DEVELOPMENT OF A METHOD TO GENERATE A SOLUBLE SUBSTRATE FOR LYTIC TRANSGLYCOSYLASES

A Thesis

Presented to

The Faculty of Graduate Studies

of

The University of Guelph

by

ADAM LAWRENCE MARK

In partial fulfilment of requirements

for the degree of

Master of Science

April, 2011

ABSTRACT

DEVELOPMENT OF A METHOD TO GENERATE A SOLUBLE SUBSTRATE FOR LYTIC TRANSGLYCOSYLASES

Adam L. Mark
University of Guelph, 2011

Advisor:
Dr. Anthony J. Clarke

Peptidoglycan, the major component of the bacterial cell wall, is essential for cell viability. Several important antibiotics disrupt peptidoglycan metabolism, including the β-lactams and vancomycin. There are several bacterial enzymes involved in peptidoglycan metabolism that are not yet the target of antibiotics, such as the lytic transglycosylases (LTs). Relatively little experimental characterization has been done on LTs, due largely to the difficulties of working with insoluble, heterogeneous, and highly variable peptidoglycan. This research develops a method for the generation of a soluble, homogeneous oligosaccharide substrate that can be used to study LTs. The approach taken was based on the enzymatic degradation of peptidoglycan into fragments of a specific nature, and their separation by HPLC. This work identifies the challenges associated with this approach, and discusses the potential flaws in the 'top-down' generation of a soluble substrate.

Acknowledgements

First I would like to thank everyone from the Clarke lab, past and present. It has been a pleasure working with all of you. You've made this experience enjoyable both inside and outside the lab. In particular I would like to thank my advisor, Anthony Clarke. I am truly grateful to have met you and to have the privilege to work under your wing. You are an inspiration.

Additionally, I would like to thank my family. It is because of you I have made it this far. You guys have been a huge support that I could always count on. Mom, dad, and Dave – I am so fortunate to have you. It is to you that I dedicate this work.

Table of Contents

List of Tables

List of Figures

List of Abbreviations

A	Absorbance
AmiB	*N*-Acetylmuramyl-L-alanine amidase B
AP	Alkaline phosphatase
APS	Ammonium persulphate
BCA	Bicinchoninic acid
BSA	Bovine serum albumin
Cam	Chloramphenicol
CCA	α-Cyano-4-hydroxycinnamic acid
CMBT	5-Chloro-2-mercaptobenzothiazole
DHB	2,5-Dihydroxybenzoic acid
DNFB	1-Fluoro-2,4-dinitrobenzene
DTT	Dithiothreitol
EDTA	Ethylenediamine tetraacetic acid
GlcNAc	*N*-Acetylglucosamine
HEWL	Hen egg-white lysozyme
HPAEC	High-performance anion-exchange chromatography
HPLC	High-performance liquid chromatography
IMAC	Immobilized metal ion affinity chromatography
IPTG	Isopropyl β-D-1-thiogalactopyranoside
Kan	Kanamycin
LB	Luria-Bertani
LT	Lytic transglycosylase
m-DAP	*meso*-Diaminopimelic acid
MALDI	Matrix-assisted laser desorption/ionization
Mlt	Membrane-bound lytic transglycosylase
MOPS	3-(*N*-Morpholino)propanesulfonic acid
MS	Mass spectrometry
MurNAc	*N*-Acetylmuramic acid
Ni-NTA	Nickel-nitrilotriacetic acid

OD	Optical density
PAD	Pulsed amperometric detection
PAGE	Polyacrylamide gel electrophoresis
PBP	Penicillin-binding protein
PEG	Polyethylene glycol
SDS	Sodium dodecyl sulfate
Slt	Soluble lytic transglycosylase
tAmiB	Truncated *N*-acetylmuramyl-L-alanine amidase B
TCA	Trichloroacetic acid
TFA	Trifluoroacetic acid
TOF	Time-of-flight
UV	Ultraviolet

Chapter 1

Introduction

1.1 Peptidoglycan

Almost all bacterial cells are surrounded by a layer of peptidoglycan (PG; murein) on the outside of the cytoplasmic membrane. This major component of the cell wall functions primarily to maintain cell strength and integrity to withstand internal turgor pressure (reviewed in Schleifer and Kandler, 1972). PG forms a mesh-like 'sacculus' surrounding the bacterial cell, serving as a scaffold to anchor other cell envelope components including proteins (Dramsi *et al.*, 2008) and teichoic acids (Neuhaus and Baddiley, 2003). Because this heteropolymer is both essential and exclusive to bacteria, its metabolism is the target of several important antibiotics; inhibition of its biosynthesis or its specific degradation results in cell lysis.

1.2 PG structure and arrangement

In Gram-positive organisms, PG is multi-layered, and for those bacteria characterized it is observed to be 15–80 nm thick (Figure 1.1) (Touhami *et al.*, 2004). In Gram-negative organisms, the PG layer is localized to the periplasm, sandwiched between the cytoplasmic and outer membranes, and is comparatively thin at 2.5–7.5 nm (Labischinski *et al.*, 1991; Murray *et al.*, 1965).

PG consists of linear glycan chains of alternating units of β-1,4-linked *N*-acetylglucosamine (GlcNAc) and *N*-acetylmuramic acid (MurNAc) residues, which are cross-linked by short peptides (Figure 1.2) (reviewed in Schleifer and Kandler, 1972). Stem peptides are attached to the C3 lactyl moiety of MurNAc, most often consisting of L-alanine, D-glutamic acid, *meso*-diaminopimelic acid (*m*-DAP), D-alanine, and D-alanine. This pentapeptide stem is present in nascent PG; however, in the mature macromolecule the terminal D-alanine residue is lost. The stem peptide serves as the point of covalent attachment of cell envelope proteins to PG (Braun and Rehn, 1969; Braun and Sieglin, 1970), and peptides from neighbouring glycans can form cross-links with each other. Cross-links are generally between the carboxyl group of D-alanine at position 4 and the amino group of *m*-DAP (or L-lysine) at position 3, either directly (Figure 1.3) or via an inter-peptide bridge. In the case of *Micrococcus luteus*, cross-links are formed via one or several peptide subunits of the same nature as

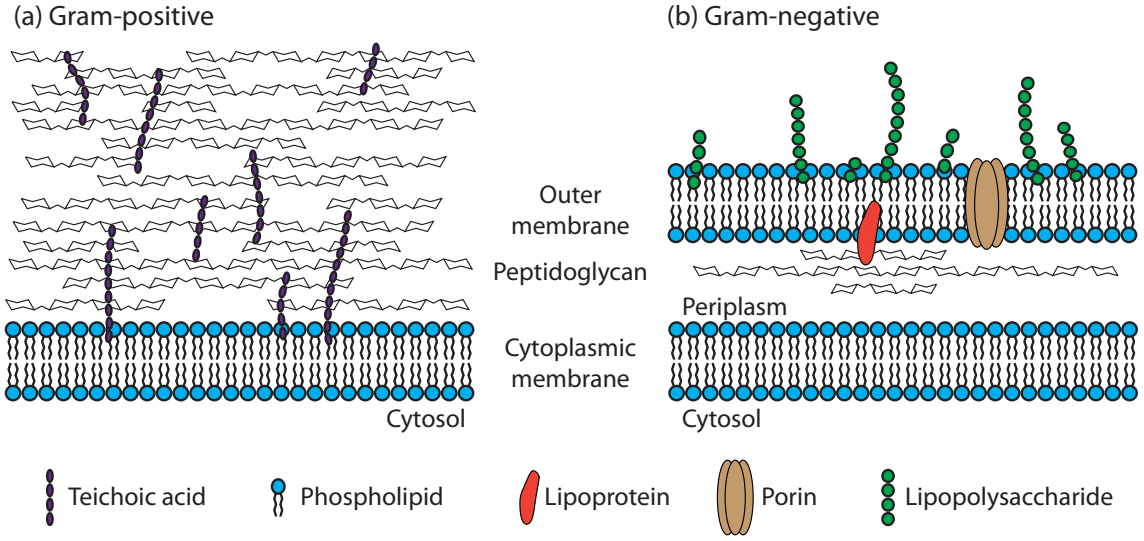

Figure 1.1: The Gram-positive and Gram-negative cell envelope. (a) Gram-positive bacteria have a thick layer of PG (15–80 nm) external to the cytoplasmic membrane, embedded with teichoic acids. (b) Gram-negative bacteria have a relatively thin layer of PG (2.5–7.5 nm) located between the inner and outer membranes, anchored by lipoproteins to the outer membrane.

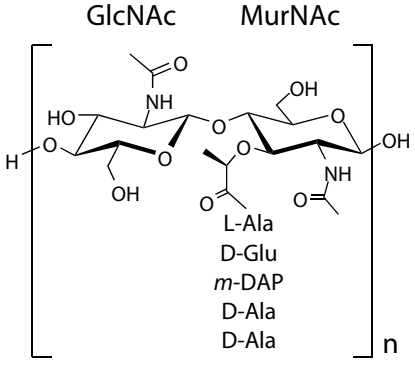

Figure 1.2: The PG monomer. PG consists of linear glycan chains of alternating units of β-1,4-linked *N*-acetylglucosamine (GlcNAc) and *N*-acetylmuramic acid (MurNAc), with short stem peptides covalently bound to the lactyl moiety of MurNAc. In *Escherichia coli*, the peptide stem consists of L-alanine, D-glutamic acid, *meso*-diaminopimelic acid, D-alanine, and D-alanine.

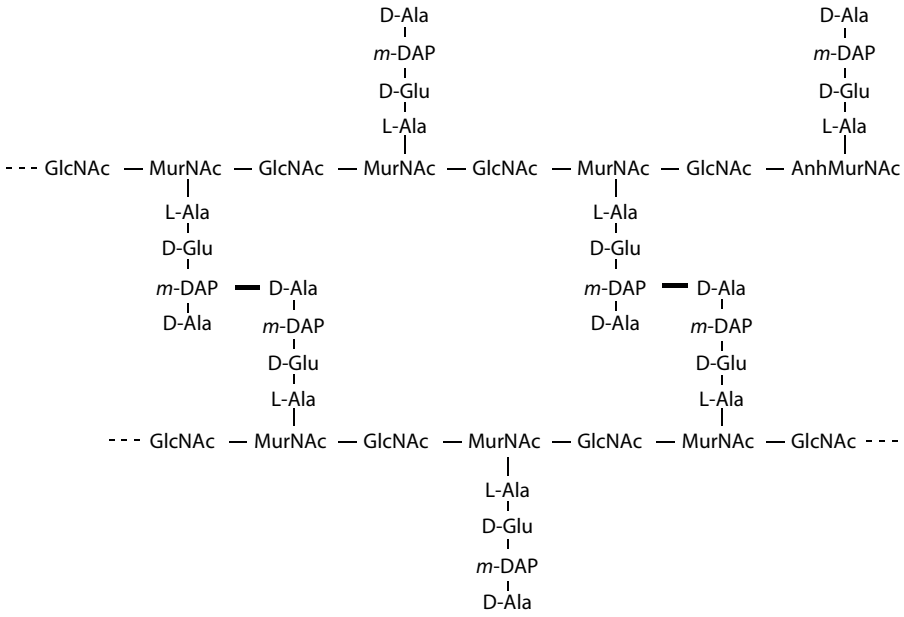

Figure 1.3: PG structure of *Escherichia coli* (chemotype A1γ). The stem peptides are directly cross-linked between the carboxyl group of D-alanine at position 4 and the amino group of *meso*-diaminopimelic acid (*m*-DAP) at position 3 (emphasized in bold). This heteropolymer forms the mesh-like sacculus that surrounds the cell. Adapted from Höltje (1995).

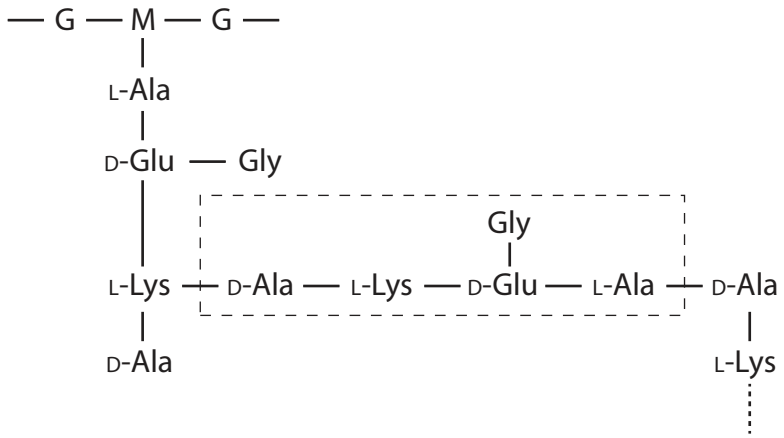

Figure 1.4: PG structure of *Micrococcus luteus* (chemotype A2). The stem peptides are connected via a peptide bridge between the carboxyl group of D-alanine at position 4 and the amino group of L-lysine at position 3 (indicated by a dashed frame). Adapted from Schleifer and Kandler (1972).

the stem peptide itself (Figure 1.4) (Schleifer and Kandler, 1972). These structures are the basis of the heteropolymer that creates the mesh-like sacculus surrounding the cell.

These structural features of PG are found in all PG-containing bacterial species known to date. However, variations in this basic architecture do exist, whether in the glycan chain, the stem peptide, or in the position or composition of the inter-peptide bridge.

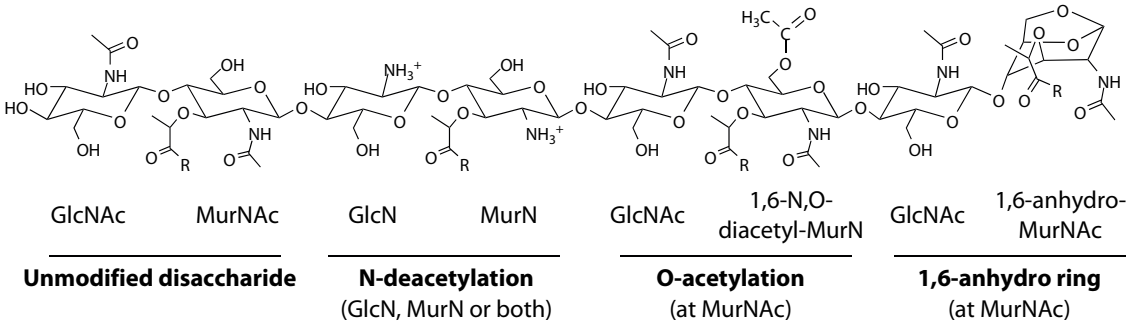

Figure 1.5: Modifications to the glycan chain. Structures of the unmodified GlcNAc-MurNAc disaccharide and some of the possible modifications to the glycan chain. Modifications (left to right) include N-deacetylation of GlcNAc and/or MurNAc, O-acetylation of the C6 position of MurNAc, and enzymatic conversion of the terminal MurNAc residue to 1,6-anhydromuramic acid (an intramolecular ring from C1 to C6). R, stem peptide. Adapted from Vollmer (2008).

1.2.1 Variation in glycan strands

During PG maturation, glycan modifications may develop. Such modifications include N-deacetylation of GlcNAc and/or MurNAc (Vollmer and Tomasz, 2000, 2002), phosphorylation (Ghuysen, 1968) or O-acetylation (Abrams, 1958; Brumfitt *et al.*, 1958) of the C6 position of MurNAc, and enzymatic conversion of the terminal MurNAc residue to 1,6-anhydromuramic acid, an intramolecular ring from C1 to C6 (Gmeiner *et al.*, 1982; Ward, 1973) (Figure 1.5). This terminal 1,6-anhydroMurNAc residue is known to exist in all Gram-negative and some Gram-positive species (*e.g., Bacillus subtilis*), which involves an intramolecular linkage between C1 and C6 (Höltje *et al.*, 1975).

The average glycan chain length of PG in *Escherichia coli* has been determined based on two methods. The first, an indirect method, determines the amount of terminal units relative to the amount of all fragments (Glauner, 1988), while the second is by the direct measurement of glycan chain distribution in cell wall digests with L-alanine amidase (discussed below) followed by high-performance liquid chromatography (HPLC) quantitative analysis (Harz *et al.*, 1990). Results from the first, indirect method, estimates the average chain length to be 33 disaccharide units (Glauner *et al.*, 1988), whereas data from the second, direct method estimates in the order of 8–12 disaccharides (Harz *et al.*, 1990). The average length of glycan chains is estimated to be much longer in Gram-positive bacteria. None of these glycan chains are long enough to encompass the cell, hence the need for a cross-linked network.

1.2.2 Variation in the stem peptide

There is an even greater diversity in peptide structure among bacteria. Peptide variations include differences in amino acids (greatest variation at position 3), different cross-links, and different types of inter-peptide bridges. These variations allow for over 100 possible PG chemotypes (Glauner *et al.*, 1988). Schleifer and Kandler (1972) proposed a classification scheme that brought organization to the various chemotypes (Table 1.1). Most Gram-negative bacteria, including *E. coli* (group A1γ), have a direct cross-linkage, whereas most Gram-positive bacteria have an inter-peptide bridge.

Table 1.1: Summary of the PG classification scheme by Schleifer and Kandler (1972).

Group A – cross-linkage between position 3 (diamino acid) and 4 (D-alanine)			
Subgroup	Type of cross-linkage	Variation(s)	Amino acid in position 3
A1	Direct (no interpeptide bridge)	α	L-lysine
		β	L-ornithine
		γ	*meso*-diaminopimelic acid
A2	Polymerized peptide subunits	None	L-lysine
A3	Monocarboxylic L-amino acids	α	L-lysine
	or glycine, or both	β	L-ornithine
		γ	*meso*-diaminopimelic acid
A4	Contains a dicarboxylic amino acid	α	L-lysine
		β	L-ornithine
		γ	*meso*-diaminopimelic acid
Group B – cross-linkage between position 2 (D-glutamic acid) and 4 (D-alanine)			
Subgroup	Type of cross-linkage	Variation(s)	Amino acid in position 3
B1	Contains an L-diamino acid	α	L-lysine
		β	L-homoserine
		γ	L-glutamic acid
		δ	L-alanine
B2	Contains a D-diamino acid	α	L-ornithine
		β	L-homoserine
		γ	L-diaminobutyric acid

PG has a flexible, heterogeneous structure and is not crystalline, making its structure impossible to directly determine at high resolution with presently available techniques. PG spatial arrangement with respect to the cell surface is still a matter of debate. The classical model of PG architecture predicts the glycan chains to be parallel to the cytoplasmic membrane, with peptide cross-links forming a planar layer (Figure 1.6). In another model, now largely discounted, the glycan strands run perpendicular to the cytoplasmic membrane, each strand being cross-linked by peptide bridges with four other strands (Dmitriev *et al.*, 1999; Meroueh *et al.*, 2006). Demchick and Koch (1996) proposed that the glycan strands follow a zig-zag line to form a layer with hexagonal tessera, the smallest pores (2 nm diameter), based on permeability studies in which globular proteins less than 25 kDa could fit through the natural pores of the sacculus while proteins around 50 kDa could not. The prevailing theory suggests that horizontal glycan strands run predominantly perpendicular to the long axis, whereas the flexible peptides run predominantly in the direction of the long axis (reviewed in Vollmer and Seligman, 2010). This model is in accordance with estimates of PG thickness (Labischinski *et al.*, 1991), length of glycan chains (Glauner *et al.*, 1988; Harz *et al.*, 1990), permeability of the sacculus (Demchick and Koch, 1996; Yao *et al.*, 1999), and the estimated amount of PG present in a cell (Wientjes *et al.*, 1991).

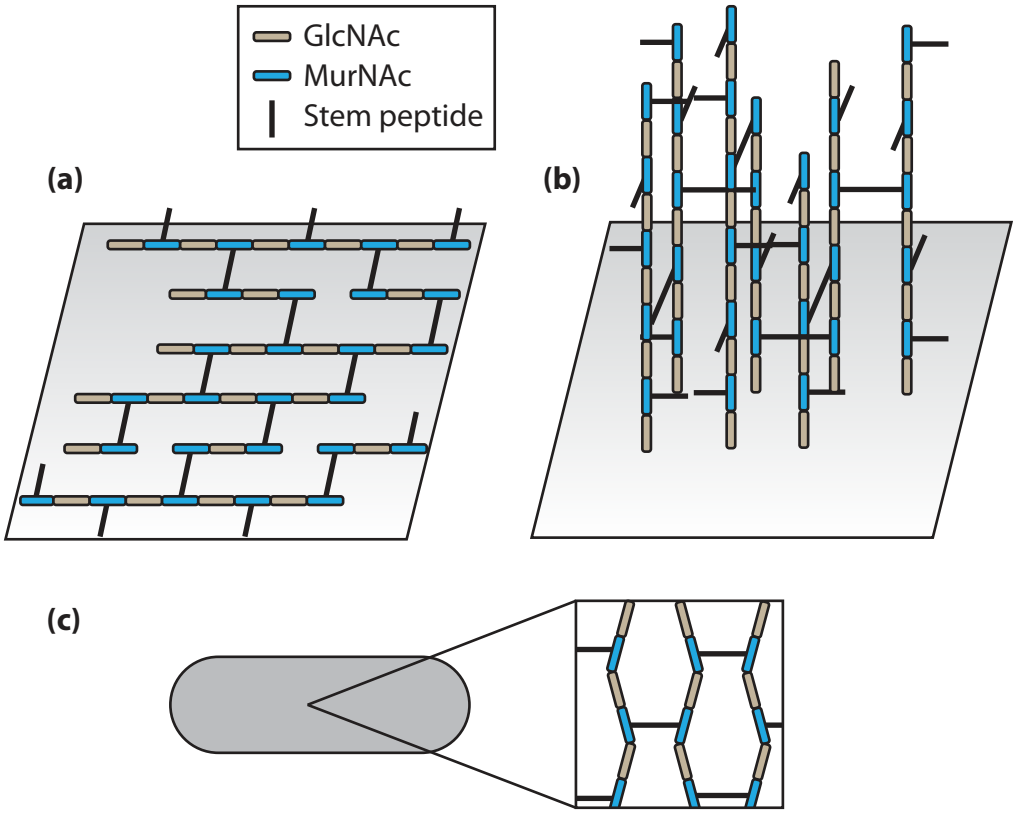

Figure 1.6: Spatial arrangement of PG with respect to the cell surface. (a) The classical model of PG architecture predicts the glycan chains to be parallel to the cytoplasmic membrane, with peptide cross-links forming a planar layer, (b) a largely discounted model in which the glycan chains run perpendicular to the cytoplasmic membrane with peptide stems protruding in a helical pattern, and (c) the prevailing theory in which horizontal glycan chains run predominantly perpendicular to the long axis and the peptides run predominantly in the direction of the long axis.

1.3 Biosynthesis of the PG sacculus

The growth of the PG sacculus involves the synthesis of disaccharide pentapeptide subunits (Figure 1.2) and their integration into the existing sacculus. This biosynthesis occurs in two different cellular compartments: the precursor (lipid II) is synthesized in the cytoplasm, which is then flipped across the cytoplasmic membrane into the periplasm where the new material is integrated. Several important antibiotics inhibit various stages of this process, including PG synthetase inhibitors (*e.g.,* fosfomycin), transpeptidase inhibitors which prevent glycan cross-linking (*e.g.,* β-lactams), and transglycosylase inhibitors which inhibit glycan polymerization (*e.g.,* moenomycin, vancomycin) (Kahne *et al.*, 2005; Barreteau *et al.*, 2008).

The biosynthesis of the disaccharide pentapeptide monomer occurs within the cytoplasm via a series of uridine diphosphate (UDP) precursors and lipid intermediates (reviewed in van Heijenoort, 2001; Barreteau *et al.*, 2008). Six steps (mediated by MurA through MurF) lead to the formation of the UDP-MurNAc-pentapeptide precursor from UDP-GlcNAc (Figure 1.7). At the cytoplasmic membrane, the UDP-MurNAc-pentapeptide from the cytoplasmic precursor is transferred to the mem-

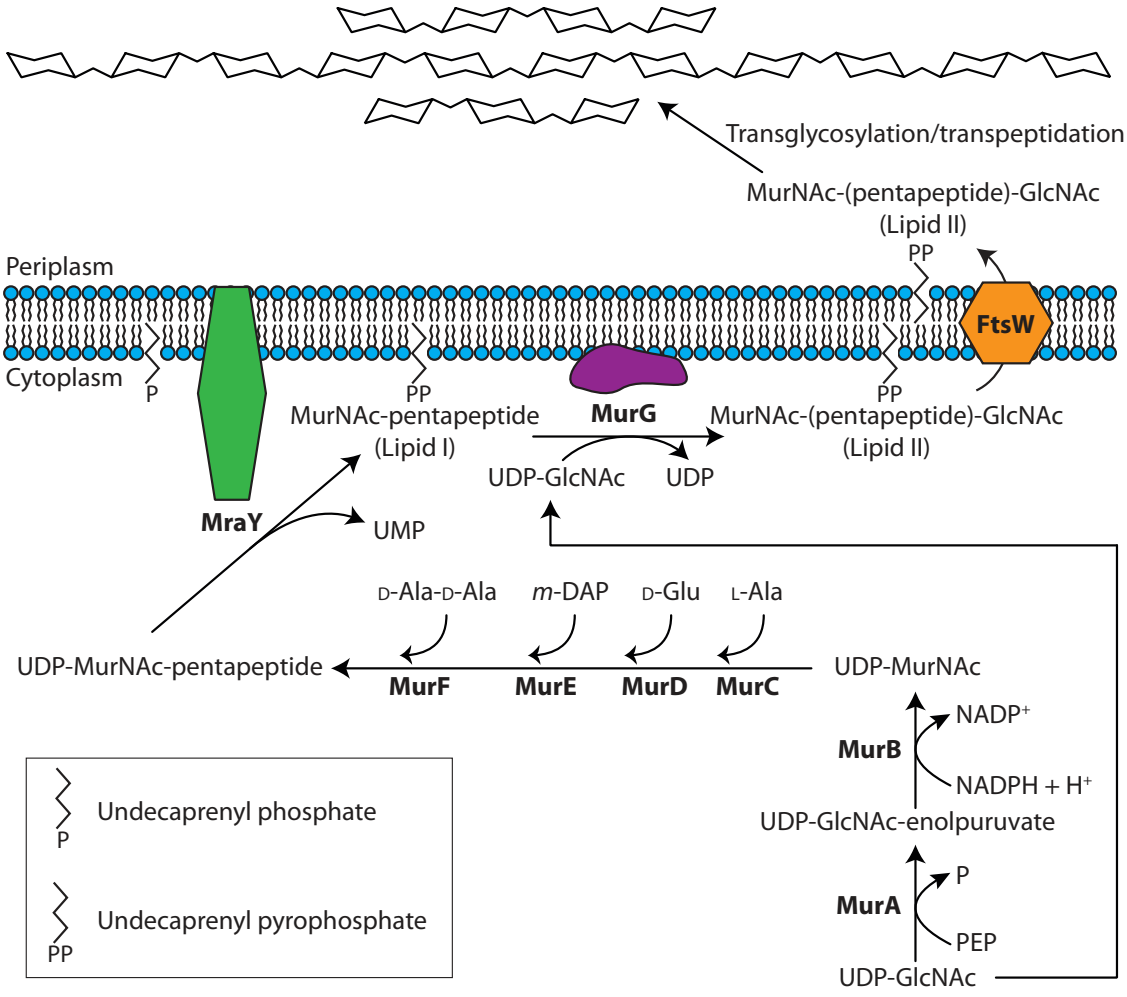

Figure 1.7: PG biosynthesis. In the cytoplasm, MurA and MurB catalyze the synthesis of UDP-MurNAc. The amino acids of the pentapeptide are sequentially added via a series of four enzymes, MurC–F, to the lactyl moiety of UDP-MurNAc using ATP hydrolysis. At the cytoplasmic membrane, MraY catalyzes the transfer of UDP-MurNAc-pentapeptide to the membrane acceptor undecaprenyl phosphate (C_{55}-P), forming lipid I. MurG catalyzes the transfer of the GlcNAc moiety from UDP-GlcNAc to lipid I, yielding lipid II. This complete PG monomer linked to the lipid carrier is translocated across the cytoplasmic membrane by FtsW where it is integrated into the existing sacculus through transglycosylation and transpeptidation reactions. Adapted from Nanninga (1998).

Table 1.2: High molecular mass PBPs of *Escherichia coli*. PBPs may carry out transpeptidation (TP), transglycosylation (TG), or both. PBP1a and PBP1b are the major transpeptidases-transglycosylases.

Class	Gene	Enzyme	Size (kDa)	Activity	Reference
A	*ponA*	PBP1a	93.5	TP & TG	Broome-Smith *et al.* (1985)
	ponB	PBP1b	94.1	TP & TG	Broome-Smith *et al.* (1985)
	pbpC	PBP1c	85.1	TP & TG	Schiffer and Höltje (1999)
B	*pbpA*	PBP2	70.9	TP & cell elongation	Stoker *et al.* (1983)
	pbpB	PBP3	63.9	TP & cell division	Botta and Park (1981)

brane acceptor undecaprenyl phosphate (C_{55}-P). This is catalyzed by the transferase MraY, an integral cytoplasmic membrane protein (Ikeda *et al.*, 1991), resulting in undecaprenyl-pyrophosphoryl-MurNAc-pentapeptide (lipid I). Thereafter, the GlcNAc moiety of UDP-GlcNAc is transferred to lipid I by the transferase MurG, an enzyme peripherally associated with the inner face of the cytoplasmic membrane, yielding undecaprenyl-pyrophosphoryl-MurNAc-(pentapeptide)-GlcNAc (lipid II) (Ha *et al.*, 2001; Mengin-Lecreulx *et al.*, 1991). Lipid II, the complete PG monomer unit linked to the carrier, is translocated across the cytoplasmic membrane by FtsW (Mohammadi *et al.*, 2011), where it is added to the existing sacculus via actions of both PG-cleaving and PG synthetic enzymes. PG-cleaving enzymes, such as lytic transglycosylases (LTs) and peptidases, catalyze the cleavage of glycan chains and peptide bonds, respectively. This results in the release of existing material as turnover products, and creates space for the addition of new material. Penicillin-binding proteins (PBPs) catalyze the polymerization of the glycan strand (transglycosylation) and the cross-linking between glycan chains (transpeptidation) (Figure 1.8). PBPs are divided into two main categories, the high molecular mass (HMM) PBPs and the low molecular mass (LMM) PBPs. *E. coli* possesses 12 PBPs; 5 HMM PBPs and 7 LMM PBPs. HMM PBPs are multi-modular and are responsible for PG polymerization and insertion into the pre-existing sacculus (Table 1.2) (Goffin and Ghuysen, 1998). LMM PBPs are involved in cell separation, PG maturation, or recycling. Of the LMM PBPs, PBP5 is the most abundant and is the major carboxypeptidase. This enzyme cleaves the terminal D-Ala-D-Ala bond, making the stem peptide unavailable for transpeptidation (reviewed in Sauvage *et al.*, 2008).

1.4 Growth of PG sacculus

The insertion site of new PG material has been the subject of numerous studies (recently reviewed in den Blaauwen *et al.*, 2008). Bacterial cells require lytic enzymes that participate in assembly of the PG sacculus, daughter cell separation, and maintenance of cell morphology. Bacterial cells lacking these various lytic enzymes are affected in septum cleavage, resulting in a chaining phenotype (Heidrich *et al.*, 2002), suggesting the essentiality of PG-cleaving enzymes for normal cell division and viability.

Newly synthesized PG must be carefully inserted into the existing sacculus, as disruption could lead to lysis. It has been theorized that bacteria utilize a "make-before-break" strategy for growth of the sacculus (Koch, 1990). In this theory, nascent strands are attached to the existing sacculus before cleavage of old bonds. In Gram-positive species this results in an inside-to-outside mode of growth,

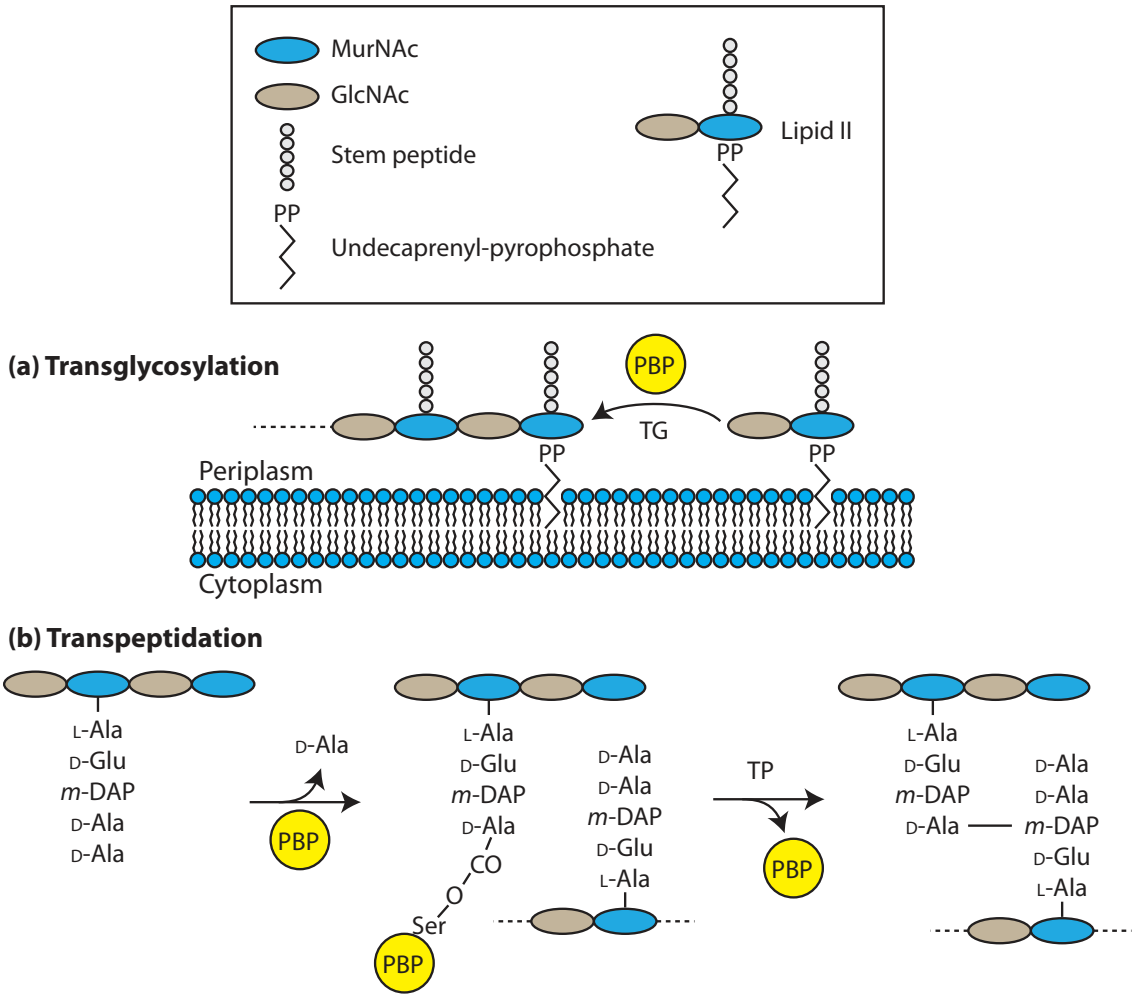

Figure 1.8: Transglycosylation and transpeptidation reactions catalyzed by penicillin-binding proteins (PBPs). (a) PBPs catalyze transglycosylation (TG) reactions through the formation of a glycosidic linkage between the growing glycan strand and lipid II, releasing undecaprenyl-pyrophosphate which is recycled for subsequent use. (b) Transpeptidation (TP) reactions occur in two steps. First, a covalent intermediate is formed between the donor stem peptide and the PBP with the concomitant release of the terminal D-alanine. Subsequently, the cross-link is formed with the acceptor strand and the PBP is released. Adapted from Mainardi *et al.* (2008).

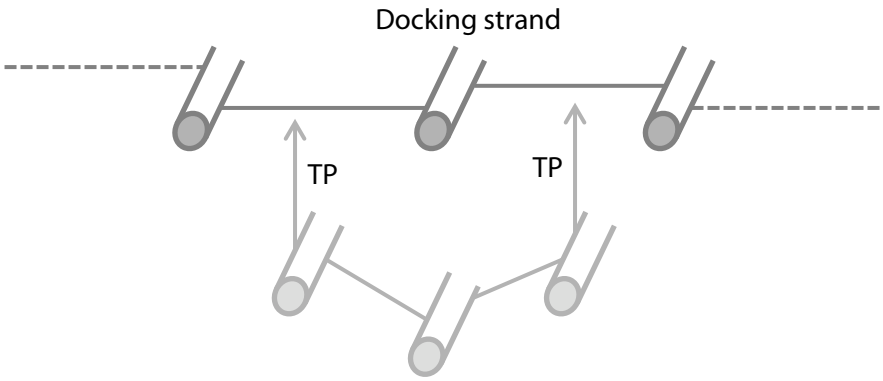

Figure 1.9: The hypothetical three-for-one growth mechanism of PG. A triplet of cross-linked glycan strands are linked to the sacculus below the docking strand by transpeptidation (TP). Subsequently, the single docking strand is cleaved and released from the sacculus, and the three nascent strands become part of the stress-bearing wall. Rods represent glycan strands, lines indicate existing cross-links, and arrows indicate new cross-links. Adapted from Höltje (1996).

with layers of nascent PG found closest to the cytoplasmic membrane (Koch and Doyle, 1985). In Gram-negative bacteria, this idea has been developed into the "three-for-one" growth model (Figure 1.9) (Höltje, 1995). In this model, a triplet of cross-linked glycan strands are linked to the sacculus below the docking strand by transpeptidation (TP). Subsequently, the docking strand is cleaved and released from the sacculus, and the three nascent strands become part of the stress-bearing wall. This model allows the expansion of the sacculus without loss of its structural integrity.

As described above, the regular maintenance of the PG sacculus requires the actions of both PG synthetic and PG cleaving enzymes. These activities must be coordinated not only to maintain the integrity of the sacculus, but ultimately for cell viability. It has been proposed that some of these enzymes exist in multi-enzyme complexes, which would allow for streamlined synthesis and degradation (Höltje, 1996). Protein complexes involved in PG metabolism have been detected in *E. coli* (Romeis and Höltje, 1994; Schiffer and Höltje, 1999; Vollmer *et al.*, 1999), *Haemophilus influenzae* (Alaedini and Day, 1999), and *Pseudomonas aeruginosa* (Legaree and Clarke, 2008) using affinity chromatography and surface plasmon resonance. Interactions between a number of LTs and PBPs have been identified, including PBP3/7/8 with soluble lytic transglycosylase 70 (Slt70) (Romeis and Höltje, 1994), PBP1B with membrane-bound lytic transglycosylase A (MltA) (Vollmer *et al.*, 1999), and PBP2 with MltB (Legaree and Clarke, 2008).

1.5 PG recycling

PG is continuously being turned over, as demonstrated by pulse-chase labelling experiments with ^{3}H-labelled *m*-DAP (Goodell, 1985). As the cell ages, maturation of the sacculus includes shortening of the glycan chains, changes in the degree of cross-linking, and loss of material through turnover. The Gram-positive *B. subtilis* has been shown to lose 25–50% of its muropeptides within each generation, presumably into the surrounding medium (Goodell, 1985). In *E. coli*, the loss of PG has been shown

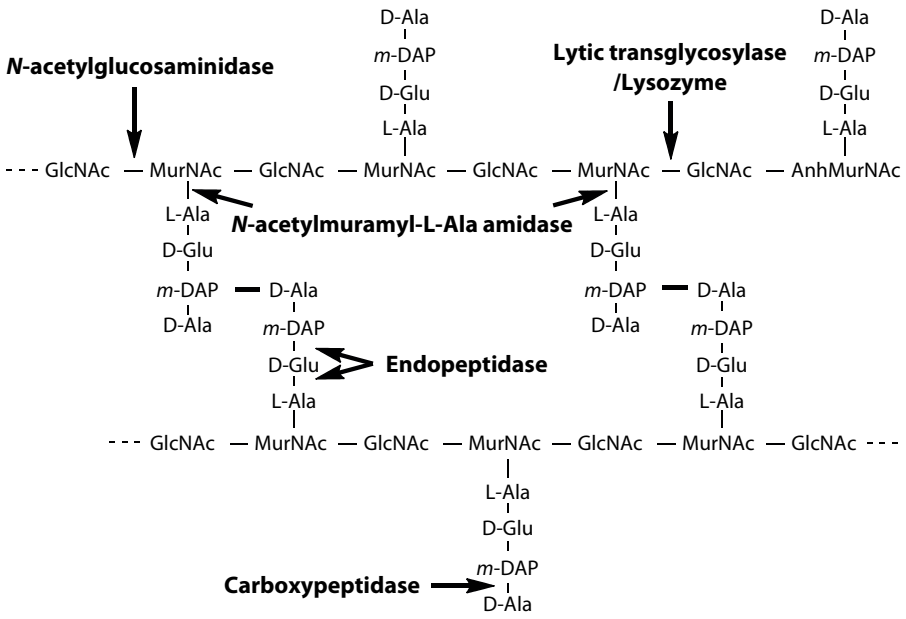

Figure 1.10: PG-cleaving enzymes. The different types of PG-cleaving enzymes (indicated in bold) are capable of cleaving specific bonds within the sacculus. If left unregulated these enzymes can be autolytic, leading to cell lysis. Lytic transglycosylases and lysozymes catalyze cleavage of the same bond, albeit with different reaction products. *m*-DAP, *meso*-diaminopimelic acid. Adapted from Höltje (1995).

to be only 6–8%; however, 50% of the turnover products are returned to the cytoplasm where they are digested into various subunits, and then used to build new PG (Park, 1993). This recycling process not only serves as an energy efficient mechanism, but may also be a signalling and sensing process the cell uses to monitor the condition of the sacculus during periods of growth and/or nutrient deprivation (Wiedemann *et al.*, 1998).

1.6 PG-cleaving enzymes

As described above, a number of metabolic activities involving PG require cleavage of the sacculus. There are several types of endogenous PG-lytic enzymes, each capable of cleaving specific bonds within the sacculus (Figure 1.10). These include *N*-acetylmuramyl-L-alanine amidases that hydrolyze the amide bond between MurNAc and the stem peptide, peptidases (carboxy- and endopeptidases) that hydrolyze amide bonds in stem peptides, and glycosidases (β-*N*-acetylhexosaminidases, lysozymes, and lytic transglycosylases) that cleave the glycan strand (reviewed in Vollmer *et al.*, 2008). Several of these enzymes can be autolytic if left unregulated; they can disrupt the PG sacculus, often leading to cell lysis. Nonetheless, it appears that bacteria possess a number of lytic enzymes that may have redundant roles, or more than one function. The following subsections describe the various enzymes involved in PG metabolism.

1.6.1 *N*-Acetylmuramyl-L-alanine amidase

N-Acetylmuramyl-L-alanine amidase (EC 3.5.1.28; herein referred to as amidase) cleaves the amide bond between the lactyl moiety of MurNAc and the N-terminal L-alanine residue of the stem peptide (Figure 1.10) (Kuroda *et al.*, 1992). Of the five amidases present in *E. coli*, four have periplasmic localization (soluble AmiA, AmiB, and AmiC, and membrane-anchored AmiD), whereas AmpD is cytoplasmic. Amidases play an important role in cleaving the septum to release daughter cells after cell division (Wolf-Watz and Normark, 1976), and in trimming soluble released PG fragments during turnover for recycling (Jacobs *et al.*, 1995). AmpD has been found to be essential for both its role in PG recycling and β-lactamase regulation. Like other hydrolases, these amidases show substrate specificity. For example, the cytoplasmic AmpD only degrades the 1,6-anhydroMurNAc-tetra- and -tripeptide resulting from PG turnover (Höltje *et al.*, 1994; Jacobs *et al.*, 1995).

The gene encoding *N*-Acetylmuramyl-L-alanine amidase from *P. aeruginosa* has been cloned and over-expressed in *E. coli* (Scheurwater *et al.*, 2007). The recombinant protein has an N-terminal truncation which was necessary for the majority of protein to remain in the cytoplasm where it could not act on PG, and a C-terminal His-tag to facilitate purification. This protein was found to accept the intact, high molecular weight PG sacculus as a substrate, unlike the *E. coli* homolog (Parquet *et al.*, 1983).

1.6.2 Peptidase

Peptidases cleave amide bonds between amino acids in PG or its soluble products (Figure 1.10) (Höltje, 1995). Endopeptidases cleave within the peptide, whereas carboxypeptidases remove a C-terminal amino acid. DD-Peptidases cleave between two D-amino acids, whereas LD- or DL-peptidases cleave between D- and L-amino acids (Smith *et al.*, 2000). Many endopeptidases belong to the low molecular mass PBPs as they share typical sequence motifs of PBPs and are inhibited by β-lactams (Goffin and Ghuysen, 1998). The two types of endopeptidases (type-4 and type-7 PBPs) are anchored to the cytoplasmic membrane where they perform hydrolytic functions, such as the hydrolysis of the peptide cross-linkage between glycan chains. This can be considered the reverse reaction of the HMM PBPs involved in transpeptidation. There are also endopeptidases unrelated to the PBPs, which are not inhibited by β-lactams, such as MepA which cleaves the cross-link between D-Ala and *m*-DAP in *E. coli* PG (chemotype A1γ) (Keck *et al.*, 1990). LD-Carboxypeptidases cleave between *m*-DAP (position 3) and D-Ala (position 4) in the tetrapeptide to remove the terminal D-Ala residue. Of the DD-carboxypeptidases, most belong to type-5 PBPs and are the most abundant LMM PBPs, and are crucial for maintaining a uniform shape in *E. coli* (Nelson and Young, 2000).

1.6.3 β-*N*-Acetylhexosaminidase

The first type of glycosidase are the β-*N*-acetylhexosaminidases (EC 3.2.1.52; *N*-acetyl-β-glucosaminidase), which are widespread in nature. These enzymes hydrolyze the glycosidic linkage between GlcNAc and adjacent monosaccharides in a number of oligosaccharide substrates, including PG (Fig-

ure 1.10) (Karamanos, 1997). In *E. coli*, the β-*N*-acetylhexosaminidase NagZ acts on the GlcNAc-1,6-anhydroMurNAc disaccharide (with or without the stem peptide), an intermediate in the PG recycling pathway (Vötsch and Templin, 2000). It hydrolyzes the β-1,4 glycosidic linkage between GlcNAc and 1,6-anhydroMurNAc of PG degradation products following their import to the cytoplasm. When the gene *nagZ* is knocked out in *E. coli*, this substrate accumulates within the cytoplasm, indicating this is the only protein to serve this purpose (Cheng *et al.*, 2000). The formation of intracellular 1,6-anhydroMurNAc-peptides is important for the expression control of inducible β-lactamases such as AmpC, as mutants lacking active NagZ cannot establish AmpC-mediated β-lactam resistance (Vötsch and Templin, 2000).

1.6.4 Lysozyme

The second type of glycosidase, lysozyme (EC 3.2.1.17; muramidase), is widespread in nature. It is produced by bacteria, bacteriophages, fungi, invertebrates, and vertebrates, and is amongst the most studied enzymes in biochemistry. There are nine classes of proteins with a lysozyme-like fold (Pei and Grishin, 2005). Four of these classes cleave the β-1,4 glycosidic linkage in PG; their best-known members being hen egg-white lysozyme (HEWL, or C-type lysozyme), goose egg-white lysozyme (GEWL), bacteriophage T4 lysozyme (T4L), and *Chalaropsis* lysozyme (Evrard *et al.*, 1999). Lysozyme can be either exo-specific, processively degrading glycan strands from their GlcNAc end, or endo-specific (Vollmer *et al.*, 1997).

Lysozymes function as a first line of defense against bacterial infection. Humans have lysozyme in concentrations up to 50 μg/mL in tears, mucous, and other secretions (Abergel *et al.*, 2007). Lysozymes are also used by bacteriophages to aid in host infection or the release of progeny (Borysowski *et al.*, 2006). These enzymes are more effective against Gram-positive organisms, as their PG is more easily accessible. Gram-negative organisms do not appear to encode any true lysozymes; however, they do produce several lytic transglycosylases, which act on the same glycosidic linkage (Figure 1.10).

1.6.5 Lytic transglycosylase

The third and final type of glycosidase is the lytic transglycosylase (LT), an important enzyme and the major focus of this project.

1.7 Lytic transglycosylases

LTs (EC 4.2.2.n) are ubiquitous among all bacteria that produce PG, and most bacteria encode a variety of them (Blackburn and Clarke, 2001). This important class of enzyme is responsible for cleaving the sacculus to accommodate PG expansion, turnover, and facilitation of the insertion of protein complexes such as flagella, pili, and secretion systems (reviewed in Scheurwater *et al.*, 2008). Such complexes are too large to pass through the natural pores within the sacculus, and therefore

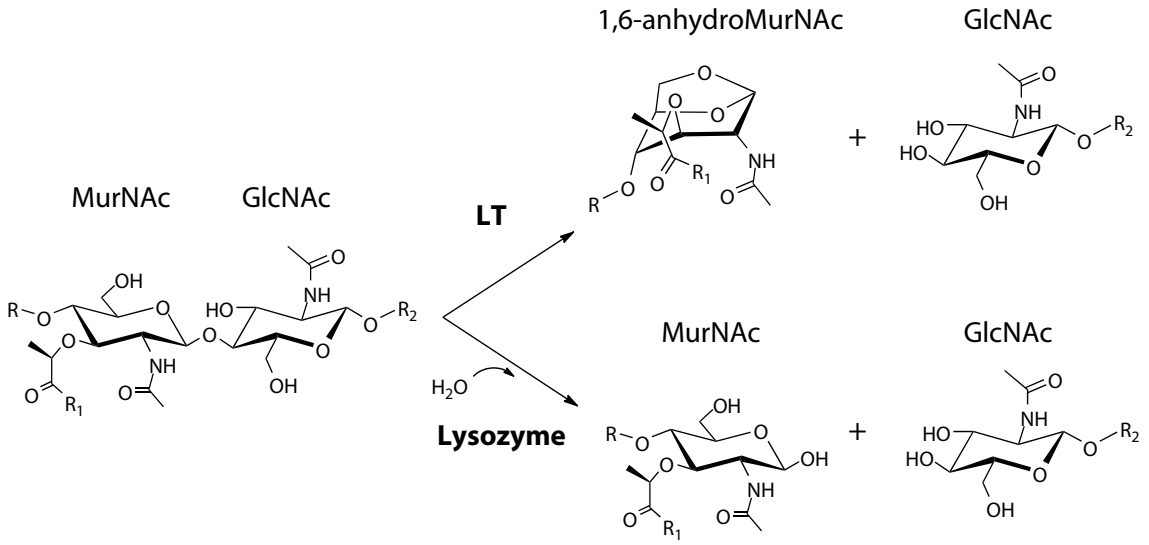

Figure 1.11: Comparison of the catalytic activity between lytic transglycosylases and lysozymes. Both LTs and lysozyme catalyze the cleavage of the β-1,4 glycosidic linkage between MurNAc and GlcNAc. However, unlike lysozymes which are hydrolytic enzymes, LTs are lyases which catalyze the cleavage of the glycosidic linkage with the concomitant formation of a 1,6-anhydromuramoyl residue (1,6-anhydroMurNAc). R, polymerized repeat units; R_1, stem peptide; R_2, polymerized repeat units. Adapted from Blackburn and Clarke (2000).

require remodelling of PG. The importance of these bacterial enzymes in cell wall metabolism is proposed to present an attractive new target for the development of broad-spectrum antibiotics.

LTs act on PG with the same substrate specificity as lysozyme, cleaving the β-1,4 glycosidic linkage between MurNAc and GlcNAc (Figure 1.10). However, unlike lysozymes which are hydrolytic enzymes, LTs are lyases which catalyze the cleavage of the glycosidic linkage with the concomitant formation of a 1,6-anhydrobond in the MurNAc residue (anhydroMurNAc) (Figure 1.11) (Höltje *et al.*, 1975). PG fragments containing this 1,6-anhydromuramoyl residue have been shown to cause a variety of pathobiological effects in the human host. For example, the released GlcNAc-anhydro-MurNAc-tetrapeptide acts as a tracheal cytotoxin by inducing cell damage in the respiratory tract during *Bordetella pertussis* infection, the etiological agent of whooping cough (Luker *et al.*, 1993). This same fragment can cause damage to fallopian tubes during *Neisseria gonorrhoeae* infection (Cloud and Dillard, 2002). Other apparent effects of anhydromuropeptides include pyrogenicity (fever induction), somnogenicity (promotion of sleep), the induction of rheumatoid arthritis, and complement activation (reviewed in Cloud-Hansen *et al.*, 2006). As many bacteria release this PG metabolite, it is likely that other pathobiological effects will be attributed to it.

1.7.1 LT families

Blackburn and Clarke (2001) have grouped LTs into four families based on their amino acid sequence and conserved motifs. Family 1 is a superfamily of five subfamilies; A through E. Family 4 enzymes primarily belong to bacteriophages. *E. coli* is known to produce LTs from each family with the ex-

Table 1.3: Family archetypes of lytic transglycosylases in *Escherichia coli*. LTs are either membrane-bound (Mlt) or soluble (Slt), and have either exo- or endo-specificity. Molecular weights are given for the unprocessed form.

Family	Gene	Enzyme	Amino acids	MW (Da)	Specificity	Reference(s)
1A	*sltY*	Slt70	645	73,353	exo	Höltje *et al.* (1975)
1B	*yfhD*	MltF (YfhD)	518	58,302	**n.d.**	Scheurwater and Clarke (2008)
1C	*mltC*	MltC	359	40,113	exo	Dijkstra and Keck (1996)
1D	*mltD*	MltD	452	49,417	exo	Kajie *et al.* (1991)
1E	*mltE*	MltE (EmtA)	203	22,227	**endo**	Kraft *et al.* (1998)
2	*mltA*	MltA	365	40,411	exo	Ursinus and Höltje (1994); Lommatzsch *et al.* (1997)
3	*mltB*	MltB	361	40,256	exo	Engel *et al.* (1992); Ehlert *et al.* (1995)

ception of family 4 (Table 1.3). In contrast, *P. aeruginosa* does not appear to encode family 1C or 1E enzymes, but instead produces four MltB isozymes in addition to the other *E. coli* LTs (Blackburn and Clarke, 2001). The apparent redundancy in LTs is similar to that observed with the variety of PBPs responsible for late stages of PG biosynthesis. Furthermore, functional equivalence among the LTs appears to allow for elimination of one or more LT without being lethal to the cell (Blackburn and Clarke, 2002; Heidrich *et al.*, 2002). A seventh *E. coli* LT was identified (MltF) (Scheurwater and Clarke, 2008) when deletion of the six known LTs resulted in a viable strain, albeit with a chaining phenotype (Heidrich *et al.*, 2002).

Crystal structures have been solved for several LTs, including *E. coli* Slt70 (Thunnissen *et al.*, 1995), *E. coli* MltA (van Straaten *et al.*, 2005), *N. gonorrhoeae* MltA (Powell *et al.*, 2006), *E. coli* Slt35 (a soluble product of MltB) (van Asselt *et al.*, 1999a), and bacteriophage lambda LT (Leung *et al.*, 2001). Both amino acid sequences and overall tertiary structures lack similarity between members of respective families, although family 1A, 3, and 4 LTs are mostly α-helical and possess a lysozyme-like fold at their catalytic domains. Family 2 enzymes are structured as a β-barrel. Aside from these differences, the active site clefts of Slt70, MltA, and MltB are comprised of four substrate-binding subsites that can accommodate the aminosugar residues of a tetrasaccharide substrate. The exo-activity of these LTs (Table 1.3) is supported by this subsite architecture, as these LTs catalyze the release of disaccharide anhydromuropeptides from either the reducing or non-reducing ends of PG. In contrast, the endo-acting bacteriophage LTs (Table 1.3) can accommodate hexasaccharide substrates within their active site clefts (Leung *et al.*, 2001). Although not yet solved, it will be interesting to compare these structures to the putative endo-acting *E. coli* MltE (Kraft *et al.*, 1998) and MltF (Scheurwater and Clarke, 2008).

1.7.2 Mechanism of LT action

The MurNAc and GlcNAc residues are shown to bind to the -1 and +1 subsites, respectively, indicating the substrate specificity of the LTs. For example, the amino acid residues at subsite -1 interact with both the lactyl moiety of MurNAc and its associated peptide, and this interaction is critical

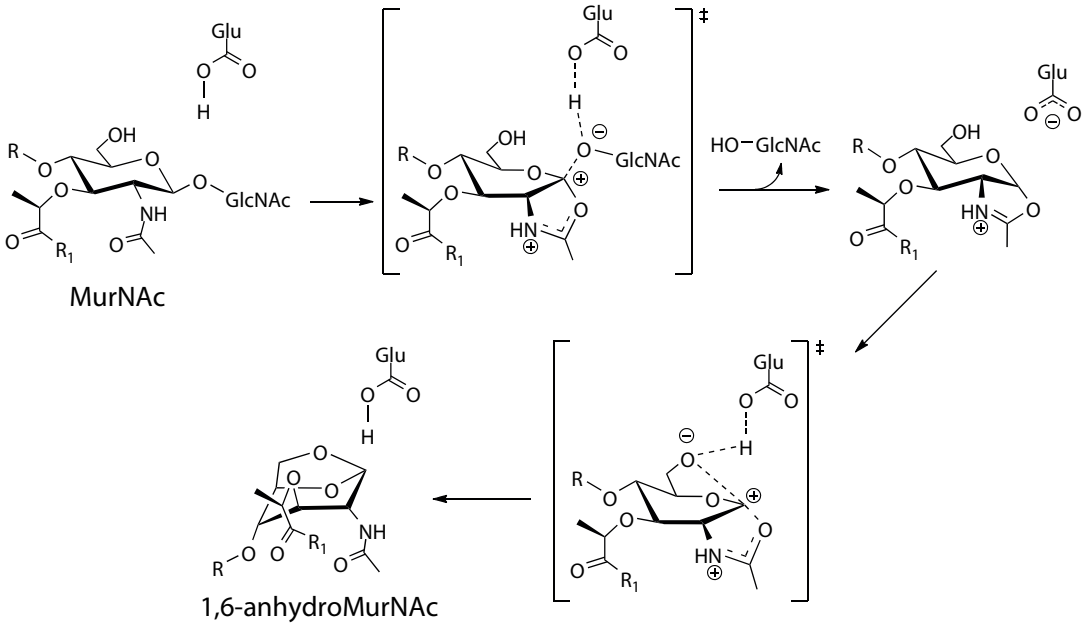

Figure 1.12: Proposed reaction mechanism catalyzed by lytic transglycosylases. Initially, the catalytic glutamic acid serves as an acid to protonate the glycosidic linkage between MurNAc and GlcNAc, leading to the formation of a muramoyl oxazolinium ion intermediate. Subsequently, the catalytic glutamate serves as a base to abstract the C6 hydroxyl proton, promoting the collapse of the oxazolinium ion with concomitant formation of the 1,6-anhydromuramoyl product. Adapted from Scheurwater *et al.* (2008).

for the proper orientation of substrate for lytic activity (Reid *et al.*, 2004c, 2006). The proposed intramolecular reaction involves a single catalytic acid residue, often a glutamic acid, positioned at the centre of the active site clefts between subsite -1 and +1. This residue is thought to function as the catalytic acid/base for bond cleavage by substrate-assisted catalysis (Thunnissen *et al.*, 1994; van Asselt *et al.*, 1999a; Reid *et al.*, 2004b). Initially, the catalytic residue acts as an acid by donating its proton to the oxygen between MurNAc and GlcNAc (Figure 1.12). As bond cleavage occurs, the transient oxocarbenium ion would be stabilized through formation of an oxazolinium intermediate involving the *N*-acetyl group of the muramoyl residue. The deprotonated catalytic residue then acts as a base by abstracting a proton from the C6 hydroxyl group of MurNAc, allowing for an intramolecular nucleophilic attack at C1, collapsing the oxazoline intermediate with the concomitant forming the 1,6-anhydromuramoyl product (Reid *et al.*, 2004a,b). This unique activity of LTs makes them attractive targets for the development of antimicrobial agents, as mechanism-based inhibitors should not interfere with innate immunity, such as human lysozyme.

1.7.3 Control of LT activity

LTs get their name because they are considered to be autolytic if their activity is not controlled. Little is known regarding the control of LT activity, although one mechanism appears to involve chemical modification of the PG. An example of this is the O-acetylation of PG at the C6 hydroxyl group of MurNAc (Figure 1.5), preventing the formation of the 1,6-anhydromuramoyl product by LTs (Black-

burn and Clarke, 2002). Another level of control is physical association and separation. In *E. coli* and *P. aeruginosa*, most LTs are peripheral membrane-bound lipoproteins on the inner (periplasmic) leaflet of the outer membrane (Höltje, 1998; Blackburn and Clarke, 2002). This localization is in accordance with the three-for-one growth model, which assumes old PG strands are removed from the side facing the outer membrane (Höltje, 1995). Both the membrane-bound and soluble LTs appear to form complexes with the PBPs (Koraimann, 2003), which are also peripheral membrane proteins but are associated with the outer leaflet of the cytoplasmic membrane (Barbas *et al.*, 1986). These complexes serve to bring the enzymes together with their substrate, sandwiching the PG between them. This association would allow lysis to be coupled with the biosynthetic transglycosylase activity of the PBPs.

1.7.4 Exo- versus endo-acting LTs

Cooperation between exo- and endo-acting enzymes is well known in chitin and cellulose degradation (reviewed in Davies and Henrissat, 1995). One advantage of endoenzymes is the production of more chain ends for the processive degradation of polymers by exoenzymes. A possible function of endo-type LTs is the formatting of PG strands to form the length distribution, a process that is still unknown (Harz *et al.*, 1990). Another function is the remodelling of PG to accommodate large, membrane-spanning structures. To accomplish this the use of endo-type enzymes would be more energetically favourable than a processive, exo-type enzyme.

Overproduction of the proposed endo-acting MltE has been shown to alter two important morphological features of *E. coli* (Kraft *et al.*, 1998). The first is a twofold increase in the amount of anhydromuropeptides, indicating the shortening of glycan strands. The second is a threefold increase in cross-linked anhydromuropeptides which appears to indicate a preference for cross-linked PG *in vivo*. Formation of such cross-links has been reported prior to the onset of bacteriolysis by various agents and growth conditions, and has been speculated as a kind of defense mechanism to avoid lysis (Glauner and Höltje, 1990; Höltje, 1998). When the activity of MltE was assayed *in vitro* using intact sacculi, no increase in the release of soluble PG breakdown products could be detected, although zymogram analysis did demonstrate autolytic activity (Kraft *et al.*, 1998).

1.7.5 Questions that remain unanswered

The LTs are far from exhaustively studied. Although they propose an attractive and novel antibiotic target, they are still being discovered. Recently Scheurwater and Clarke (2008) identified the seventh *E. coli* LT, MltF. This enzyme is unique as it possesses two domains, of which only the C-terminal domain bears sequence similarity to other family 1 LTs. The N-terminal, non-LT domain is similar to ATP-binding cassette-type (ABC) periplasmic binding proteins, in particular a lysine/arginine/ornithine-binding protein (LAO). As no cleavage site is predicted between the two domains, it appears that MltF is a bi-modular protein with two potential functions. Disruption of the *mltF* gene in *E. coli* had no obvious phenotype, although attempts to disrupt this gene in an *E. coli* strain lacking the six previously identified LTs were unsuccessful (Scheurwater and Clarke, 2008).

This suggests the essentiality and redundancy of LTs.

Preliminary studies found that MltF behaved uniquely among the LT family. The non-LT domain, devoid of both PG-binding capacity and lytic activity, was found to modulate the activity of the LT domain (Scheurwater and Clarke, 2008). Using the turbidometric assay of Hash (1967) which is based on the reduction in absorbance as insoluble PG is cleaved into soluble products, MltF was found to solubilize PG in a linear, time-dependent fashion, analogous to lysozyme. However, upon removal of the non-LT domain, the isolated C-terminal LT domain solubilized PG with an initial rapid burst of activity, followed by a slower gradual rate of activity, as seen with other LTs (Scheurwater and Clarke, 2008).

MltF shares the most identity with MltE (Blackburn and Clarke, 2001), the only proposed endo-acting LT (Kraft *et al.*, 1998). This suggests that MltF may also be an endo-acting enzyme, and the relatively low activity found by Scheurwater and Clarke (2008) would thus be a consequence of inappropriate assays. If MltF is indeed an endo-acting LT, the larger cleavage products would remain insoluble or unresolved by HPLC separation, as the products may remain cross-linked to each other. In order to obtain conclusive proof, a defined substrate is required.

1.8 Challenges when working with PG

One of the greatest challenges when working with PG arises from its inherent insolubility and heterogeneity. Some enzymes involved in PG metabolism can be studied relatively easily, particularly if they are active against substrates that are either commercially available or easily generated. An example of one such enzyme is lysozyme, which is active against commercially available disaccharides and oligosaccharides. Another example is NagZ, which hydrolyzes the glycosidic linkage in the disaccharide GlcNAc-anhydroMurNAc, with or without a stem peptide, a substrate which can be easily generated or acquired (Vötsch and Templin, 2000). On the other hand, several enzymes involved in PG metabolism are not active against such simple substrates, and these are the focus of this study.

Unlike lysozymes, lytic transglycosylases require the lactyl moiety of MurNAc for proper orientation in the active site cleft and for substrate-assisted catalysis, and as such are inactive against commercially available chitooligosaccharides ($GlcNAc_n$ oligomers) or their derivatives (Reid *et al.*, 2004c). While naturally occurring PG contains stem peptides, some of the LTs have been shown to degrade unsubstituted $(GlcNAc\text{-}MurNAc)_n$ oligosaccharides *in vitro*. Examples of such enzymes include MltA (Romeis *et al.*, 1993) and MltE (Kraft *et al.*, 1998), indicating that a homogeneous $(GlcNAc\text{-}MurNAc)_n$ substrate can be used to conduct biochemical tests on several of the LTs. An assay using this substrate could provide evidence for the substrate specificity of LTs, in particular whether they are exo- or endo-specific. This would also provide evidence for the function of LTs within the cell.

1.9 Research proposal

As pathogens continue to gain resistance to current antimicrobials, work on potential novel antibiotic targets is imperative. LTs appear to present a promising target as they are critical to bacterial cell function and reproduction. LTs act on a structure unique to bacteria which is important for cell viability. In contrast with other important antibiotics which target the metabolism of the stem peptide (*e.g.,* β-lactams and vancomycin), LTs act on the carbohydrate residues which are unique to and invariant in PG. The consistency of this structure suggests that evolution of resistance to inhibitors would be slow to develop. Understanding the functions and chemistry of the LTs is a fundamental step in developing antibiotic agents that target them.

Biochemical characterizations of key members from each of the four families of LTs have been carried out to varying degrees, the least studied of which is family 1B. Work done by Scheurwater and Clarke (2008) suggested the need for a defined, homogeneous substrate by isolation of glycan chains of defined size (see HPAEC-based assay in discussion). Thus, this study focuses on developing a method to generate a defined substrate for further characterization of MltF and other LTs. I propose that the use of various enzymes to degrade PG and fractionating of products using HPLC will lead to the generation of this substrate. This will be referred to as a 'top-down' approach to substrate generation, as opposed to the biosynthesis of a substrate, or 'bottom-up' approach.

To generate this defined substrate, isolated insoluble PG was exhaustively digested with the *N*-acetylmuramyl-L-alanine amidase to remove all stem peptides, generating a collection of muroglycans. The *N*-acetylmuramyl-L-alanine amidase B (AmiB) from *P. aeruginosa* was used because this enzyme accepts the intact high molecular weight PG sacculus as a substrate, unlike the amidase present in *E. coli* (Parquet *et al.*, 1983; Scheurwater *et al.*, 2007). Since the degree of polymerization of the glycan strands can be very long (Glauner *et al.*, 1988; Harz *et al.*, 1990), the muroglycans were partially digested with commercially available hen egg-white lysozyme (HEWL), an endo-acting glycosidase, under controlled conditions to limit the extent of digestion. The shorter, soluble fragments (~6–8 disaccharide units long) were then collected by HPLC and identified by MALDI-TOF mass spectrometry.

Chapter 2

Materials and Methods

2.1 Chemical reagents

DNase I, RNase A, Pronase, IPTG, and EDTA-free protease inhibitor tablets were purchased from Roche Diagnostics (Laval, QC). Molecular biology kits and nickel-nitrilotriacetic acid (Ni-NTA) agarose were purchased from Qiagen (Mississauga, ON), while carbohydrate standards were purchased from Toronto Research Chemicals (North York, ON). Resins for ion-exchange chromatography were purchased from GE Healthcare (Baie-d'Urfé, QC) and unless otherwise stated, all other chemical reagents were purchased from Sigma-Aldrich (Oakville, ON) or Fisher Scientific (Ottawa, ON). Reagent concentrations expressed as percentages are weight per volume unless otherwise noted.

2.2 Strains, plasmids, and culture conditions

The bacterial strains and plasmids used in this study are listed in Table 2.1. Cultures were routinely

Table 2.1: Bacterial strains and plasmids used in this study.

Strain or plasmid	Genotype or relevant characteristic	Reference or source
Strains		
E. coli BL21(DE3)pLysS	F^- *ompT hsdS*$_B$ (r_B^-, m_B^-) *gal dcm* (DE3) pLysS (Cam^R)	Novagen
E. coli DH5α	F^- φ80*lac*ZΔM15 Δ(*lac*ZYA–*arg*F)U169 *rec*A1 *end*A1 *hsd*R17(r_k^-, m_k^+) *pho*A *sup*E44 *thi*–1 *gyr*A96 *rel*A1 λ^-	Invitrogen
M. luteus ATCC 4698	Type strain; freeze-dried	Sigma-Aldrich
P. aeruginosa PAO1	A^+B^+; serotype O5	Hancock and Carey (1979)
Plasmids		
pET-30a(+)	IPTG-inducible expression vector; Kan^R	Novagen
pACJP-2	pET-30a(+) derivative containing truncated *P. aeruginosa amiB* encoding AmiB lacking its N-terminal 27 amino acids; C-terminal His_6-tag; Kan^R	Scheurwater *et al.* (2007)

grown in Luria-Bertani (LB) broth (Appendix A) at 37 °C with agitation. For protein expression, cells were grown in Super Broth (Appendix A) at 37 °C with agitation. For cells harbouring the pLysS plasmid, the medium was supplemented with 34 μg/mL chloramphenicol (Cam). For cells harbouring pET-30a(+) or its derivative pACJP-2, the medium was supplemented with 50 μg/mL kanamycin (Kan). *Escherichia coli* DH5α was used for all plasmid preparation while *E. coli* BL21(DE3)pLysS was used for all gene expressions. All strains were maintained by storage at -80 °C in 25% glycerol. Bacterial media and solutions are listed in Appendix A.

2.3 Preparation of PG

2.3.1 PG isolation

Insoluble PG was isolated from *P. aeruginosa* PAO1 and *M. luteus* ATCC 4698 lyophilized cells (Sigma-Aldrich). Overnight cultures of *P. aeruginosa* were used to inoculate large cultures which were grown in LB for 3–4 h at 37 °C with agitation. Cells were harvested at mid-exponential phase (OD_{600}~0.6) by centrifugation (5000 × *g*, 15 min, 4 °C) and frozen until required. For large-scale preparations of PG, pellets from 18 L of *P. aeruginosa* culture or 4 g lyophilized *M. luteus* cells were used.

PG was isolated using a modification of the boiling SDS procedure and subsequent purification by enzyme treatment described by Höltje *et al.* (1975). Cells resuspended in 200 mL of Milli-Q water were added slowly to an equal volume of a boiling solution of 8% SDS (4% SDS final concentration) under reflux with vigorous stirring. The mixture was kept boiling for 3 h, then allowed to cool overnight. This step solubilizes all components of the cell, while PG (and anything tightly attached) remains insoluble. The PG was recovered by ultracentrifugation (41,000 × *g*, 1 h, 25 °C). Remaining SDS was removed by washing the PG at least three times[1] with Milli-Q water (41,000 × *g*, 1 h, 25 °C). PG sacculi were resuspended in a small volume of Milli-Q water and sonicated for 2 min (10 s on, 10 s off) prior to freezing and lyophilization. Lyophilized PG was stored at -20 °C.

2.3.2 PG purification

Purification of crude PG was accomplished by a modification of the methods of Höltje *et al.* (1975) and Hoyle and Beveridge (1984). Isolated sacculi were resuspended in a minimal volume of 10 mM Tris-HCl buffer, pH 7.4, containing 20 mM $MgSO_4$, and sonicated for 2 min (10 s on, 10 s off). The suspension was incubated for 2 h at room temperature in the presence of α-amylase (100 μg/mL), DNase I (10 μg/mL), and RNase A (50 μg/mL). These enzymes served to degrade high molecular weight glycogen (Leutgeb and Weidel, 1963), DNA, and RNA trapped inside the sacculi, respectively. Following this digestion, pronase was added (200 μg/mL, incubated 1 h at 60 °C), releasing covalently bound lipoprotein (Braun, 1975). The pronase stock solution had been incubated (2 h at 60 °C) prior to its addition to the sacculi suspension in order to inactivate possible contamination by lysozyme

[1] Pellets were stored at room temperature if left overnight.

(Harz *et al.*, 1990). Once again, the sample was treated with boiling SDS (4% final concentration) for 15 min. After cooling, sacculi were recovered by ultracentrifugation (41,000 × *g*, 1 h, 25 °C).

O-Acetylation is a common modification to the glycan strand in both Gram-positive and Gram-negative bacteria (reviewed in Clarke and Dupont, 1992; Clarke *et al.*, 2002), and is known to interfere with the lytic activity of enzymes including lysozyme and lytic transglycosylases (Blackburn and Clarke, 2002). In order to remove *O*-acetyl groups, purified PG was subjected to mild alkaline hydrolysis by incubation in 20 mM NaOH overnight at room temperature (Dupont and Clarke, 1991). Sacculi were washed at least three times in Milli-Q water, frozen, lyophilized, and stored at -20 °C as described above.

In the case of PG isolated from Gram-positive organisms, teichoic acids were removed by treatment with trichloroacetic acid (TCA) using the methods of Hash (1967) as modified by Amako *et al.* (1982). PG was extracted with 5% TCA at 4 °C for 45 h and then with 10% TCA at 90 °C for 10 min. Once cool, the PG was washed four times in Milli-Q water, frozen, lyophilized, and stored at -20 °C as described above.

2.4 DNA techniques

2.4.1 General DNA techniques

The QIAprep Spin Miniprep Kit from Qiagen (Mississauga, ON) was used to isolate plasmid DNA from 5 mL overnight cultures according to the manufacturer's protocol. Plasmid sequencing was performed by Laboratory Services Division of the University of Guelph (Guelph, ON). Plasmid DNA was stored at -20 °C until required. Agarose gel electrophoresis was performed using gels prepared to a final concentration of 0.8% agarose in TAE buffer (Appendix A). Samples were mixed with DNA loading buffer (Appendix A) and loaded into the wells. Electrophoresis was carried out at 100 V for 1 h. Visualization of DNA was accomplished by staining the gel in SYBR Safe DNA gel stain (Invitrogen) and exposure to ultraviolet light.

2.4.2 Preparation of competent cells

Chemically competent cells of *E. coli* DH5α and *E. coli* BL21(DE3)pLysS were prepared by a variation of the method of Cohen *et al.* (1972). Cells were grown overnight in 5 mL of LB broth (supplemented as necessary). The cells were then subcultured into 100 mL of LB (supplemented as necessary) and grown to mid-exponential phase, reaching an OD_{600} of approximately 0.5. At this point, the cells were chilled on ice and harvested by centrifugation (7,000 × *g*, 10 min, 4 °C). Cells were resuspended in 50 mL of cold, filter-sterilized α-solution (30 mM potassium acetate, 100 mM KCl, 10 mM $CaCl_2$, 50 mM $MnCl_2$, 15% (v/v) glycerol, pH 5.8). The cells were again harvested by centrifugation and resuspended in 10 mL of cold, filter-sterilized β-solution (10 mM 3-(*N*-morpholino)propanesulfonic acid (MOPS), 75 mM $CaCl_2$, 10 mM KCl, 15% (v/v) glycerol, pH 6.5) and left on ice for 2–3 h. Cells were divided into 200 µL aliquots and frozen immediately at -80 °C for storage.

2.4.3 Competent cell transformations

A heat-shock transformation procedure was used to transform DNA into chemically competent cells. A 200 µL aliquot of competent cells was thawed on ice for 10 min prior to the addition of 1 µL of plasmid DNA. The cells were then incubated on ice for 30 min, heat shocked at 37 °C for 3 min, and incubated on ice for another 10 min. To allow cells to recover and develop resistance, 500 µL of LB was added and the cells were incubated at 37 °C for 1 h. Cells were collected by centrifugation (13,000 × *g*, 5 min), resuspended in sterile water, and plated on LB agar containing the appropriate antibiotic(s). Plates were incubated at 37 °C overnight. A colony was streaked out on LB agar (containing the appropriate antibiotics) and incubated at 37 °C overnight. An isolated colony was used to inoculate 5 mL LB (containing the appropriate antibiotics) and incubated at 37 °C overnight. Glycerol stocks were made by combining 500 µL of culture with 500 µL of sterile 50% glycerol and frozen immediately at -80 °C. The remainder of the culture was used to prepare plasmid DNA.

2.5 Protein production and purification

The construct pACJP-2 was used for protein production (Scheurwater *et al*., 2007) (Table 2.1). This plasmid encodes *P. aeruginosa amiB* lacking its N-terminal 27 amino acids, and contains a C-terminal His_6-tag to facilitate purification. This protein was chosen for several reasons: it remains soluble within the cytoplasm, it has previously been expressed and purified (Scheurwater *et al*., 2007), and it accepts the intact high molecular weight PG sacculus as a substrate, unlike the *E. coli* homolog (Parquet *et al*., 1983). This truncated AmiB will be referred to herein as tAmiB.

2.5.1 Culture growth for preparative purification

Glycerol stocks of *E. coli* BL21(DE3)pLysS cells harbouring the pACJP-2 plasmid were used to inoculate 50 mL LB containing 50 µg/mL Kan and 34 µg/mL Cam and incubated at 37 °C overnight. Fifteen mL of overnight culture was used to inoculate 1 L of prewarmed Super Broth (containing 50 µg/mL Kan, 34 µg/mL Cam). The culture was incubated at 37 °C until the OD_{600} was 0.5 to 0.6. A 1 mL sample was taken immediately before induction; cell pellet was resuspended in 30 µL H_2O containing 10 µL 4X DualColor™ protein loading buffer (Fermentas, Burlington, ON; Appendix A) and frozen. Protein expression was induced by adding isopropyl β-D-1-thiogalactopyranoside (IPTG) to a final concentration of 1 mM and the culture was incubated for an additional 4 h. A second 1 mL sample was collected; cell pellet was resuspended in 60 µL H_2O containing 20 µL 4X DualColor™ protein loading buffer and frozen. Cells were harvested by centrifugation (4000 × *g*, 20 min, 4 °C) and stored at -20 °C for 1 to 3 nights.

2.5.2 Preparation of cleared cell lysates

All protein purifications in this study were performed under native conditions. Cell pellets were thawed on ice and resuspended in 20 mL lysis buffer (Table 2.2) per litre original culture. The cells

Table 2.2: IMAC buffers for purification under native conditions (Appendix A).

Buffer	NaH_2PO_4 (mM)	NaCl (mM)	Imidazole (mM)	Triton X-100 (%)	pH
Lysis	50	300	10	0.1	8.0
Wash	50	300	20	0.1	8.0
Elution	50	300	250	0.1	8.0

were then treated with three Complete, Mini, EDTA-free protease inhibitor cocktail tablets, RNase A (10 µg/mL), DNase I (5 µg/mL), and lysozyme (1 mg/mL) and incubated on ice for 30 min. Cells were then sonicated on ice for 3 min (10 s on, 10 s off) using a Sonics & Materials Vibra-Cell VCX130 ultrasonic processor equipped with a 6 mm microtip. Insoluble cellular debris and remaining intact cells were removed by centrifugation (10,000 × *g*, 30 min, 4 °C). The lysate was syringe-filtered with a 0.2 µm filter. A 30 µL sample was taken and added to 10 µL 4X DualColor™ protein loading buffer and frozen.

2.5.3 Immobilized metal ion affinity chromatography (IMAC)

tAmiB was recovered from the clarified lysate using Ni-NTA metal-affinity chromatography (Qiagen), exploiting the His_6-tag on the overproduced recombinant enzyme. To the clarified lysate, 1 mL of 50% Ni-NTA agarose resin slurry (Qiagen) was added per litre original culture volume and mixed gently at 4 °C for 1 h. The following steps were performed at 4 °C. The lysate-Ni-NTA mixture was loaded into a disposable column and the flow-through was collected. The column was then washed twice with 20 mL lysis buffer and twice with 20 mL wash buffer (Table 2.2). Fractions were collected for sodium dodecyl sulfate polyacrylamide gel electrophoresis (SDS-PAGE) analysis. Protein was eluted in 4 × 2.5 mL elution buffer after each volume was allowed to remain in the column for 1–2 min prior to collecting. Recovered protein fractions were combined and dialyzed three times against 1 L of 50 mM sodium phosphate buffer, pH 7.0, containing 0.1% Triton X-100 at 4 °C.

2.5.4 Cation-exchange chromatography

As the predicted pI of tAmiB is 9.71, the partially purified tAmiB was further purified by cation-exchange chromatography on SOURCE 15S (GE Healthcare), a resin with a methyl sulfonate strong cation exchange group. Protein in dialysis buffer was applied to a 4.6 mm × 100 mm column equilibrated in 50 mM sodium phosphate buffer, pH 7.0, at a flow rate of 0.7 mL/min at room temperature using a Dionex BioLC® HPLC system (Dionex, Sunnyvale, CA). The amidase was eluted from the column by increasing the ionic strength of the buffer using a linear gradient of 0–1 M NaCl (in starting buffer) over 40 min. Collected fractions were analyzed by SDS-PAGE with the most pure protein being pooled and dialyzed three times against 1 L of 50 mM sodium phosphate buffer, pH 7.0, containing 0.1% Triton X-100 at 4 °C. Purified protein preparations were stored at 4 °C until required.

2.6 Protein analyses

2.6.1 SDS-PAGE

Two SDS-PAGE gels were run concurrently; one for staining with Coomassie Brilliant Blue (PageBlue™), the other for Western blot and immunodetection. SDS-PAGE analyses were performed according to the method of Laemmli (1970) using 12% acrylamide separating gels and 4% acrylamide stacking gels (Appendix A). Samples (30 µL) mixed with 10 µL of 4X DualColor™ protein loading buffer were heated for 10 min at 95 °C and insoluble material was removed by centrifugation (15,000 × *g*, 1 min) prior to loading. Samples were loaded and subjected to electrophoresis at 150 V in electrophoresis buffer (25 mM Tris, 192 mM glycine, 0.1% SDS, pH 8.3) for 60–80 min. Gels were stained using PageBlue™ Protein Staining Solution (Fermentas) according to the manufacturer's microwave protocol. The PageRuler™ prestained protein ladder (Fermentas) containing proteins ranging from 10 to 170 kDa was used for molecular mass markers.

2.6.2 Western blot and immunodetection

To generate a Western blot, proteins in the polyacrylamide gel were transferred to a nitrocellulose membrane in a tank-blotting apparatus (Mini Trans-Blot electrophoretic transfer cell, Bio-Rad) in transfer buffer (10 mM $NaHCO_3$, 3 mM Na_2CO_3, 20% methanol, pH 9.9) for 1 h at 50 V at 4 °C with stirring. Immunodetection was performed according to the procedure of Burnette (1981) using an anti-His probe (H-3), a mouse anti-His monoclonal IgG antibody (Santa Cruz Biotechnology, Santa Cruz, CA) for detection of the His_6-tagged proteins, followed by goat anti-mouse IgG-alkaline phosphatase (AP) conjugate (Bio-Rad) secondary antibody. The 1-Step NBT/BCIP substrate from Pierce Biotechnology (Rockford, IL) was used as the staining solution for AP. Solution components are listed in Appendix A and the protocol in Appendix B.

2.6.3 Protein quantification

Protein concentrations were determined using a bicinchoninic acid (BCA) protein assay kit (Pierce Biotechnology, Rockford, IL). Bovine serum albumin (BSA) ranging from 0–1 mg/mL (in water) was used as a standard. For each standard and unknown sample[2], 25 µL was added into a 96-well microplate in triplicate. To each well, 200 µL of working reagent (50:1, BCA:cupric sulfate) was added, mixed, and the plate was incubated at 37 °C covered for 30 min. The absorbance was measured using a FLUOstar Optima plate reader (BMG LABTECH, Germany) at 560 nm. A standard curve was prepared by plotting the average blank-corrected 560 nm measurement for each BSA standard versus its concentration in µg/mL. The standard curve was used to determine the protein concentration of unknown samples.

[2] When the protein concentration of a sample was greater than 1 mg/mL, a 1:10 dilution was used.

2.7 Enzyme activity assays

Three assays were used to confirm the catalytic activity of purified tAmiB *in vitro*: zymography, turbidometry, and detection of released free amines by the DNFB (Sanger's reagent) assay.

2.7.1 Zymography

Zymographic analyses were performed as described (Bernadsky *et al*., 1994; Watt and Clarke, 1994). In this assay, PG is incorporated into SDS-PAGE gels and run normally. Following renaturation of separated proteins, clear zones in a background of PG indicate the solubilization of PG, and hence autolytic activity.

Purified PG was incorporated into a 12% polyacrylamide separating gel to a final concentration of 0.1%. To cast the gels, PG was thoroughly sonicated in the appropriate volume of water and buffer (Appendix A), and gels were run as normal (SDS-PAGE as described above) at 25 mA for 1.5–2 h. Gels were rinsed and then soaked first in water for 15–30 min, followed by three times in renaturation solution (25 mM sodium phosphate, 10 mM $MgCl_2$, 0.1% Triton X-100, pH 7.0). Gels were left in renaturation solution overnight, and then rinsed with water and stained with 0.1% Methylene Blue in 0.01% KOH for 1–2 h. Gels were destained with repeated changes of water until zones of clearing were visible. Lysozyme (10–20 µg) was used as a positive control.

2.7.2 Turbidometry

The turbidometric assay of Hash (1967) is based on the solubilization of PG by autolytic enzymes, monitored by the reduction in turbidity. This assay was used to determine the activity of both tAmiB and lysozyme. Whole cells of *M. luteus* were sonicated briefly in 50 mM sodium phosphate buffer, pH 7.0. Purified tAmiB (0–150 µg/mL final concentration) was added to samples in a 1 mL cuvette at room temperature and the decrease in OD at 600 nm was monitored using a Beckman Coulter DU 530 Life Science UV/Vis Spectrophotometer with a Multicell Module (Beckman Coulter, CA). Depicted are representative curves.

2.7.3 Free amino group assay

The hydrolysis of stem peptides from PG generates free amino groups. The generation of free amino groups was determined with the method of Ghuysen *et al*. (1966), using sodium borate ($Na_2B_4O_7$) instead of potassium borate ($K_2B_4O_7$) due to availability. This assay uses 1-fluoro-2,4-dinitrobenzene (DNFB; Sanger's reagent) which reacts with the amine group in amino acids to produce dinitrophenyl-amino acids (Sanger, 1945), which are bright yellow and can be detected at 420 nm.

This assay was used to determine the release of free amino groups from tAmiB-digested PG. Soluble fractions recovered from digestions following centrifugation (13,000 × *g*, 10 min) and standards (40 µL of each) were dried down and resuspended in 40 µL $Na_2B_4O_7$. To each, 4 µL of 1.3% DNFB (in ethanol) was added and incubated at 60 °C for 30 min in the dark. Samples were acidified with 160 µL of 2 N HCl, transferred to a 96-well microplate, and the absorbance was measured using a

FLUOstar Optima plate reader (BMG LABTECH, Germany) at 420 nm. L-Alanine (0–0.25 mg/mL) was used to generate a standard curve.

2.8 Generation of oligoglycans from purified PG

2.8.1 Removal of stem peptides

Glycan strands were freed of stem peptides using a modification of the methods of Harz *et al*. (1990). Enzymatically purified PG from either *P. aeruginosa* PAO1 or *M. luteus* was treated with purified *P. aeruginosa* tAmiB (purified as described above). This enzyme is an *N*-acetylmuramoyl-L-alanine amidase (EC 3.5.1.28), which catalyzes the hydrolysis of the link between MurNAc residues and L-amino acid residues in the PG sacculus. Digestion conditions typically consisted of 250 µg/mL PG, 150 µg/mL tAmiB in buffer (50 mM sodium phosphate, pH 7.0), overnight at 37 °C on a nutator. To ensure complete hydrolysis of all amide bonds, the sample was incubated a second time for several hours with another portion of amidase. Samples were stored at -20 °C until required.

2.8.2 Partial digestion of glycan strands

Because the average degree of polymerization of glycans can be very long (Glauner *et al*., 1988; Harz *et al*., 1990), the glycan strands were treated with hen egg-white lysozyme (HEWL; EC 3.2.1.17; Sigma-Aldrich) under controlled conditions to limit the extent of digestion. The activity of lysozyme was determined using the turbidometric assay (as above with amidase) using whole cells of *M. luteus* as substrate. A series of digestions with increasing concentrations of HEWL were used to determine optimal conditions to generate glycan strands of an ideal length. Lysozyme was added to amidase-digested PG (already in 50 mM sodium phosphate, pH 7.0) at final concentrations of 0, 0.01 µg/mL, 0.1 µg/mL, and 1.0 µg/mL. The reactions were incubated at room temperature for 1 h. To quench reactions and denature proteins, samples were adjusted to pH~4.0 with 20% phosphoric acid, and heated in a boiling water bath for 3 min. Insoluble material was removed by centrifugation (13,000 × *g*, 10 min), and the supernatant was filtered with a 0.22 µm filter.

2.8.3 Isolation of soluble glycans

Remaining proteins or peptides were removed by cation-exchange chromatography on SOURCE 15S. Amidase-digested samples adjusted to pH 2.0 with 20% phosphoric acid were applied to a 4.6 mm × 100 mm column equilibrated with 10 mM sodium phosphate, pH 2.0, at a flow rate of 0.7 mL/min at room temperature. At this pH, glycans have a neutral charge while the free peptides have a positive charge. Therefore, glycans elute immediately while peptides are retained on the column. Following collection of the flow-through, proteins were washed off the column with 1 M NaCl in starting buffer. Purified glycans were concentrated and stored at -20 °C.

2.8.4 HPAEC-PAD separation of glycans

Isolated glycans were then separated using high-performance anion-exchange chromatography with pulsed amperometric detection (HPAEC-PAD). This system allows separation and detection of sugars at high pH without the need for derivatization. At high pH, the hydroxyl groups of carbohydrates are transformed into oxyanions enabling their separation as anions. Separations of oligomuroglycans are based on structural features – in this case size – due to the increasing anionic nature of the increasing number of hydroxyl residues associated with the oligomers of higher mass. The separated carbohydrates are detected with PAD and the signal is reported in coulombs (C). Amperometric detection is used to measure the current or charge resulting from oxidation or reduction of analyte molecules at the surface of an electrode. During oxidation reactions, electrons are transferred from electroactive analytes (carbohydrates) to the electrode in the amperometry cell.

The HPAEC equipment consisted of a Dionex GS50 pump, Dionex AS50 sampler, and Dionex ED50A electrochemical detector (Dionex, Sunnyvale, CA) operating with the carbohydrate waveform. The isolated glycans were applied to a CarboPac PA-100 column equilibrated with 100 mM NaOH. The AS50 sampler was programmed to inject 20 µL of sample, unless otherwise stated. Resolution was achieved by application of a linear salt gradient from 0–500 mM sodium acetate in 100 mM NaOH. Individual species of glycans were identified based on their retention time and by matrix-assisted laser desorption/ionization time-of-flight mass spectrometry (MALDI-TOF MS) analysis.

2.8.5 MALDI-TOF mass spectrometry

MALDI-TOF mass spectrometry was used to determine the identities of separated digestion products. As the fractions collected from HPAEC had a very high concentration of NaOH, their pH was adjusted with 6 N HCl to form NaCl and water. Once the pH was below 4.0, samples were dried *in vacuo*, resuspended in 0.1% TFA, and desalted using ZipTip® pipette tips with C_{18} resin (Millipore) according to the manufacturer's protocol.

The matrix chosen for MALDI-TOF analyses was 5-chloro-2-mercaptobenzothiazole (CMBT) as it has been shown to be a practical matrix for analysis of oligosaccharides (Xu *et al.*, 1997). Ten mg of CMBT was dissolved in 1 mL ethanol and 3 mL HPLC grade water was added. CMBT was collected by centrifugation (5,000 × *g*, 10 min, room temperature). The pellet was washed three times with 1 mL of HPLC grade water and the recrystallized matrix was dried *in vacuo*. To reconstitute the matrix, 3 mg of recrystallized CMBT was dissolved in 100 µL acetonitrile.

An on-plate crystallization method using CMBT was developed. Deionized samples (1 µL) were spotted onto a MALDI plate, and an equal volume of CMBT matrix in solution was added. This method replaces in-tube sample preparation because CMBT precipitates very quickly in the presence of aqueous solvent, thus precluding co-crystallization with the analyte. The sample/matrix mixtures were allowed to air-dry, and were analyzed in a Bruker Reflex III (Bruker Daltonik, Germany) equipped with a 337 nm nitrogen laser (Mass Spectrometry Facility, Advanced Analysis Centre, University of Guelph). Samples were analyzed in reflectron and positive ion modes scanning from 0–5000 m/z using ion suppression up to 150 m/z. For all experiments, the ion sources 1 and 2 were

held at 20 kV and 16.35 kV, respectively, and the guiding lens voltage at 9.75 kV. The reflector detection gain was set up at 5.3 with pulsed ion extraction at 200 ns. The nitrogen laser power was set to the minimal level necessary to generate a reasonable signal and to avoid degradation of analytes. Typically 5% of laser energy was used, which is equal to ~2 mJ per laser shot. A four point external calibration was performed using standard compounds ranging from 155 to 2500 m/z. The mass accuracy with this external calibration is estimated to be below 10 ppm. External glycan standards were also submitted, including chitotetraose, chitopentaose, and chitohexaose (each GlcNAc oligomer at 100 µM), which were analyzed the same day as the samples. Spectra were acquired from an average of at least 30 shots.

2.9 HPLC Performance

All columns were operated with a guard column. Ultrapure water was generated on a Milli-Q (Millipore) water purification system. Buffers were prepared using HPLC-grade reagents, filtered using 0.2 µm filters, degassed prior to HPLC for 10–15 min with helium, and stored at 4 °C.

2.10 *In silico* analyses

DNA and amino acid sequences were analyzed using A Plasmid Editor (ApE)[3]. Multiple sequence alignments were generated with ClustalW2 (Chenna *et al.*, 2003). Signal peptides and cleavage sites were predicted using SignalP 3.0 (Nielsen *et al.*, 1997; Bendtsen *et al.*, 2004). Protein molecular mass and pI values were calculated using ProtParam (Wilkins *et al.*, 1999). Mass spectrometric data were analyzed using mMass (Strohalm *et al.*, 2008, 2010). Unless otherwise stated, all tools were used with their default values.

[3] `http://biologylabs.utah.edu/jorgensen/wayned/ape/`

Chapter 3

Results

3.1 Preparation of PG

Four g lyophilized *M. luteus* cells yielded 1.63 g of PG following isolation and purification. The yield following TCA treatment to remove teichoic acids was 1.21 g. PG prepared from 18 L of the Gram-negative bacterium *P. aeruginosa* PAO1 culture yielded 40.6 mg following isolation and purification.

3.2 Plasmid DNA

Initially, the truncated *amiB* construct pACJP-2 was transformed into *E. coli* DH5α to make a plasmid stock (Table 2.1). The DNA sequence was confirmed to contain an open reading frame encoding a polypeptide with the N-terminal truncation and C-terminal His_6-tag (Figure 3.1). This polypeptide consisted of 456 amino acids with a theoretical molecular mass of 48,913 and a pI value of 9.71. The N-terminal truncation is necessary for the majority of the protein produced to remain in the cytoplasm where it cannot act on PG which would result in autolysis (Scheurwater *et al.*, 2007). Unlike the *E. coli* homolog, *P. aeruginosa* AmiB contains a lysin motif domain at its C-terminus (NCBI Conserved Domains Database). This domain is found in a variety of enzymes involved in bacterial cell wall degradation, and may serve to facilitate binding with PG (Joris *et al.*, 1992; Bateman and Bycroft, 2000).

3.3 Production and purification of tAmiB

In order to use *P. aeruginosa* tAmiB on a preparative scale, we must be able to produce large amounts of active protein. A number of conditions were adjusted to optimize yield and solubility, including those involved in expression, purification, digestion, and storage.

3.3.1 IMAC using a pH gradient

The pACJP-2 construct was transformed into *E. coli* BL21(DE3)pLysS for preparative purification. Cells were grown to mid-exponential phase and expression of truncated *amiB* was induced for 4 h

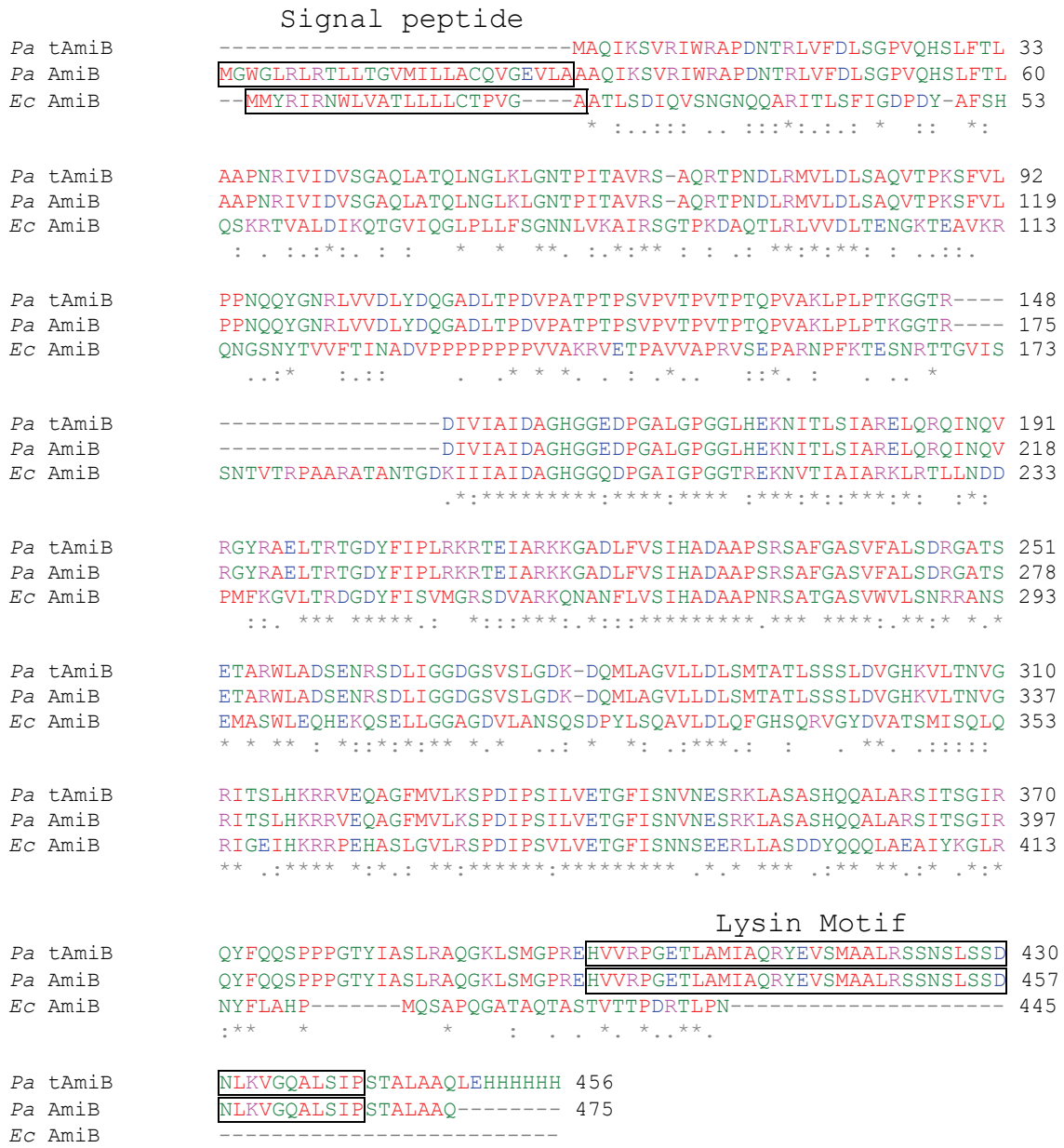

Figure 3.1: Amino acid sequence alignment between *P. aeruginosa* AmiB and *E. coli* AmiB. The upper boxes indicate signal peptides predicted using SignalP 3.0. The signal peptide is absent in the truncated, recombinant protein (tAmiB), encoded by pACJP-2. The lower boxes indicate a lysin motif at the C-terminus of the *P. aeruginosa* protein. The alignment was generated with ClustalW2; "*" indicates identical residues in all sequences, ":" indicates conserved substitutions, and "." indicates semi-conserved substitutions. Colours indicate the physiochemical characteristics of amino acids: red, small/hydrophobic; blue, acidic; magenta, basic; green, hydroxyl/sulfhydryl/amine/G. Adapted from Scheurwater *et al.* (2007).

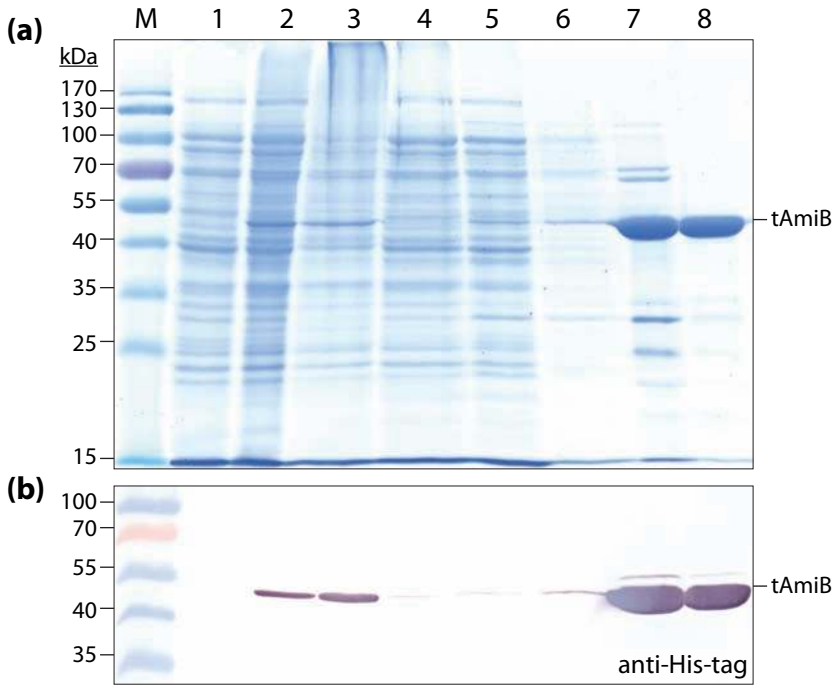

Figure 3.2: Production and purification of recombinant *P. aeruginosa* tAmiB. SDS-PAGE gels were run in duplicate; one for staining with (a) Coomassie Brilliant Blue (PageBlue™), the other for (b) Western blot and immunodetection with an anti-His antibody. M indicates the PageRuler™ prestained protein ladder. Lanes 1 and 2 contain pre- (0 h) and post-induced (4 h) samples, respectively. Lane 3 contains cell lysate. Lane 4 contains IMAC flow-through. Lanes 5 and 6 contain IMAC washes, and lane 7 is the fraction eluted with 250 mM imidazole. Eluted tAmiB was further purified by cation-exchange chromatography on SOURCE 15S (lane 8).

with 1 mM IPTG. Many attempts were made to purify the protein using the pH gradient established by Scheurwater *et al.* (2007). These attempts resulted in low yield and poor enzyme solubility. Briefly, the lysate-Ni-NTA mixture (in 50 mM sodium phosphate buffer, pH 8.0) was loaded into a disposable column, washed with a series of buffers of descending pH, and eluted at pH 4.5.

Although the solubility of tAmiB increased under suitable buffer conditions (see below), the yield from IMAC purification using a pH gradient remained very low (~0.1 mg per litre original culture). This was likely due to the instability of tAmiB in the elution buffer (pH 4.5). Since this low pH is unavoidable when using a pH gradient, an alternative approach to purification was investigated.

3.3.2 IMAC using an imidazole gradient

An IMAC purification method using increasing concentrations of imidazole (rather than a pH gradient) was established. Briefly, the lysate-Ni-NTA mixture was loaded into a disposable column, washed with a buffer containing 20 mM imidazole, and eluted in a buffer containing 250 mM imidazole. The initial buffer contained 10 mM imidazole to minimize non-specific binding of untagged, contaminating proteins. Production and purification of the recombinant protein was confirmed by SDS-PAGE and Western immunoblot analysis using anti-His antibodies (Figure 3.2, lanes 1–7). Whereas the re-

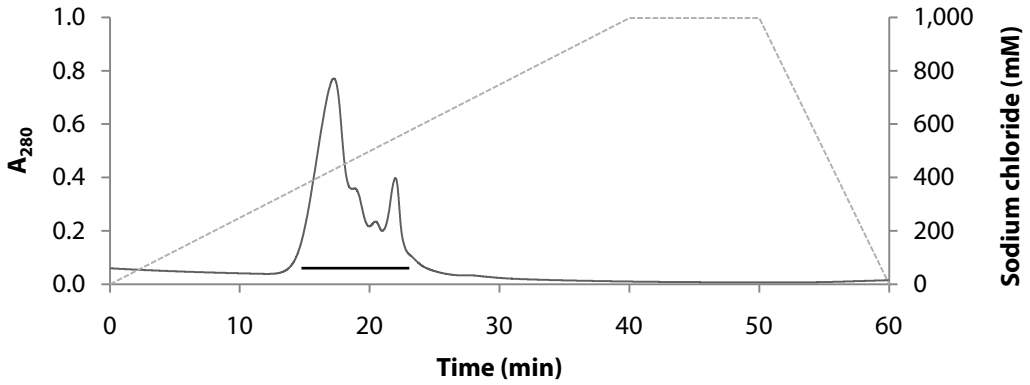

Figure 3.3: Cation-exchange chromatography for the purification of recombinant *P. aeruginosa* tAmiB. tAmiB eluted in a broad peak beginning at 15 min in approximately 300 mM NaCl. The solid line indicates the absorbance at 280 nm, while the dotted line indicates the concentration of sodium chloride (mM). The horizontal bar denotes the fraction of purified tAmiB collected and analyzed by SDS-PAGE (lane 8 in Figure 3.2).

covery of tAmiB was improved by this protocol, the protein was not sufficiently pure since other proteins were co-purified by this procedure (lane 7), and thus required further purification by ion-exchange chromatography.

3.3.3 Cation-exchange chromatography

The predicted pI value of tAmiB is high (9.71), therefore further purification was achieved by cation-exchange chromatography on SOURCE 15S (Figure 3.3). The protein was retained on the resin at pH 7.0, and was eluted by a linear gradient from 0 to 1 M NaCl. tAmiB eluted at ~300 mM NaCl. Peak fractions were collected separately for SDS-PAGE analysis. Fractions collected between 15–24 min appeared to contain tAmiB of equivalent purity (data not shown), and were pooled. This step led to improved purity following IMAC (Figure 3.2, lane 8). While enzyme purity from this method was equivalent to that reported previously (Scheurwater *et al.*, 2007), yields were approximately 5× greater at ~5 mg per litre original culture. Batch purifications were routinely made from 2 L culture.

3.4 Activity of tAmiB

To confirm the catalytic activity of tAmiB *in vitro*, three assays were used: zymography, turbidometry, and detection of released free amines by the DNFB (Sanger's reagent) assay.

3.4.1 Zymography

Purified tAmiB produced a zone of clearing in the zymogram with an apparent molecular mass of ~50 kDa (Figure 3.4), corresponding to the protein detected by Western immunoblot using anti-His antibodies (Figure 3.2b). This indicated that tAmiB was active on purified insoluble *M. luteus* PG (chemotype A2) and therefore functions as an autolysin.

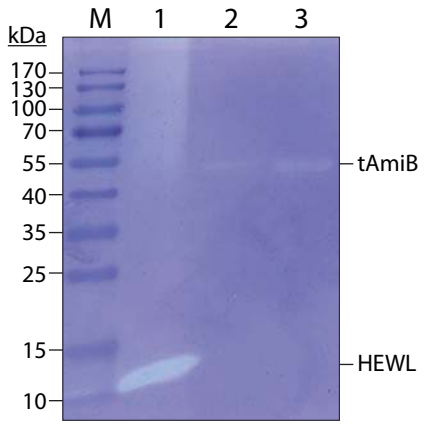

Figure 3.4: Zymogram analysis of tAmiB using 0.1% *M. luteus* PG as substrate. SDS-PAGE was run at 40 mA for 80 min, renatured, and stained with Methylene Blue in KOH. Clear zones indicate the solubilization of PG by 42 µg hen egg-white lysozyme (lane 1, positive control), 1.23 µg tAmiB (lane 2), and 4.91 µg tAmiB (lane 3). M, PageRuler™ prestained protein ladder.

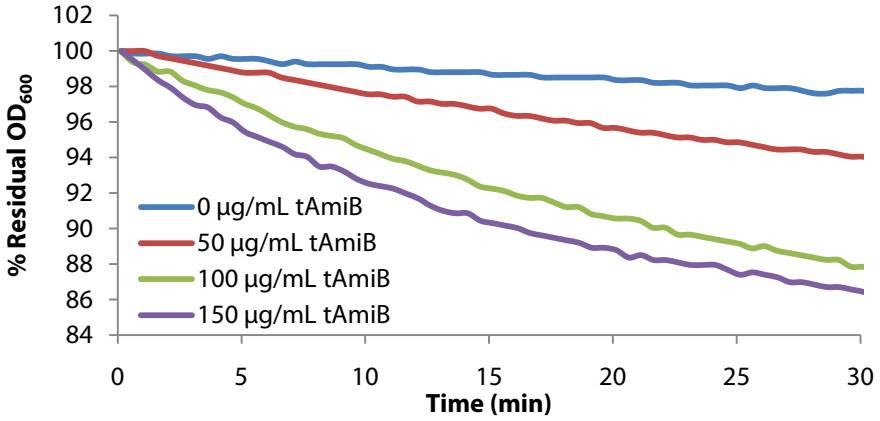

Figure 3.5: Turbidometric analysis of tAmiB using whole cells of *M. luteus* as substrate. Cells were incubated in the presence of tAmiB at 0 µg/mL (blue, control for settling), 50 µg/mL (red), 100 µg/mL (green), and 150 µg/mL (purple). The decrease in turbidity at 600 nm was monitored for 30 min.

3.4.2 Turbidometry

The time-dependent solubilization of PG by tAmiB was determined using the turbidometric assay of Hash (1967). For this assay, whole cells of *M. luteus* were used as a substrate. Cells suspended in 50 mM sodium phosphate buffer, pH 7.0, were incubated in the presence of 0–150 µg/mL tAmiB. Solubilization was monitored by the decrease in turbidity at OD_{600} (Figure 3.5). Under these conditions, the rate of solubilization for the purified enzyme was 37.6 $\Delta OD_{600} \cdot min^{-1} \cdot$ mg protein^{-1}, which was 8.5× that reported previously (Scheurwater *et al.*, 2007).

3.4.3 Free amino group assay

Attempts were made to detect stem peptides liberated by tAmiB. Digestion conditions were 250 µg/mL PG, 150 µg/mL tAmiB in buffer (50 mM sodium phosphate, pH 7.0), overnight at 37 °C on a nutator,

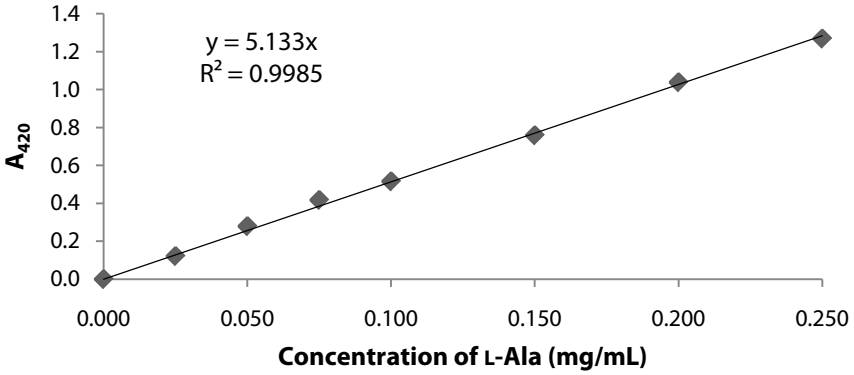

Figure 3.6: Standard curve for the detection of free amino groups in the DNFB assay. L-Alanine from 0–250 µg/mL was used as a standard. Attempts to monitor the liberation of stem peptides by tAmiB were unsuccessful, as the absorbance at 420 nm was below the detection limit ($A_{420} < 0.005$).

followed by a second digestion for several hours with another portion of amidase. Insoluble material was removed by centrifugation, and 40 µL sample or standards were dried down and resuspended in 40 µL of 1% $Na_2B_4O_7$. To this, 4 µL of 1.3% DNFB was added and incubated at 60 °C for 30 min. Following incubation, samples were acidified with 160 µL of 2 N HCl, transferred to a 96-well plate. The DNFB reacts with free amino groups, producing dinitrophenyl-amino acids, which were detected at 420 nm (Figure 3.6). This assay was unable to detect liberated free amino groups from tAmiB-digested PG, as the A_{420} was below the detection threshold ($A_{420} < 0.005$, data not shown). This could have resulted from using samples of PG that provide free amines at concentrations below detection limits of the DNFB reaction, or from protein instability during early purifications. Due to the positive results from zymography and turbidometry, the tAmiB was deemed active and suitable for use in the generation of the soluble substrate.

3.4.4 Improving enzyme solubility and activity

tAmiB was found to be unstable, resulting in its accumulation as insoluble aggregates with low functional activity. An empirical approach was taken to improve solubility. Increasing the salt concentration in IMAC buffers (from 300–500 mM NaCl) did not appear to improve solubility. Maintaining a low temperature during cell lysis by the use of a French pressure cell (instead of sonication) did not improve solubility either.

Additives in dialysis buffers were investigated. It was found that the addition of a detergent (0.3% Sarkosyl) greatly improved solubility. However, this anionic detergent prevented tAmiB from binding to the nickel resin during IMAC, and hence it eluted in the flow-through (data not shown). Alternatively, a low concentration of non-ionic surfactant (0.1% Triton X-100) was also found to greatly improve solubility without affecting IMAC purification. As Triton X-100 absorbs at 280 nm, it was removed by dialysis prior to cation-exchange chromatography, and subsequently reintroduced by dialysis. Although the presence of Triton X-100 did not appear to have an effect on enzyme activity (Figure 3.7), it greatly improved solubility during enzyme storage and was therefore included in all subsequent purifications. Using the turbidometric assay, it was found that tAmiB stored at 4 °C

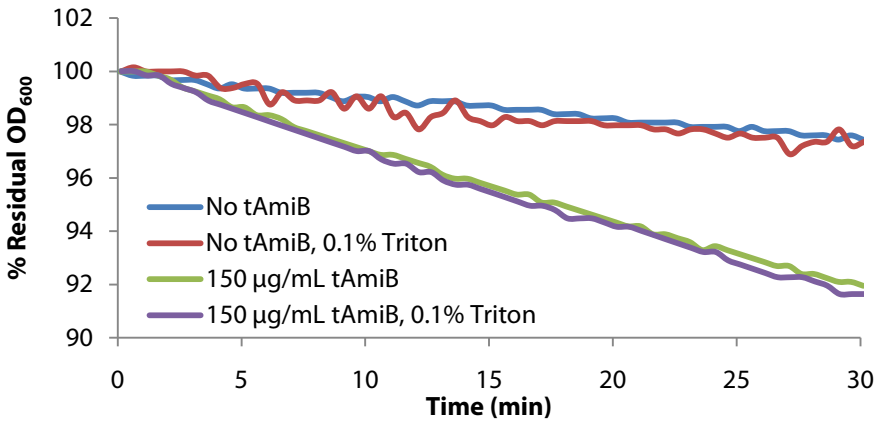

Figure 3.7: The effect of Triton X-100 on the activity of tAmiB. Whole cells of *M. luteus* were used as substrate for the turbidometric assay. Cells were incubated without tAmiB in the presence (red) or absence (blue) of 0.1% Triton X-100, and with 150 µg/mL tAmiB in the presence (purple) or absence (green) of 0.1% Triton X-100. The decrease in turbidity at 600 nm was monitored for 30 min.

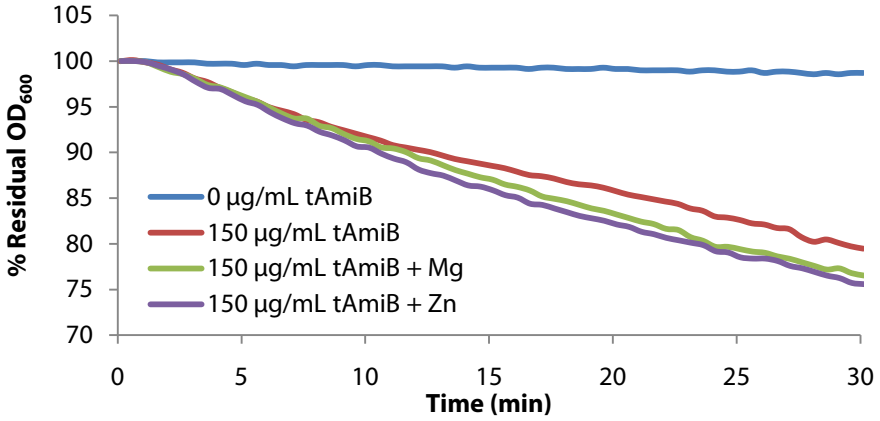

Figure 3.8: The activity of tAmiB in the presence of divalent cations. Whole cells of *M. luteus* were used as the substrate for turbidometry. Cells were incubated in the presence of 0 µg/mL tAmiB (blue), 150 µg/mL tAmiB (red), 150 µg/mL tAmiB in 5 mM $MgCl_2$ (green), or 150 µg/mL tAmiB in 1 µM $ZnCl_2$ (purple). All reactions took place in 25 mM sodium phosphate, pH 7.0, and 0.02% sodium azide. The decrease in turbidity at 600 nm was monitored for 30 min.

began to lose activity after 8–10 days.

The generation of a soluble substrate in this study depends on the complete removal of stem peptides by tAmiB, and as such it is very important that the enzyme be highly active. Since the activity of tAmiB was found to be relatively low (as compared to lysozyme), attempts were made to increase activity. Because AmiB is a Zn-dependent peptidase (Korndörfer *et al.*, 2006), the effect of divalent cations in digestion buffers were tested (Figure 3.8). The inclusion of either zinc ($ZnCl_2$) or magnesium ($MgCl_2$) increased the activity of tAmiB by less than 5%, and was not investigated further. That tAmiB is nearly as active in the absence of these cations is most likely due to the acquisition of zinc ions from the growth medium during translation.

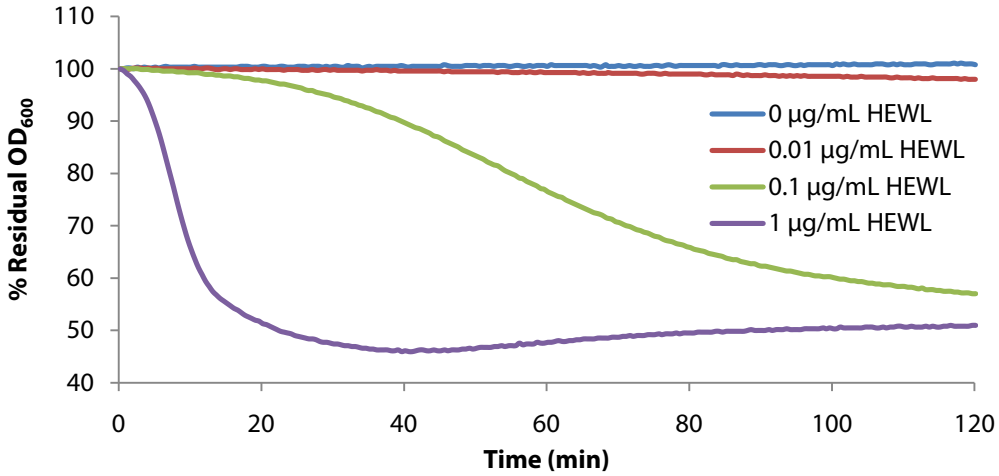

Figure 3.9: Turbidometric analysis of hen egg-white lysozyme using whole cells of *M. luteus* as substrate. Cells were incubated in the presence of HEWL at 0 µg/mL (blue, control for settling), 10 ng/mL (red), 100 ng/mL (green), and 1 µg/mL (purple). The decrease in turbidity at 600 nm was monitored for 120 min.

3.5 Generation of oligoglycans from purified PG

3.5.1 Digestion of PG

For the generation of large quantities of oligomuroglycans, purified PG was incubated with tAmiB to liberate stem peptides. To ensure complete digestion, a high concentration of tAmiB was used (150 µg/mL) to digest PG (250 µg/mL). Because the average length of glycans can be quite long, lysozyme was used to generate shorter fragments. Lysozyme is a highly active enzyme and will continue to digest glycans into their disaccharide subunits if the reaction is allowed to proceed to completion. To generate oligomuroglycans of the desired length (~12–14 monosaccharides) using lysozyme, optimal digestion conditions must be established. Using the turbidometric assay, lysozyme concentrations of 10 ng/mL, 100 ng/mL, and 1 µg/mL were found to solubilize PG to different extents after 60 min (Figure 3.9). Prior to this digestion, insoluble material from the tAmiB digestion was not removed because the solubility of the upper limit of glycan length remains unknown. Digestions were quenched after 1 h by acidification and boiling. Insoluble material was removed by centrifugation and filtration prior to glycan purification by cation-exchange chromatography.

3.5.2 Purification of glycan strands by cation-exchange chromatography

The soluble fraction of the PG digest was applied to a cation-exchange column at pH 2.0. At this pH, muroglycans have a neutral charge and are collected immediately in the flow-through, while peptides with a positive charge are retained on the column (Harz *et al.*, 1990). The column was washed with 1 M NaCl to elute muropeptides. This purification step serves to avoid interference of muropeptides and added enzymes during subsequent HPLC separation of oligosaccharides.

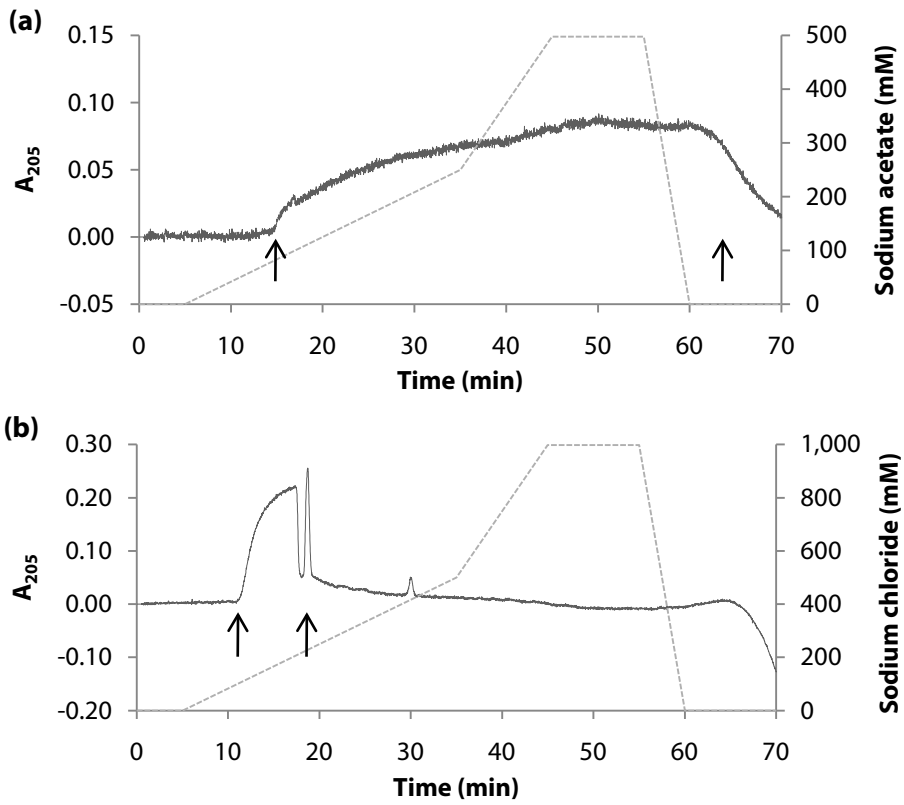

Figure 3.10: Representative blank HPAEC-A chromatograms using (a) sodium acetate or (b) sodium chloride as the eluent. Nothing was injected before the run was initiated. The solid line indicates the absorbance at 205 nm, while the dotted line indicates the concentration of eluent (mM). The baseline interference from each eluent results in a characteristic 'hump' (arrows).

3.5.3 HPAEC separation of glycans using absorbance

Many attempts were made to resolve glycans (both muroglycans and model chitooligosaccharides) using HPAEC with detection by absorbance at 205 nm and 210 nm. The column used in each case was the CarboPac PA-100 carbohydrate column (Dionex). Carbohydrate analysis with this column is intended to be paired with amperometric detection, although due to equipment availability, detection by absorbance was attempted. Using a gradient of either sodium acetate (Figure 3.10a) or sodium chloride (Figure 3.10b) resulted in strong baseline drift and background noise. This was found to interfere with the resolution of glycans, whether they were standards in a mixture (Figure 3.11) or the products of enzymatic digestions (Figure 3.12). The chitooligosaccharides eluted early in the chromatogram, indicating weak interaction with the resin (Figure 3.11). This was expected due to their lack of carboxylic acid groups, such as those present in the MurNAc-containing muroglycans of PG origin (Figure 3.12). The characteristic 'humps' of both sodium chloride and sodium acetate lie within the range of analytes, thus indicating the impracticality of the use of these eluants coupled with detection by absorbance. The humps also appeared to mask peaks that eluted within the same time. The peaks which were resolved were of very low intensity, which is likely explained by the low sensitivity of detection by absorbance.

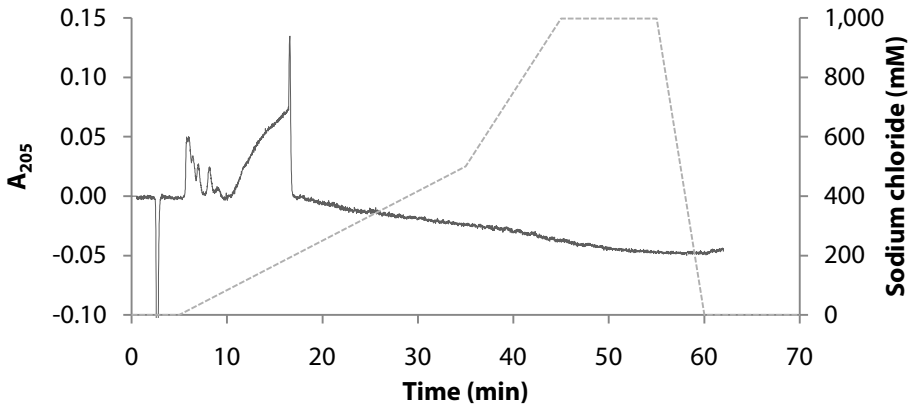

Figure 3.11: HPAEC-A separation of glycan standards (chitooligosaccharides). A mixture containing 20 nmol each of $GlcNAc_2$, $GlcNAc_3$, $GlcNAc_4$, $GlcNAc_5$, and $GlcNAc_6$ was injected. The solid line indicates the absorbance at 205 nm, while the dotted line indicates the concentration of sodium chloride (mM).

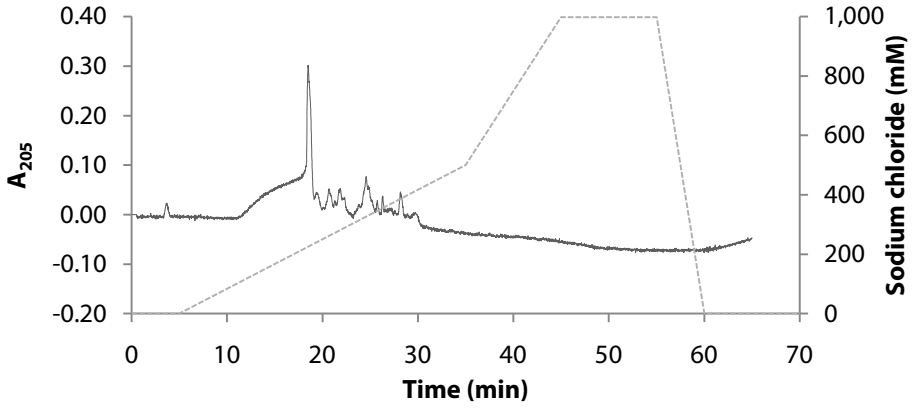

Figure 3.12: HPAEC-A separation of tAmiB and HEWL digestion products. PG which had been digested completely with tAmiB was partially digested with HEWL (20 ng/mL HEWL at 37 °C for 2 h). This reaction was quenched by directly injecting 100 µL of sample. The solid line indicates the absorbance at 205 nm, while the dotted line indicates the concentration of sodium chloride (mM).

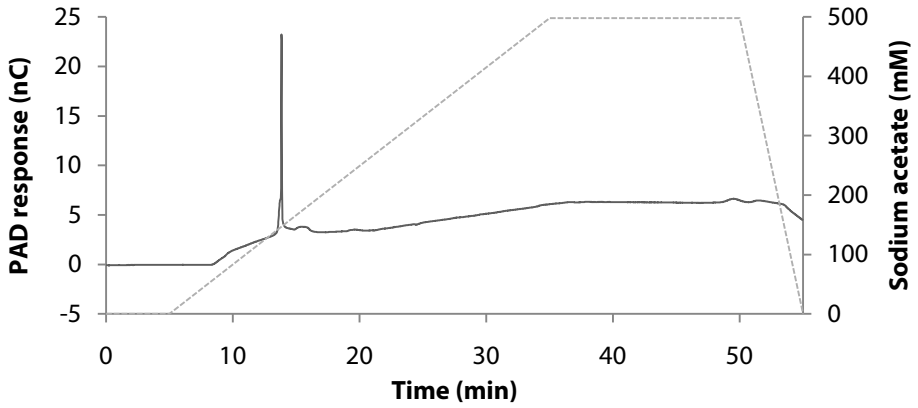

Figure 3.13: A representative blank HPAEC-PAD chromatogram using sodium acetate as the eluent. This chromatographic profile was subtracted from subsequent runs to account for baseline drift. A blank chromatogram was generated for each series of runs. The solid line indicates amperometric detection in coulombs (nC), while the dotted line indicates the concentration of sodium acetate (mM).

Numerous attempts were made to minimize baseline interference, including different gradients and initial equilibration in a low percentage of eluant. Two different HPLC machines were used to attempt to improve the method – a Beckman System Gold with 168 detector, and a Dionex GP40 pump with AD20 detector. All attempts to improved the resolution of glycans using HPAEC with detection by absorbance were unsuccessful. An HPLC system coupled with pulsed amperometric detection was available in the laboratory of Dr. Joseph Lam and was used for the remainder of this study.

3.5.4 HPAEC separation of glycans using PAD

Chromatographic separation of glycans coupled with pulsed amperometric detection is far more sensitive than detection by absorbance. Furthermore, baseline fluctuation is minimal when using sodium acetate (500 mM), and thus does not interfere with peak resolution (Figure 3.13). When the blank chromatogram is subtracted from subsequent runs, a very clean profile is generated with minimal baseline drift.

To test this method, standards of chitooligosaccharides were separated from a mixture (Figure 3.14). The GlcNAc oligomers eluted quickly from the column and with poor resolution. This was attributed to their lack of carboxylic acid groups, thus weak interactions with the resin. When such groups are stripped of their hydrogen in high pH, they are stabilized by resonance between the two oxygen molecules. The lack of such a group likely gives rise to relatively weak interactions with the resin. To support this, a solution containing GlcNAc-MurNAc and $GlcNAc_2$ was resolved by the same method (Figure 3.15). With just one carboxylic acid group (*i.e.,* the lactyl moiety of MurNAc), the standard bound more tightly to the column and eluted in a higher concentration of sodium acetate (~200 mM). This interaction is expected to be stronger for molecules with multiple carboxylic acid groups, such as in the case of $(GlcNAc\text{-}MurNAc)_n$ oligomers greater than the disaccharide. However, the GlcNAc-MurNAc disaccharide is the only commercially available PG oligosaccharide.

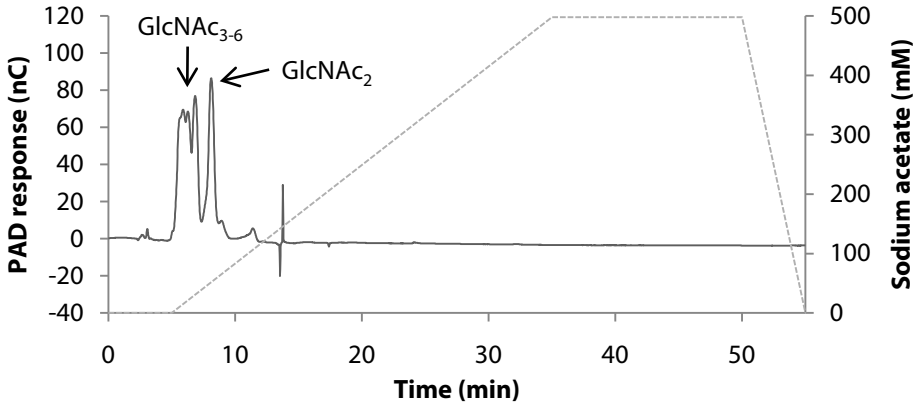

Figure 3.14: HPAEC-PAD separation of neutral carboyhydrate standards. A chitooligosaccharide mixture containing 4 nmol each of GlcNAc oligomers between 2 and 6 monosaccharides was injected. The standards eluted quickly and with poor resolution. The solid line indicates PAD response (nC), while the dotted line indicates the concentration of sodium acetate (mM).

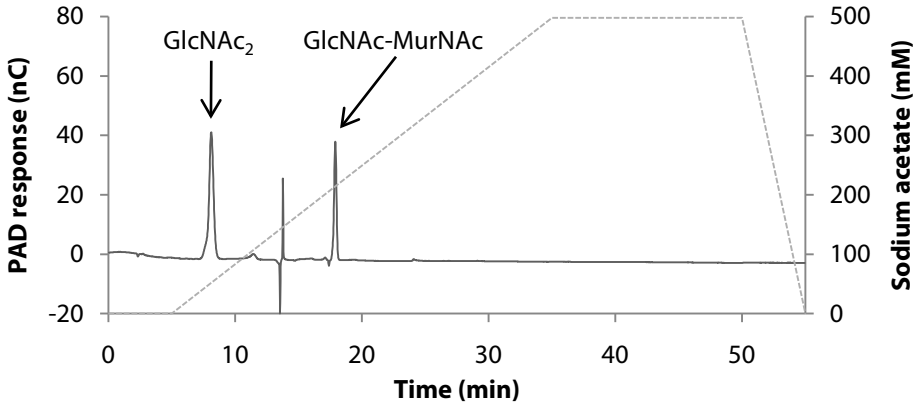

Figure 3.15: HPAEC-PAD separation of neutral and acidic carboyhydrate standards. A mixture containing 10 nmol each of $GlcNAc_2$ and GlcNAc-MurNAc was injected. $GlcNAc_2$ eluted at 8.1 min, while GlcNAc-MurNAc eluted much later at 17.9 min. The solid line indicates PAD response (nC), while the dotted line indicates the concentration of sodium acetate (mM).

3.5.5 Chromatographic separation of digestion products

Using the established HPAEC-PAD method, attempts were made to isolate and recover reaction products based on their degree of oligomerization. Some success was made isolating product species from digestions using lysozyme and tAmiB. To generate these samples, purified PG was digested with 0 μg/mL, 0.01 μg/mL, 0.1 μg/mL, and 1 μg/mL lysozyme. Following a 1 h incubation at room temperature, the samples were acidified with 20% phosphoric acid to pH~4.0 and heated in a boiling water bath to denature the lysozyme. Since the lysozyme-digested PG may remain insoluble (due to stem peptide cross-links), insoluble material was not removed. The samples were adjusted to pH 7.0 with NaOH, and the tAmiB digestion was allowed to proceed overnight (Figure 3.16).

Shortly after tAmiB was added to these samples a cloudy precipitate formed (less than 2 h). This was observed again with the addition of a second aliquot of tAmiB. Insoluble material was separated by centrifugation (13,000 × *g*, 5 min), and upon SDS-PAGE analysis it was found that the tAmiB had completely precipitated from solution (Figure 3.17). This insolubility was not attributed to the presence of lysozyme since samples without lysozyme were also insoluble, but rather to the high ionic strength resulting from pH adjustment – first to quench the lysozyme digestion and again to re-neutralize the samples. These data suggested the need to conduct the tAmiB digestion first, allowing it to run to completion, followed by subsequent digestion with lysozyme. In this order, the lysozyme digestion can be quenched by denaturation without affecting the tAmiB digestion.

3.6 MALDI-TOF mass spectrometry

Analysis of carbohydrates by mass spectrometry proved to be the most challenging aspect of this project. Although much work has been done on PG, the vast majority of analytes have contained at least part of the stem peptide, which can assist analysis by MALDI-TOF mass spectrometry.

3.6.1 Maximizing sensitivity with various matrices

CCA

Amongst the commonly used matrices, each is ideal for a specific type of molecule. One matrix in particular, α-cyano-4-hydroxycinnamic acid (CCA), has been used in many studies involving PG. This matrix is apparently ideal for peptide analysis, and as such is useful when analyzing molecules with a stem peptide. In this study, attempts were made to analyze carbohydrates using the CCA matrix. However, no peaks representing analytes were observed in the spectra (*e.g.,* Figure D.1). This was likely due to the inadequacy of this matrix when used to assist the ionization of carbohydrates. This was further confirmed by failure to identify chitooligosaccharide standards (data not shown).

DHB

When analyzing peptides and proteins by MALDI-TOF MS, the most abundant signals arise from the protonation of analyte molecules, even though sodium and potassium adducts are almost al-

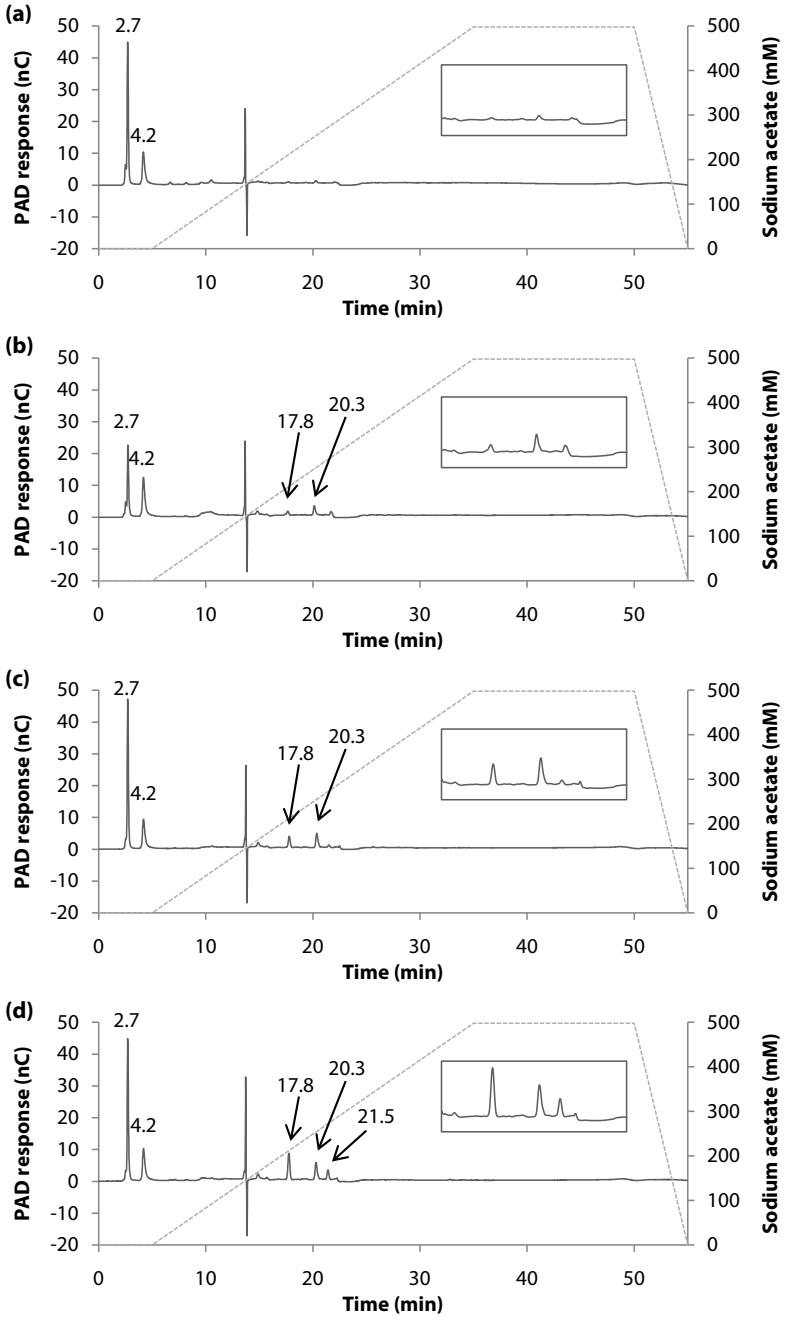

Figure 3.16: HPAEC-PAD separation of lysozyme and tAmiB-digestion products from *P. aeruginosa* PG. PG samples were first digested with (a) 0 µg/mL, (b) 0.01 µg/mL, (c) 0.1 µg/mL, and (d) 1 µg/mL lysozyme. Subsequently, all samples were digested with tAmiB. As lysozyme concentration increased, the abundance of product species which eluted at 17.8, 20.3, and 21.5 min also increased. The solid line indicates PAD response (nC), while the dotted line indicates the concentration of sodium acetate (mM). Insets: expanded region between 15 and 25 min scaled from -2 to 10 nC.

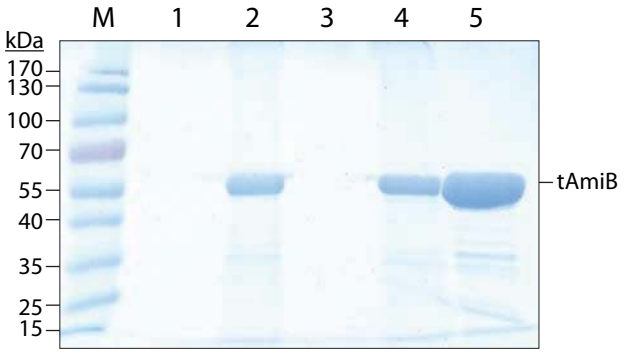

Figure 3.17: SDS-PAGE analysis of lysozyme and tAmiB digestions. Samples were first digested with lysozyme, followed by tAmiB. Insoluble material was removed by centrifugation (13,000 × *g*, 5 min). M indicates the PageRuler™ prestained protein ladder. Lanes 1 and 2 contain soluble and insoluble material, respectively, of a sample that was digested with only tAmiB. Lanes 3 and 4 contain soluble and insoluble material, respectively, of a sample that was digested first with 1 µg/mL lysozyme followed by tAmiB. Lane 5 contains tAmiB (11.1 µg) as a positive control.

ways present. However, when analyzing carbohydrates, cation attachment usually predominates and protonated species are rarely detected (Xu *et al.*, 1997). Therefore a good cationizing matrix should be used for the analysis of carbohydrates. One commonly used matrix for carbohydrate analysis is 2,5-dihydroxybenzoic acid (DHB).

In this study, some success was attained using DHB as the matrix in positive mode, although sensitivity was quite low when detecting carbohydrate standards (~20 µM for pure GlcNAc and MurNAc). The predominant species observed were the $[M+Na]^+$ ion, and to a lesser extent the $[M+K]^+$ ion (Figure 3.18). Several attempts were made to improve the sensitivity with DHB, including mixing the matrix and sample prior to spotting on the plate, spotting as a matrix-sample sandwich, matrix-sample-matrix sandwich, and using a combination of DHB and CCA matrices. The sensitivity was highest either when mixing sample with the matrix, or the matrix-sample sandwich. However, the sensitivity remained quite low. Since the DHB matrix is primarily used for neutral glycans, alternative matrices were investigated.

CMBT

Amongst the literature a vast number of matrices have been examined. Narrowing this down to oligosaccharides, and in particular acidic oligosaccharides, a chemical within the mercaptobenzothiazole class appeared suitable. Xu *et al.* (1997) found that 5-chloro-2-mercaptobenzothiazole (CMBT) is an excellent cationizing matrix with a much higher signal-to-noise ratio when compared to DHB. Using this matrix, we were able to increase the sensitivity of carbohydrate detection to low-picomole levels (Figure 3.18). The sensitivity when using CMBT was found to be superior to that of DHB, as indicated by the signal-to-noise ratio. As with DHB, the major peak in the mass spectrum represents the sodium adduct, $[M+Na]^+$. A potassium adduct ion, $[M+K]^+$, is also observed but to a lesser extent. The protonated species ($[M+H]^+$) is only observed when using CMBT as the matrix, but at very low intensity.

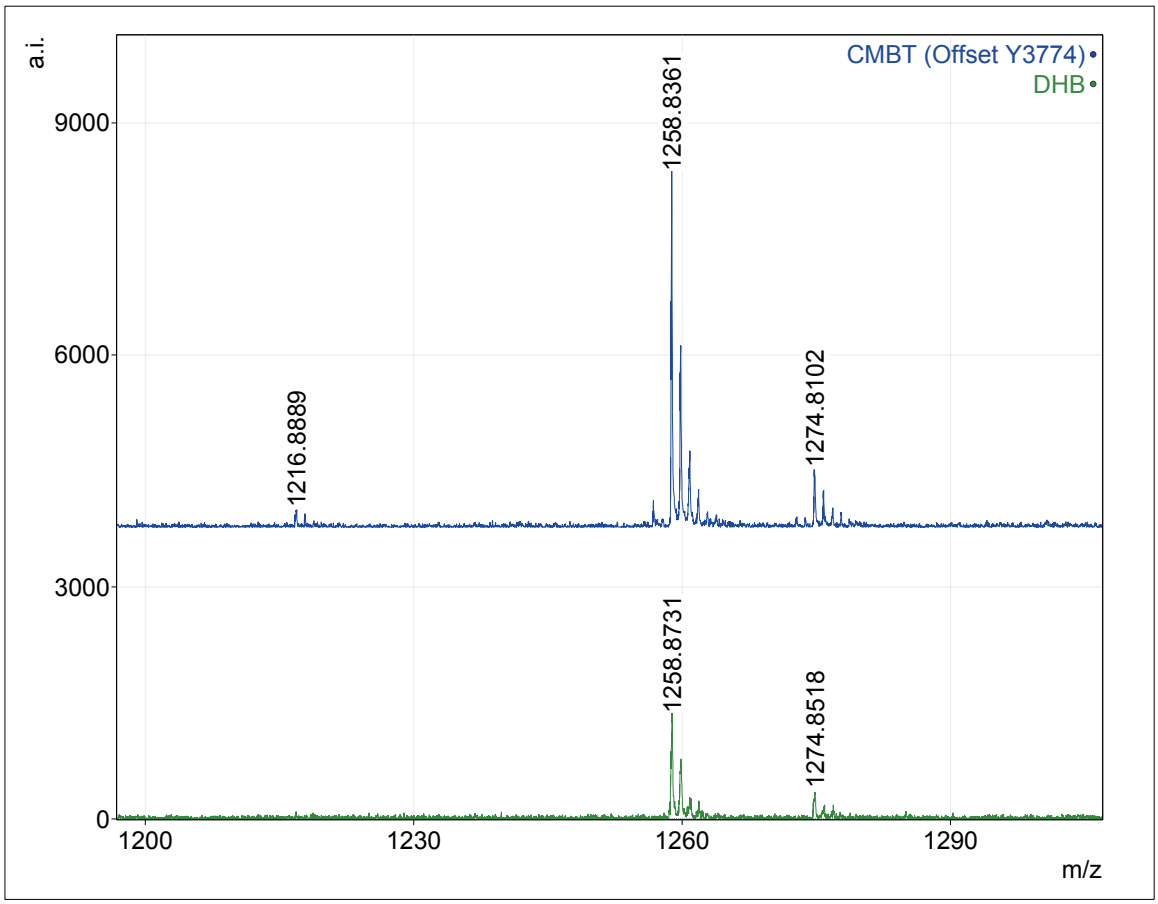

Figure 3.18: MALDI-TOF MS matrix comparison for the detection of oligosaccharides. Two matrices were tested: CMBT (blue), and DHB (green). Each spectrum represents 100 pmol of $GlcNAc_6$. Baseline correction was applied, and the CMBT spectrum was offset to emphasize the difference in sensitivity. The most intense peak in either spectra (m/z 1258.8) represents $GlcNAc_6$ with a sodium adduct, $[M+Na]^+$. The potassium adduct (m/z 1274.8, $[M+K]^+$) is observed to a lesser extent, while the protonated species (m/z 1216.9, $[M+H]^+$) is only observed in the CMBT spectrum.

One potential problem with both the CMBT and DHB matrices is interference in the lower mass range (m/z < 700) (Figure 3.19). This profile may interfere with the analysis of small molecules such as the GlcNAc-MurNAc disaccharide (expected m/z of 519.18, $[M+Na]^+$), or may lead to the suppression of their signal. However, as the sensitivity and signal-to-noise is superior to that of DHB, the CMBT matrix was used in all subsequent analyses.

3.6.2 Analysis of digestion products

Many attempts were made to identify digestion products by MALDI-TOF MS, whether from tAmiB, lyzosyme, or a combination of digestions. Attempts were made to identify products both from the crude digestion (*e.g.,* Figure D.2) and chromatographically separated products (*e.g.,* Figure D.3). Using the calculated monoisotopic masses (Appendix C), all attempts to identify product molecules failed. The analysis of glycans derived from PG digestion proved to be extremely difficult, even with

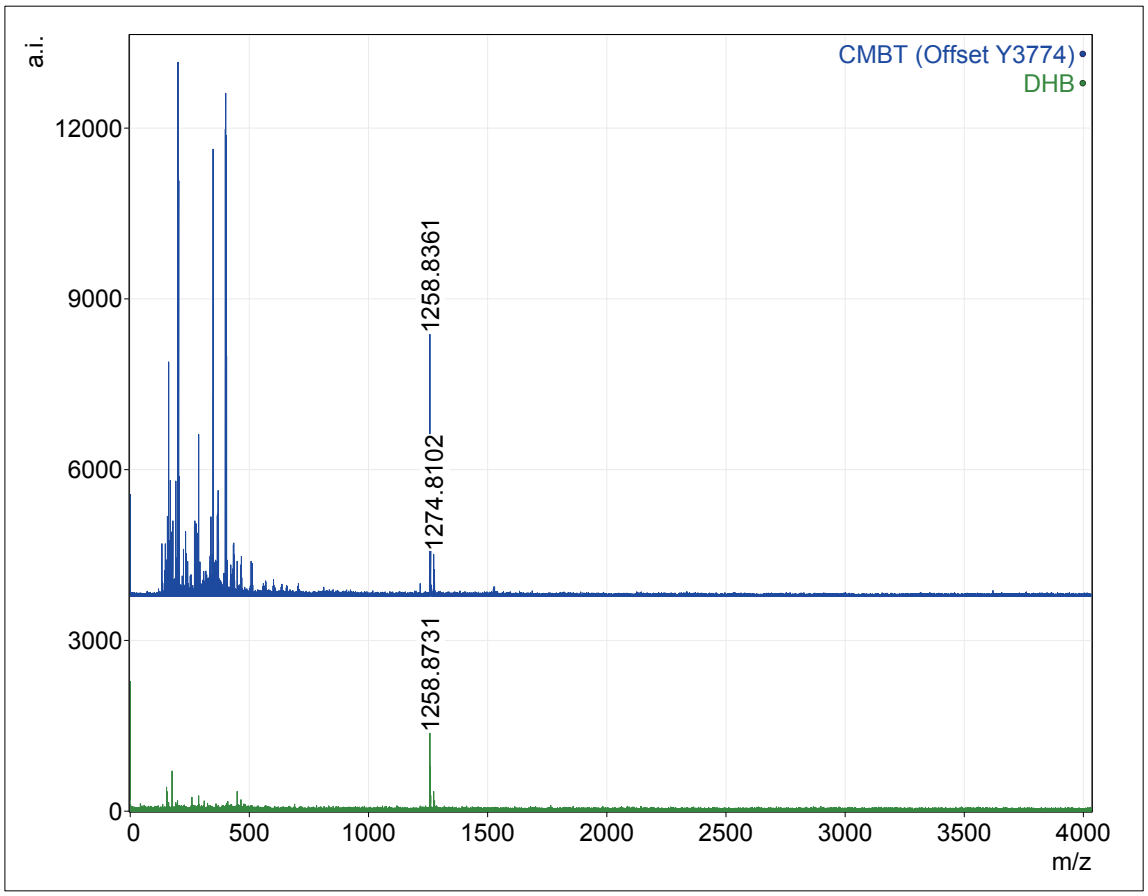

Figure 3.19: MALDI-TOF MS matrix comparison showing the full spectra from Figure 3.18. While the CMBT matrix (blue) has higher sensitivity than DHB (green), both produce significant background in the low m/z range.

the established MALDI-TOF method. Attempts to identify the same collected analytes using LC-MS were also unsuccessful, which may have been due to the increased sensitivity to signal suppression from salt. The possible reasons for these analytical failures were investigated.

The peaks isolated in Figure 3.16 were collected, desalted, and analyzed by MALDI-TOF MS. One peak in particular (17.8 min) was thought to be the GlcNAc-MurNAc disaccharide as it eluted at the same time (Figure 3.15). However, upon analysis by MALDI-TOF MS there were no peaks representing the sodium adduct (m/z 519.18, $[M+Na]^+$), the potassium adduct (m/z 535.15, $[M+K]^+$), or the protonated ion (m/z 497.20, $[M+H]^+$) (Figure 3.20). The lack of a peak representing GlcNAc-MurNAc or any other species could be due to several possibilities: the isolated product could be too low a concentration for detection, the matrix could be suppressing the signal, or it is a different molecule altogether and which may not be detected using this matrix. A likely explanation is that the CMBT matrix generates significant background in this low range, and as such may not be able to identify low molecular weight analytes.

The spectra generated by the remaining peaks from Figure 3.16d were indistinguishable to that of Figure 3.20, with no identifiable products. One option would be to try a complete lysozyme digest;

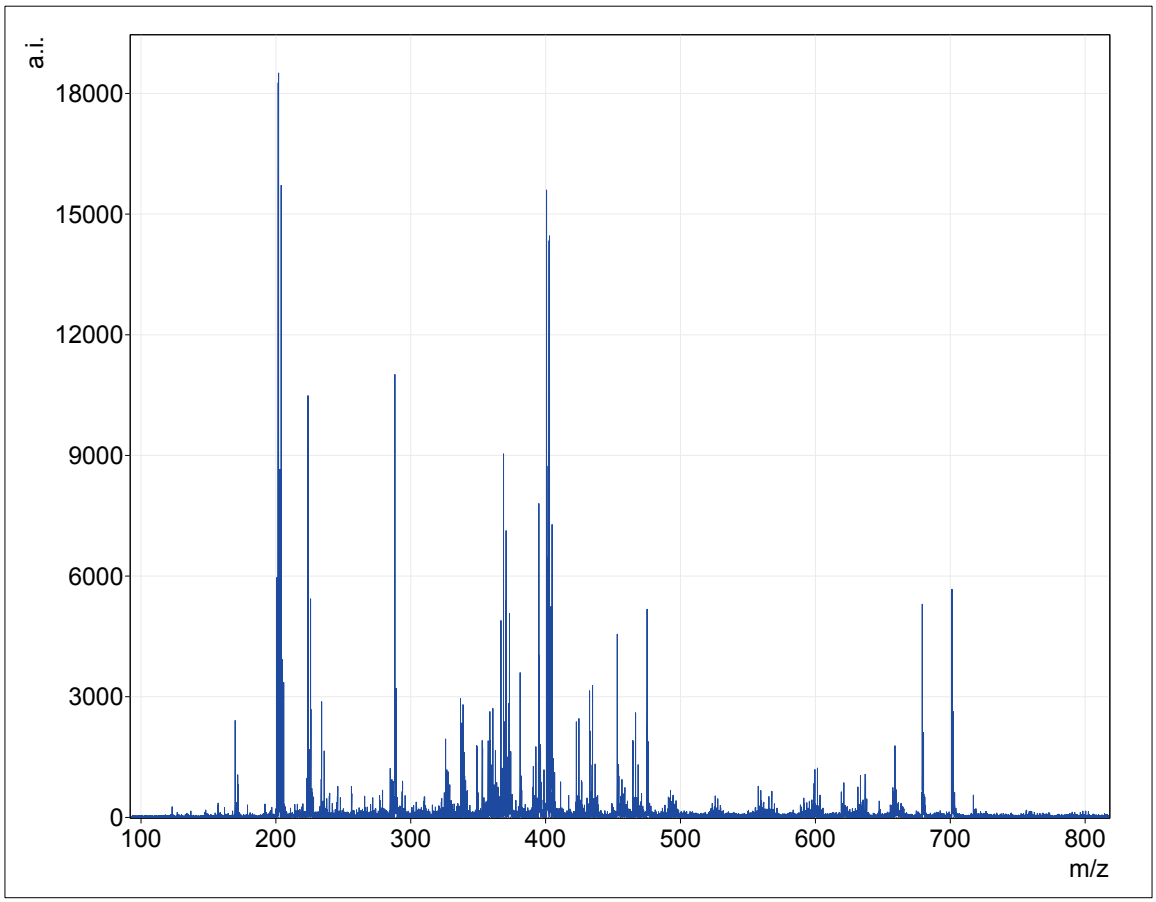

Figure 3.20: MALDI-TOF MS analysis of an isolated product. The peak at 17.8 min in Figure 3.16d was collected, desalted, and analyzed using the CMBT matrix. There are no obvious peaks representing product species when compared to the spectrum of pure matrix. There was no signal below m/z 100 or above m/z 800.

however, this would end in the generation of the GlcNAc-MurNAc disaccharide which may not be identifiable using this method. The remainder of this research focused on the troubleshooting and optimization of sample preparation for MALDI-TOF mass spectrometry.

3.7 MALDI-TOF MS troubleshooting

Spectra from crude digests had a great deal of background, and at best separated products generated numerous peaks with unknown identities based on the monoisotopic mass calculations for the expected products (Appendix C). These peaks were often of low abundance, and could have arisen from larger, undetectable low abundance molecules being broken apart by the ionization of the laser. Several attempts were made to overcome this challenge.

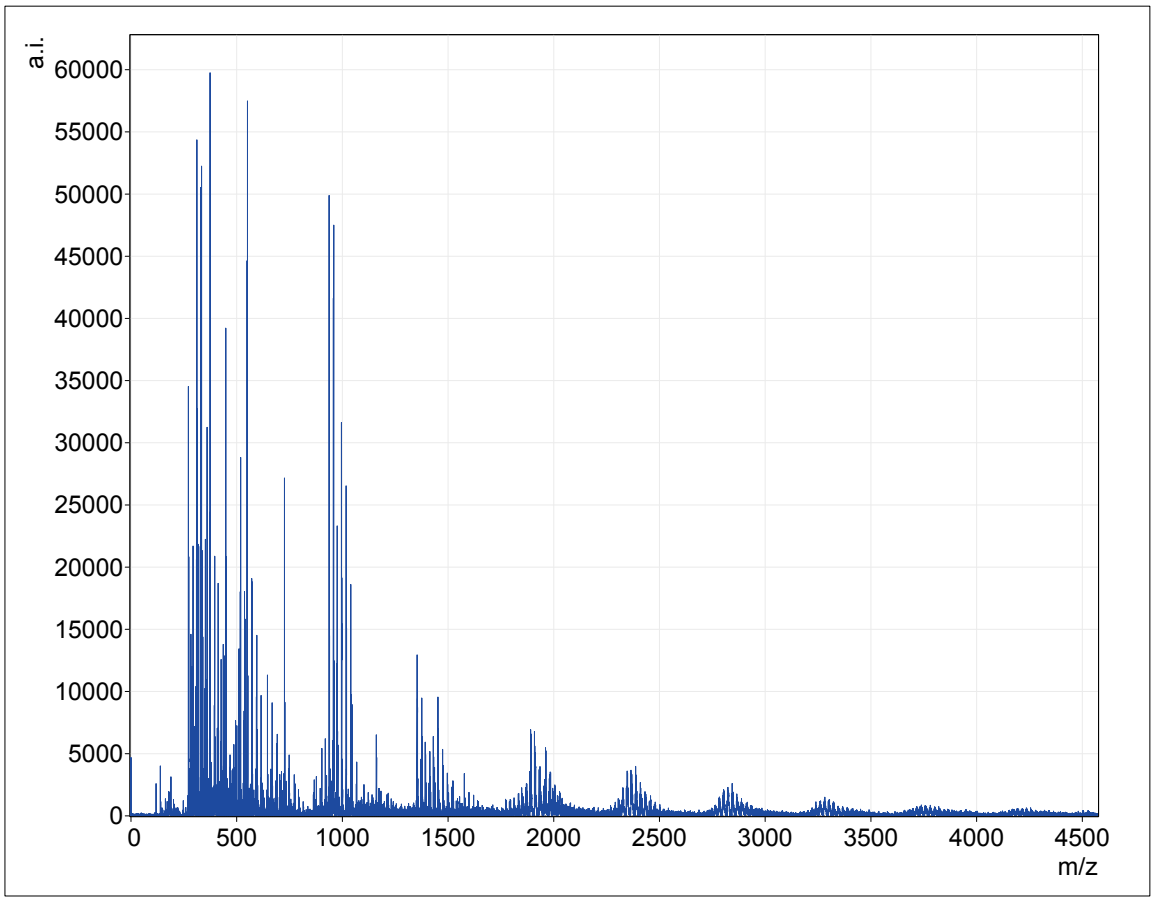

Figure 3.21: MALDI-TOF MS contamination by a polymer. tAmiB-digested PG was incubated with lysozyme (0.25 mg/mL) for 1 h, mixed with DHB and spotted directly onto a MALDI-TOF plate. The bell-shaped groups of peaks (*e.g.,* between m/z 2700 and 3000) are characteristic of PEG contamination, which was attributed to the presence of Triton X-100 in the digestion buffer.

3.7.1 PEG contamination

Early MALDI-TOF analyses produced spectra with what appeared to be contamination by polyethylene glycol (PEG) (Figure 3.21). This was first thought to have come from sample preparation or storage, possibly from cuvettes or the microtubes used to collect products. The use of siliconized, low-retention microtubes did not seem to make a difference. It was later found that the contaminating compound was Triton X-100, which contains a polyethylene oxide group, and thus the PEG-like spectra. Although Triton X-100 was useful for maintaining protein solubility, it was omitted from digestions when an efficient means of its removal prior to mass spectrometry had not yet been established. However, this was undesirable as tAmiB was very unstable in the absence of this detergent, so instead methods to remove Triton X-100 were investigated.

3.7.2 Desalting

Analyses of chitooligosaccharide standards indicated that the presence of as low as 10 mM sodium phosphate was enough to suppress the MALDI-TOF signal (data not shown). Therefore, the inab-

ility to identify analytes using MALDI-TOF MS could be attributed to a high sodium content. The presence of sodium could be from the sodium phosphate buffer used in digestions, or sodium acetate from HPLC separation. Since the removal of sodium azide (0.02% as a preservative) from the buffer during overnight digestions did not appear to improve spectra, a good desalting method was required.

Various methods of desalting were attempted. An on-plate desalting method was attempted, in which samples were spotted directly onto the MALDI-TOF plate, and distilled water was pipetted repeatedly on top of the sample. The generated spectra appeared to have somewhat cleaner signal with less baseline noise, although this did not improve sensitivity and products remained unidentified.

Another method to desalt samples was the use of ZipTip® pipette tips. These pipette tips contain a C_{18} resin which binds hydrophobic analytes. Excess salts are washed away using trifluoroacetic acid, and the analytes are subsequently eluted in acetonitrile. Because samples resolved by HPAEC were at a very high pH, they were first adjusted to pH < 4.0 with HCl. This step was taken so the oligosaccharides would possess a neutral charge, otherwise they may not bind well to the hydrophobic C_{18} resin (Harz *et al.*, 1990). Samples were dried down and resuspended in a small volume of 0.1% TFA prior to the use of ZipTips®. This technique was vastly superior to on-plate desalting in the generation of mass spectrometric peaks. The obvious disadvantage of desalting by this method is that the pipette tips only have a capacity of 10 µL and can therefore only desalt a minimal amount of sample. Another option would be to use an RP-HPLC column to desalt on a more preparative scale, although other (potentially superior) options are discussed in the next chapter.

Although the ZipTip® method is designed for desalting peptides and nucleotides, it was also found to work for oligosaccharides and this has several advantages. The main advantage is that desalted analytes produce much cleaner MALDI-TOF spectra. Another advantage is that desalting removes other chemicals and therefore allows for their inclusion in upstream experiments, such as digestions. Such chemicals removed by desalting practises include sodium azide to prevent microbial growth, and Triton X-100 to improve enzyme solubility. The ZipTip® method was used for all subsequent analyses.

3.7.3 Calibration

Because MALDI-TOF MS analytes are most often proteins and peptides, the machines are calibrated with corresponding standards. Thus, one possibility of the inability to identify peaks could be inaccurate calibration for oligosaccharides. To account for this, chitooligosaccharide standards ($GlcNAc_n$) between 4 and 6 units long were submitted with samples to act as an external standard. These standards are pure, relatively inexpensive, and closely related to PG-derived oligosaccharides. Furthermore, the peaks representing these standards are above the profile of the CMBT matrix, and as such are ideally suited for calibration. Using these calibrants, the spectra were often adjusted by up to ±2 Da prior to interpretation. These standards were analyzed along with each set of samples because results can vary each day.

3.8 Ongoing challenges

These results suggest the need for further experimentation. Success has been made in several areas of this project: the purification of large amounts of tAmiB, the optimization of digestion conditions and enzyme storage, the separation of carbohydrate digestion products, and the establishment of a MALDI-TOF MS method with a suitable matrix. With these established techniques one should be able to generate a pool of $(GlcNAc\text{-}MurNAc)_n$ oligosaccharides of an ideal length. However, further work is required to generate this substrate. This may involve optimization of the limited lysozyme digestion, or it may involve a different approach altogether, each of which are discussed in the next chapter.

Chapter 4

Discussion

This research focuses on three objectives: (i) to optimize the purification and digestion conditions of *P. aeruginosa* tAmiB, (ii) to optimize the MALDI-TOF MS procedure for identification of PG-derived oligosaccharides, and (iii) to generate a soluble, defined PG derivative for the study of lytic transglycosylases. With regards to the first objective, the yield of tAmiB was increased by a factor of five, and enzyme solubility was vastly improved as determined by SDS-PAGE. The results of the MALDI-TOF MS optimization have indicated that the combination of a good desalting method and use of the CMBT matrix are optimal for oligosaccharides greater than 600 m/z. Finally, the results of the substrate generation were inconclusive, as the isolation and identification of oligosaccharide digestion products were unsuccessful. All of these findings will be discussed in more detail below.

4.1 Experimental approach

The approach taken in this study was the enzymatic degradation of insoluble PG sacculi isolated from whole cells, and the isolation of specific fragments. This top-down approach seemed a viable option as opposed to biosynthesis, as the disaccharide pentapeptide monomer (the building block of PG) is not commercially available and its biosynthesis is fairly laborious (Figure 1.7). The seemingly 'simpler' approach used here requires fewer enzymes; an *N*-acetylmuramyl-L-alanine amidase to liberate the glycan chains from stem peptides, and lysozyme to generate shorter glycans.

The required *N*-acetylmuramyl-L-alanine amidase is not commercially available, therefore the production and purification of a recombinant protein was necessary. The truncated *P. aeruginosa* amidase B used in this research was chosen for a number of reasons: it remains soluble within the cytoplasm, it has previously been expressed and purified (Scheurwater *et al.*, 2007), and it accepts the intact high molecular weight PG sacculus as a substrate (unlike the *E. coli* homologs) (Parquet *et al.*, 1983). The latter may be due to the presence of the lysin motif, which is absent in the *E. coli* homolog. This domain is found in a variety of enzymes, including others involved in cell wall degradation, and is believed to function as a PG-binding module (Joris *et al.*, 1992; Bateman and Bycroft, 2000).

4.1.1 Optimization of tAmiB

By altering the production and purification procedures for tAmiB, yields were increased by a factor of five from previously published results (Scheurwater *et al.*, 2007). This was achieved by an optimized IMAC purification protocol using an imidazole gradient, followed by cation-exchange chromatography. The purity achieved with this combination was near-homogeneous, as indicated by SDS-PAGE analysis (Figure 3.2).

Initially, tAmiB solubility was very poor. However, the presence of a non-ionic detergent, such as Triton X-100, vastly improved solubility. This not only improved tAmiB solubility during prolonged digestions, it also extended the shelf life to 10 days (at 4 °C). These accomplishments were sufficient, as large PG digestions required tAmiB to remain active for two days. Attempts to improve the activity of tAmiB were insignificant. Although the addition of Triton X-100 greatly improved solubility, it had little effect on enzyme activity (Figure 3.7). Furthermore, the inclusion of zinc did not appear to improve activity significantly (Figure 3.8).

4.1.2 Generation of muroglycans

Initial attempts to generate muroglycans began with treatment of isolated PG sacculi with lysozyme, followed by treatment with tAmiB. This order of digestions was desirable due to the relatively high activity of lysozyme and low cost. Lysozyme digestion was proposed to relax the sacculus, allowing for easy access to stem peptides by tAmiB. However, this led to the complete precipitation of tAmiB. This was due to the high ionic strength – the result of acidification, boiling, and re-neutralization of samples following lysozyme digestion. This pH adjustment was necessary to limit the extent of lysozyme digestion; acidification and boiling quenched the reaction. Another means of quenching the reaction and inactivating lysozyme is to immediately boil it. However, the concern with this is the increase in activity of lysozyme due to the slow increase in temperature before it becomes hot enough to denature the protein.

The solution to these problems was to conduct the tAmiB digestion prior to the lysozyme digestion. Using this sequence, the tAmiB digestion was allowed to run through completion. Subsequently, lysozyme was added and allowed to digest for a specific length of time prior to acidification and boiling. This allowed for the denaturation of both lysozyme and tAmiB simultaneously, followed by muroglycan purification by cation-exchange chromatography.

4.1.3 Chromatographic separation of digestion products

The initial attempts to detect resolved products using absorbance at 202 nm, 205 nm, 210 nm or 215 nm were unsuccessful. The low sensitivity of detection using absorbance appeared to be inadequate for the detection of the low levels of muroglycans derived from PG digestion (Figures 3.11, 3.12). This issue was resolved when the HPLC instrument with a PAD detector became available in the laboratory of Dr. Joseph Lam. Carbohydrate detection using PAD is extremely sensitive, as observed in Figure 3.14. Using the established conditions, reaction products were well-resolved (Figure 3.16).

4.1.4 Identification by MALDI-TOF mass spectrometry

Identification of the digestion products by MALDI-TOF MS proved to be the most challenging component of this research. Commonly used matrices, namely CCA and DHB, were found to be inadequate for the detection of muroglycans. The use of CMBT was far superior to either of these matrices, providing clean spectra and high sensitivity for the detection of oligosaccharides. However, all attempts to identify product species were unsuccessful. Many attempts were made to troubleshoot this, including the optimization of sample preparation.

Others have had success identifying HPLC-separated digestion products, although in each case at least part of the stem peptides were present (Atrih *et al.*, 1996; Xu *et al.*, 1997; Antignac *et al.*, 2003). For example, Atrih *et al.* (1996) used the CCA matrix to identify an isolated muropeptide. Similarly, Antignac *et al.* (2003) used both the CMBT and CCA matrices to identify muramidase-digested PG, and several peaks could not be determined which they attributed to the co-elution of an unidentified polymer that inhibited MALDI-MS analysis. The variation in success could also be due to limitations of the MALDI-TOF equipment used, although this remains a speculation. In many cases, digestion products were identified by complete digestion with muramidase and comparison of HPLC profiles to those of known digestion products (such as in Harz *et al.*, 1990).

4.2 Concerns with the experimental approach

Insoluble PG was prepared primarily from *M. luteus* cells due to the thick cell wall of this Gram-positive organism. While the PG of *M. luteus* is chemotype A2, the enzymes to be studied with the generated substrate are primarily from organisms with PG chemotype A1γ (*e.g., E. coli*). The difference between these chemotypes exists within the stem peptide: chemotype A1γ contains *m*-DAP at position 3 (Figure 1.3), while chemotype A2 contains L-lysine at position 3 and a glycine attached to D-glutamic acid at position 2 (Figure 1.4). Chemotype A1γ forms a direct cross-linkage, while chemotype A2 forms an interpeptide bridge consisting of 1–4 peptide subunits (Schleifer and Kandler, 1972). Although this chemotype discrepancy exists, it was of little concern for two reasons: the first is that the amidase used in this research is active against PG of either chemotype (Figure 3.5), and the second is that the substrate generated from this research will no longer possess stem peptides, and therefore will not have this chemotype discrepancy.

This removal of stem peptides gives rise to a more significant concern with this approach. Of the studied LTs of *E. coli*, Slt70, MltB, and MltC do not accept unsubstituted muroglycan as a substrate (*i.e.,* $(GlcNAc\text{-}MurNAc)_{n>30}$) (reviewed in Höltje, 1998). The requirement of the stem peptide for lytic activity by these enzymes indicates that the muroglycan substrate sought in this study cannot be used to assay all LTs. However, some of the LTs do indeed accept unsubstituted muroglycan chains as a substrate, including MltA (Romeis *et al.*, 1993) and MltE (Kraft *et al.*, 1998). The proposed endo-acting MltF has very little sequence similarity to the former exo-acting LTs and is placed closer to MltE than other family 1 enzymes (Blackburn and Clarke, 2001; Scheurwater and Clarke, 2008), and therefore may indeed accept the muroglycan substrate. If this relatively uncharacterized LT does

accept this substrate, several important conclusions can be drawn regarding its role within the cell (discussed below in HPAEC-based assay).

4.3 Alternative approaches to substrate generation

There are several alternative approaches to the generation of a defined substrate. One such approach involves the isolation of soluble PG metabolites secreted into the medium when cells are grown in sub-lethal concentrations of a cross-linking inhibitor. This approach has previously been attempted by Scheurwater (2008) using penicillin G; however, this approach proved difficult as separation by chromatography was poor and the material could not be identified by MALDI-TOF MS.

An approach similar to the one used in this study involves the use of MepA, an endopeptidase which hydrolyzes the cross-link between D-Ala and *m*-DAP in PG with chemotype A1γ (*e.g., E. coli*) (Keck *et al.*, 1990). MepA could be used with PG from a bacterial species with an average length of glycan strands of 8–9 disaccharides in the case of *Helicobacter pylori* (Chaput *et al.*, 2007) or 16 disaccharides in the case of *P. aeruginosa* (Quintela *et al.*, 1995). Glycans of this length presumably remain soluble, and their isolation should be fairly straightforward. One disadvantage to this approach is the relatively low yield of PG from such Gram-negative organisms.

The final, and perhaps superior approach involves substrate biosynthesis (bottom-up). This would involve the synthesis of the disaccharide pentapeptide monomer – the product of a series of eight enzymatic reactions (Figure 1.7) which can then be polymerized *via* transglycosylation. Although there is the inherent disadvantage of using many enzymes in this approach, there are significant advantages. First, the controlled polymerization can generate substrate with a consistent degree of polymerization, in contrast with the highly variable degree of polymerization of the heterogeneous PG sacculus. Second, the stem peptide would not only be present in the oligomer, it would be that of the native A1γ PG chemotype in *E. coli*.

4.4 Future directions

4.4.1 Sample preparation

One of the greatest disadvantages of mass spectrometry techniques is signal suppression by salt. Although there are many techniques available to desalt proteins, there is a lack of effective methods for the desalting of the relatively smaller oligosaccharides. Most of the commonly used methods are impractical; dialysis requires membranes which have an arbitrary low molecular weight cut-off, ion exchange media risks the loss of charged sugars, salt precipitation can result in the co-precipitation of oligosaccharides, and size exclusion chromatography requires long columns and small sample volumes (Packer *et al.*, 1998).

The use of reversed-phase separation, the basis of the ZipTips® used in this research, contain alkyl groups (commonly as octadecyl chains) to retain hydrophobic substances. This works well for proteins, but this adsorbent has relatively little affinity for hydrophilic solutes such as oligosacchar-

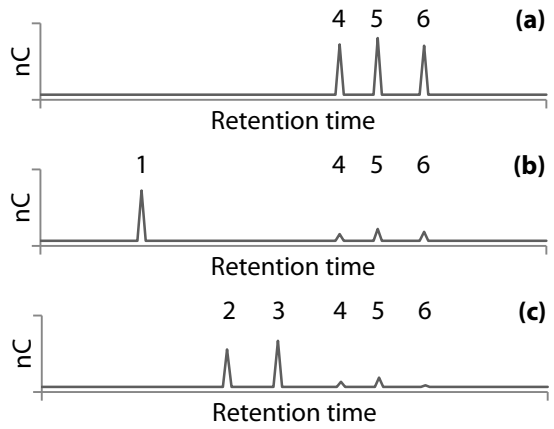

Figure 4.1: Hypothetical HPAEC-PAD chromatograms indicating enzyme substrate specificity. (a) Substrate consisting of oligomuroglycans between 4 and 6 disaccharide units. Following enzyme treatment, the loss of peaks representing high molecular weight substrate is coupled with an increase in peaks representing either (b) disaccharide units indicating exo-specificity, or (c) products greater than disaccharide units indicating endo-specificity. Numbers indicate the degree of polymerization in disaccharide units. Thus, for example, "4" indicates an octasaccharide consisting of $(GlcNAc\text{-}MurNAc)_4$.

ides. Upon a literature search, it was found that activated carbon has proven to be an excellent tool for both the desalting of oligosaccharides and their purification. Packer *et al.* (1998) found that the use of activated carbon is a quick and inexpensive way to remove contaminants including salt, detergents (*e.g.,* Triton X-100), protein, and other compounds. Furthermore, this can be used to fractionate neutral oligosaccharides from acidic oligosaccharides. Using Carbograph Ultra-Clean SPE columns (Grace, Deerfield, IL), Packer *et al.* (1998) has established a technique to purify neutral and acidic oligosaccharides. This step can improve MS analysis, enzymatic digestions, or remove salt prior to lyophilization for storage.

4.4.2 HPAEC-based assay

The generation of a defined substrate will provide several avenues, such as obtaining conclusive proof regarding the endo- or exo-specificity of LTs. Using natural PG substrates to accomplish this is complicated by the fact that digestion products may remain cross-linked to each other. Using a defined substrate, digestion samples can be removed at incremental times and resolved by HPAEC-PAD. The loss of certain peaks representing the high molecular weight substrate and the increase of peaks representing product species are monitored (Figure 4.1). The ratio of products generated with masses greater than the monomeric disaccharide GlcNAc-anhydroMurNAc to the amount of the monomeric disaccharide fragment produced will indicate whether the LT functions with exo- or endo-specificity. An authentic exo-acting LT can be used as a control, such as MltA. In this case only low molecular weight (*i.e.,* disaccharide) product accumulates (Figure 4.1b). Negative controls are also required in which no enzyme is added, as tight associations of LTs with PG have been observed (van Asselt *et al.*, 1999b), and so it is possible that some residual enzymes may be present with the substrate.

This assay is relatively simpler and more economical than that used by Kraft *et al.* (1998) for

the determination of the endo-specificity of MltE (EmtA). Kraft *et al.* (1998) generated a substrate consisting of [^{3}H]GlcNAc-labelled muroglycans – a process requiring the growth of bacteria in the presence of D-[1-^{3}H]-*N*-acetylglucosamine, murein isolation and purification, and digestion with isolated human serum amidase (Ursinus and Höltje, 1994). Fractionation was accomplished by reversed-phase HPLC and the radioactivity in the eluent was monitored by a flow-through scintillation counter. The kinetics of degradation suggested that MltE can cleave muroglycan at a distance of two disaccharide units, but preferentially cleaves at a distance of more than two disaccharide units from the ends (Kraft *et al.*, 1998). The substrate consisting of 7 disaccharides was completely digested into 2- and 3 disaccharide products; no monomeric disaccharide fragments were observed.

While the methods of Kraft *et al.* (1998) may be more expensive and labour-intensive, detection of radiolabelled material is extremely sensitive, and requires little material. When this form of detection is used with reversed-phase HPLC, the use of volatile buffers eliminates the need for subsequent desalting. A similar approach to this is the use of activated carbon resin. Several HPLC columns containing this adsorbent exist, and our group is currently investigating their use.

4.5 Conclusion

The essential nature and unique chemical structure of PG has led to the development of antibiotic agents that target its metabolism. The rise in antibiotic resistance indicates the need for new targets. Resistance to several important antibiotics is due to the highly variable nature of their target – the stem peptides. Alternatively, enzymes involved in maintenance of the glycan strand, such as the LTs, have been far less exploited as antibiotic targets. These enzymes are an attractive target, as the glycan strand is relatively invariable, and therefore antibiotic resistance may be more difficult to achieve.

The primary challenge associated with studying enzymes that act on PG is its inherent insolubility and heterogeneity, indicating the need for a refined enzyme assay based on a defined, soluble substrate. The above is an example of one such assay, the determination of endo- or exo-specificity of LTs. This determination of substrate-specificity is an important step in the development of antibiotic agents that target such enzymes. While further study is required, the findings from this work will help to shape future strategies for the generation of a defined substrate.

Appendix A

Media, Solutions, and Reagents

A.1 Bacterial media and solutions

LB medium:	10 g/L tryptone, 5 g/L yeast extract, 10 g/L NaCl
LB agar (1.5%):	LB medium containing 15 g/L agar
SuperBroth medium:	32 g/L tryptone, 20 g/L yeast extract, 5 g/L NaCl
Kanamycin stock solution:	50 mg/mL in H_2O, filter-sterilize, store in 1 mL aliquots at -20 °C
Chloramphenicol stock solution:	34 mg/mL in ethanol, filter-sterilize, store in 1 mL aliquots at -20 °C
IPTG (1 M):	238.3 mg/mL in H_2O, filter-sterilize, store in 1 mL aliquots at -20 °C

A.2 Solutions for DNA

6X DNA loading buffer:	1X TAE buffer 0.25% bromophenol blue 0.25% xylene cyanol FF 30% glycerol
0.5 M EDTA, pH 8.0	0.5 M EDTA Adjust pH to 8.0 with NaOH Note: EDTA will not go into solution until pH~8.0
50X TAE buffer (1 litre):	242 g Tris base 57.1 mL glacial acetic acid 100 mL 0.5 M EDTA, pH 8.0
TE buffer:	10 mM Tris-HCl, pH 7.4 1 mM EDTA

A.3 Solutions for SDS-PAGE

Ammonium persulfate (APS): 10% (wt/vol) in water

Sodium dodecyl sulfate (SDS): 10% (wt/vol) in water

10X Electrophoresis buffer (1 litre):

0.25 M Tris	30.3 g Tris (MW 121.14 g/mol)
1.92 M glycine	144.1 g glycine (MW 75.07 g/mol)
1% SDS	10 g SDS

pH should be 8.3 without adjusting

4X DualColor™ Protein Loading Buffer (Fermentas):

0.25 M Tris-HCl, pH 8.5
8% SDS
1.6 mM EDTA
0.024% Pyronin Y
0.04% bromophenol blue
40% glycerol
0.4 M DTT
Note: DTT was stored at -20 °C as a 2 M stock (one freeze-thaw cycle)

A.4 SDS-PAGE gel recipes

	2 gels		4 gels	
	12% separating	4% stacking	12% separating	4% stacking
Distilled water	4.35 mL	3.22 mL	8.7 mL	6.42 mL
Acrylamide/Bis (40%)	3.0 mL	0.4875 mL	6.0 mL	0.975 mL
1.5 M Tris-HCl, pH 8.8	2.5 mL	–	5.0 mL	–
0.5 M Tris-HCl, pH 6.8	–	1.25 mL	–	2.5 mL
10% (wt/vol) SDS	100 µL	50 µL	200 µL	100 µL
10% (wt/vol) APS	50 µL	25 µL	100 µL	50 µL
TEMED	5 µL	5 µL	10 µL	10 µL

A.5 Solutions for protein purification

A.5.1 IMAC buffers

Lysis buffer (1 litre):

50 mM NaH_2PO_4	6.00 g NaH_2PO_4 (MW 119.98 g/mol)
300 mM NaCl	17.53 g NaCl (MW 58.44 g/mol)
10 mM imidazole	0.68 g imidazole (MW 68.08 g/mol)
0.1% Triton X-100	1 mL Triton X-100

Adjust pH to 8.0 using NaOH.

Wash buffer (1 litre):

50 mM NaH_2PO_4	6.00 g NaH_2PO_4 (MW 119.98 g/mol)
300 mM NaCl	17.53 g NaCl (MW 58.44 g/mol)
20 mM imidazole	1.36 g imidazole (MW 68.08 g/mol)
0.1% Triton X-100	1 mL Triton X-100

Adjust pH to 8.0 using NaOH.

Elution buffer (1 litre):

50 mM NaH_2PO_4	6.00 g NaH_2PO_4 (MW 119.98 g/mol)
300 mM NaCl	17.53 g NaCl (MW 58.44 g/mol)
250 mM imidazole	17.02 g imidazole (MW 68.08 g/mol)
0.1% Triton X-100	1 mL Triton X-100

Adjust pH to 8.0 using NaOH.

A.5.2 FPLC buffers

Buffer A (1 litre):

50 mM NaH_2PO_4	6.00 g NaH_2PO_4 (MW 119.98 g/mol)

Adjust pH to 7.0 using NaOH, filter-sterilize through a 0.2 μm filter

Buffer B (1 litre):

50 mM NaH_2PO_4	6.00 g NaH_2PO_4 (MW 119.98 g/mol)
1 M NaCl	58.44 g NaCl (MW 58.44 g/mol)

Adjust pH to 7.0 using NaOH, filter-sterilize through a 0.2 μm filter

A.6 Solutions for Western blot and immunodetection

Tank-blotting transfer buffer:	10 mM $NaHCO_3$ 3 mM Na_2CO_3 20% methanol pH should be 9.9 without adjusting
TBS buffer:	10 mM Tris-HCl, pH 7.5 150 mM NaCl
TBS-Tween/Triton buffer:	20 mM Tris-HCl, pH 7.5 500 mM NaCl 0.05% Tween 20 0.2% Triton X-100
Blocking buffer:	3% BSA in TBS buffer
Primary antibody solution:	1:1000 in blocking buffer
Secondary antibody solution:	1:2000 in blocking buffer

A.7 Solutions for zymography

Zymogram gels:	0.1% peptidoglycan in SDS-PAGE separating gel
Zymogram renaturation solution:	25 mM sodium phosphate, pH 7.0 10 mM $MgCl_2$ 0.1% Triton X-100
Zymogram stain:	0.1% Methylene Blue 0.01% KOH

Appendix B

Protocols

B.1 Western blot immunodetection

The following steps were done to the membrane at room temperature on a shaker:

1. Wash twice for 10 min each time with TBS buffer (10 mM Tris-HCl, 150 mM NaCl, pH 7.5)
2. Incubate for 1 h in blocking buffer (3% BSA in TBS buffer)
3. Wash twice for 10 min each time in TBS-Tween/Triton buffer (20 mM Tris-HCl, 500 mM NaCl, 0.05% Tween 20, 0.2% Triton X-100, pH 7.5)
4. Wash for 10 min with TBS buffer
5. Incubate with anti-His antibody (1:1000 in blocking buffer) for 1 h
6. Wash twice for 10 min each time in TBS-Tween/Triton buffer
7. Wash for 10 min with TBS buffer
8. Incubate with secondary antibody (1:2000 in blocking buffer) for 1 h
9. Wash 4 times for 10 min each time in TBS-Tween/Triton buffer
10. Stain with 2 mL 1-Step NBT/BCIP for 5–10 min without shaking
11. Stop the chromogenic reaction by rinsing twice with water
12. Scan as soon as possible as the colours will fade with time

Appendix C

Calculations

Table C.1: Monoisotopic mass calculations. The mass of the most common isotope was used. Masses are indicated without an adduct, and with the hydrogen, sodium, or potassium adduct. All ion species are singly charged as observed in oligosaccharide analysis. The most abundant species observed with oligosaccharides is the $[M+Na]^+$ ion. G, GlcNAc; M, MurNAc; aM, anhydroMurNAc.

Product	[M]	$[M+H]^+$	$[M+Na]^+$	$[M+K]^+$
Adduct	0.00	1.01	22.99	38.96
G	221.09	222.10	244.08	260.05
aM	275.10	276.11	298.09	314.06
M	293.11	294.12	316.10	332.07
G_2	424.17	425.18	447.16	463.13
G-aM	478.18	479.19	501.17	517.14
G-M	496.19	497.20	519.18	535.15
G_3	627.25	628.26	650.24	666.21
M-G-aM	753.28	754.29	776.27	792.24
M-G-M	771.29	772.30	794.28	810.25
G_4	830.33	831.34	853.32	869.29
G-M-G-aM	956.36	957.37	979.35	995.32
$(G\text{-}M)_2$	974.37	975.38	997.36	1013.33
G_5	1033.41	1034.42	1056.40	1072.37
M-G-M-G-aM	1231.46	1232.47	1254.45	1270.42
G_6	1236.49	1237.49	1259.48	1275.45
$M\text{-}(G\text{-}M)_2$	1249.47	1250.48	1272.46	1288.43
$(G\text{-}M)_2$-G-aM	1434.54	1435.55	1457.53	1473.50
$(G\text{-}M)_3$	1452.55	1453.56	1475.54	1491.51
$(G\text{-}M)_3$-G-aM	1912.72	1913.73	1935.71	1951.68
$(G\text{-}M)_4$	1930.73	1931.74	1953.72	1969.69
$(G\text{-}M)_4$-G-aM	2390.90	2391.91	2413.89	2429.86
$(G\text{-}M)_5$	2408.91	2409.92	2431.90	2447.87
$(G\text{-}M)_5$-G-aM	2869.08	2870.09	2892.07	2908.04
$(G\text{-}M)_6$	2887.09	2888.10	2910.08	2926.05
$(G\text{-}M)_6$-G-aM	3347.26	3348.27	3370.25	3386.22
$(G\text{-}M)_7$	3365.27	3366.28	3388.26	3404.23
$(G\text{-}M)_7$-G-aM	3825.44	3826.45	3848.43	3864.40
$(G\text{-}M)_8$	3843.45	3844.46	3866.44	3882.41
$(G\text{-}M)_8$-G-aM	4303.62	4304.63	4326.61	4342.58
$(G\text{-}M)_9$	4321.63	4322.64	4344.62	4360.59
$(G\text{-}M)_9$-G-aM	4781.80	4782.81	4804.79	4820.76
$(G\text{-}M)_{10}$	4799.81	4800.82	4822.80	4838.77
$(G\text{-}M)_{10}$-G-aM	5259.98	5260.99	5282.97	5298.94

Appendix D

MALDI-TOF analyses

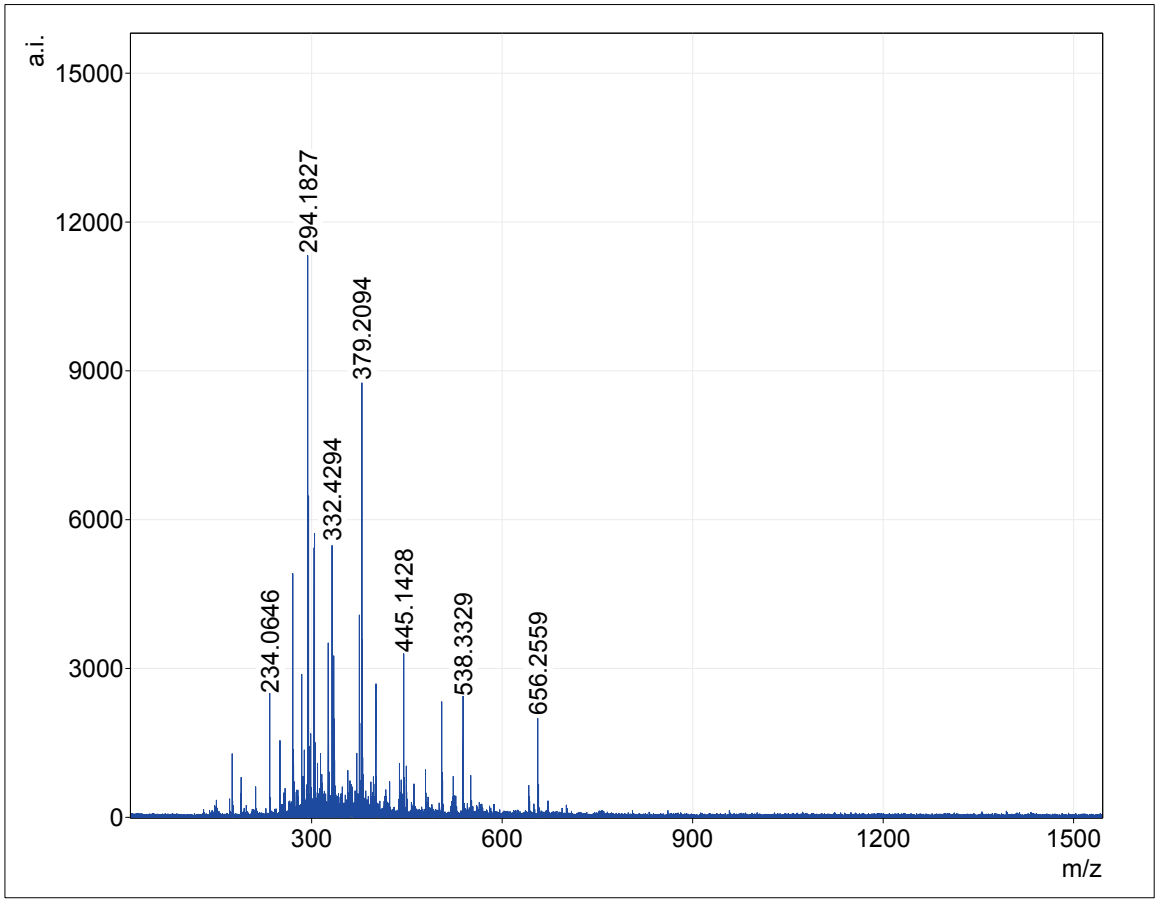

Figure D.1: MALDI-TOF MS analysis of digested PG using CCA. tAmiB-digested *P. aeruginosa* PG was incubated with lysozyme (1 mg/mL) for 1 h at 37 °C, desalted with a ZipTip®, mixed with CCA and spotted directly onto a MALDI-TOF plate. Peaks were of very low intensity and none of the peaks were identified.

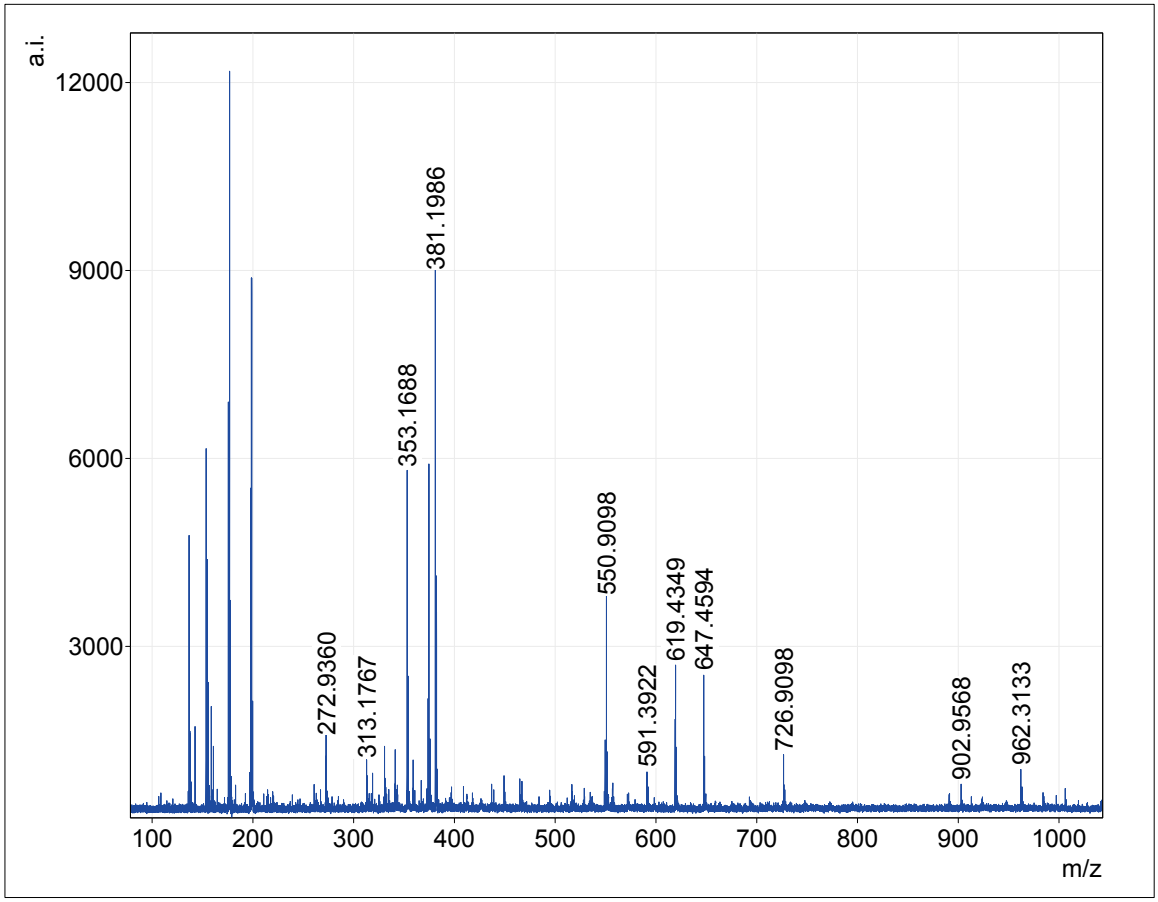

Figure D.2: MALDI-TOF MS analysis of digested PG using DHB. tAmiB-digested *P. aeruginosa* PG was incubated with lysozyme (1 mg/mL) for 1 h at 37 °C, mixed with DHB and spotted directly onto a MALDI-TOF plate. None of the peaks were identified.

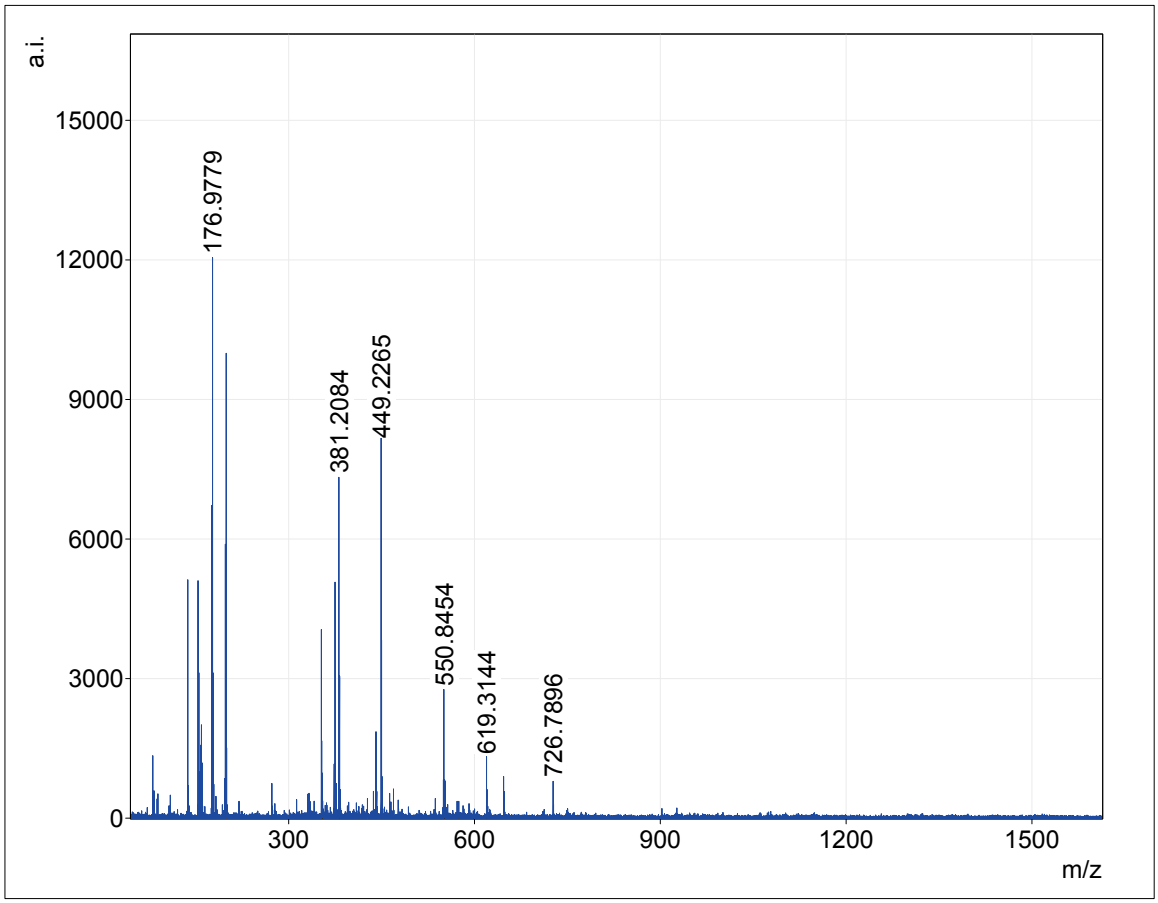

Figure D.3: MALDI-TOF MS analysis of an isolated PG digestion product using DHB. tAmiB-digested *P. aeruginosa* PG was incubated with lysozyme (20 ng/mL) for 2 h at 37 °C and resolved by HPAEC-A (Figure 3.12). The peak at 21 min was collected, desalted with a ZipTip®, mixed with DHB and spotted directly onto a MALDI-TOF plate. None of the peaks were identified.

References

Abergel, C., Monchois, V., Byrne, D., Chenivesse, S., Lembo, F., Lazzaroni, J.C., Claverie, J.M., 2007. Structure and evolution of the Ivy protein family, unexpected lysozyme inhibitors in Gram-negative bacteria. Proc. Natl. Acad. Sci. U.S.A. 104, 6394–6399.

Abrams, A., 1958. O-acetyl groups in the cell wall of *Streptococcus faecalis*. J. Biol. Chem. 230, 949–959.

Alaedini, A., Day, R.A., 1999. Identification of two penicillin-binding multienzyme complexes in *Haemophilus influenzae*. Biochem. Biophys. Res. Commun. 264, 191–195.

Amako, K., Umeda, A., Murata, K., 1982. Arrangement of peptidoglycan in the cell wall of *Staphylococcus* spp. J. Bacteriol. 150, 844–850.

Antignac, A., Rousselle, J.C., Namane, A., Labigne, A., Taha, M.K., Boneca, I.G., 2003. Detailed structural analysis of the peptidoglycan of the human pathogen *Neisseria meningitidis*. J. Biol. Chem. 278, 31521–31528.

van Asselt, E.J., Dijkstra, A.J., Kalk, K.H., Takacs, B., Keck, W., Dijkstra, B.W., 1999a. Crystal structure of *Escherichia coli* lytic transglycosylase Slt35 reveals a lysozyme-like catalytic domain with an EF-hand. Structure 7, 1167–1180.

van Asselt, E.J., Thunnissen, A.M., Dijkstra, B.W., 1999b. High resolution crystal structures of the *Escherichia coli* lytic transglycosylase Slt70 and its complex with a peptidoglycan fragment. J. Mol. Biol. 291, 877–898.

Atrih, A., Zollner, P., Allmaier, G., Foster, S.J., 1996. Structural analysis of *Bacillus subtilis* 168 endospore peptidoglycan and its role during differentiation. J. Bacteriol. 178, 6173–6183.

Barbas, J.A., Díaz, J., Rodríguez-Tébar, A., Vázquez, D., 1986. Specific location of penicillin-binding proteins within the cell envelope of *Escherichia coli*. J. Bacteriol. 165, 269–275.

Barreteau, H., Kovac, A., Boniface, A., Sova, M., Gobec, S., Blanot, D., 2008. Cytoplasmic steps of peptidoglycan biosynthesis. FEMS Microbiol. Rev. 32, 168–207.

Bateman, A., Bycroft, M., 2000. The structure of a LysM domain from *E. coli* membrane-bound lytic murein transglycosylase D (MltD). J. Mol. Biol. 299, 1113–1119.

Bendtsen, J.D., Nielsen, H., von Heijne, G., Brunak, S., 2004. Improved prediction of signal peptides: SignalP 3.0. J. Mol. Biol. 340, 783–795.

Bernadsky, G., Beveridge, T.J., Clarke, A.J., 1994. Analysis of the sodium dodecyl sulfate-stable peptidoglycan autolysins of select Gram-negative pathogens by using renaturing polyacrylamide gel electrophoresis. J. Bacteriol. 176, 5225–5232.

den Blaauwen, T., de Pedro, M.A., Nguyen-Distèche, M., Ayala, J.A., 2008. Morphogenesis of rod-shaped sacculi. FEMS Microbiol. Rev. 32, 321–344.

Blackburn, N.T., Clarke, A.J., 2000. Assay for lytic transglycosylases: a family of peptidoglycan lyases. Anal. Biochem. 284, 388–393.

Blackburn, N.T., Clarke, A.J., 2001. Identification of four families of peptidoglycan lytic transglycosylases. J. Mol. Evol. 52, 78–84.

Blackburn, N.T., Clarke, A.J., 2002. Characterization of soluble and membrane-bound family 3 lytic transglycosylases from *Pseudomonas aeruginosa*. Biochemistry 41, 1001–1013.

Borysowski, J., Weber-Dabrowska, B., Górski, A., 2006. Bacteriophage endolysins as a novel class of antibacterial agents. Exp. Biol. Med. (Maywood) 231, 366–377.

Botta, G.A., Park, J.T., 1981. Evidence for involvement of penicillin-binding protein 3 in murein synthesis during septation but not during cell elongation. J. Bacteriol. 145, 333–340.

Braun, V., 1975. Covalent lipoprotein from the outer membrane of Escherichia coli. Biochim. Biophys. Acta 415, 335–377.

Braun, V., Rehn, K., 1969. Chemical characterization, spatial distribution and function of a lipoprotein (murein-lipoprotein) of the *E. coli* cell wall. The specific effect of trypsin on the membrane structure. Eur. J. Biochem. 10, 426–438.

Braun, V., Sieglin, U., 1970. The covalent murein-lipoprotein structure of the *Escherichia coli* cell wall. The attachment site of the lipoprotein on the murein. Eur. J. Biochem. 13, 336–346.

Broome-Smith, J.K., Edelman, A., Yousif, S., Spratt, B.G., 1985. The nucleotide sequences of the *ponA* and *ponB* genes encoding penicillin-binding protein 1A and 1B of *Escherichia coli* K12. Eur. J. Biochem. 147, 437–446.

Brumfitt, W., Wardlaw, A.C., Park, J.T., 1958. Development of lysozyme-resistance in *Micrococcus lysodiekticus* and its association with an increased O-acetyl content of the cell wall. Nature 181, 1783–1784.

Burnette, W.N., 1981. "Western blotting": electrophoretic transfer of proteins from sodium dodecyl sulfate–polyacrylamide gels to unmodified nitrocellulose and radiographic detection with antibody and radioiodinated protein A. Anal. Biochem. 112, 195–203.

Chaput, C., Labigne, A., Boneca, I.G., 2007. Characterization of *Helicobacter pylori* lytic transglycosylases Slt and MltD. J. Bacteriol. 189, 422–429.

Cheng, Q., Li, H., Merdek, K., Park, J.T., 2000. Molecular characterization of the β-*N*-acetylglucosaminidase of *Escherichia coli* and its role in cell wall recycling. J. Bacteriol. 182, 4836–4840.

Chenna, R., Sugawara, H., Koike, T., Lopez, R., Gibson, T.J., Higgins, D.G., Thompson, J.D., 2003. Multiple sequence alignment with the Clustal series of programs. Nucleic Acids Res. 31, 3497–3500.

Clarke, A.J., Dupont, C., 1992. O-acetylated peptidoglycan: its occurrence, pathobiological significance, and biosynthesis. Can. J. Microbiol. 38, 85–91.

Clarke, A.J., Strating, H., Blackburn, N.T., 2002. Pathways for the O-acetylation of bacterial cell wall polysaccharides, in: Doyle, R.J. (Ed.), Glycomicrobiology. Springer US, pp. 187–223.

Cloud, K.A., Dillard, J.P., 2002. A lytic transglycosylase of *Neisseria gonorrhoeae* is involved in peptidoglycan-derived cytotoxin production. Infect. Immun. 70, 2752–2757.

Cloud-Hansen, K.A., Peterson, S.B., Stabb, E.V., Goldman, W.E., McFall-Ngai, M.J., Handelsman, J., 2006. Breaching the great wall: peptidoglycan and microbial interactions. Nat. Rev. Microbiol. 4, 710–716.

Cohen, S.N., Chang, A.C., Hsu, L., 1972. Nonchromosomal antibiotic resistance in bacteria: genetic transformation of *Escherichia coli* by R-factor DNA. Proc. Natl. Acad. Sci. U.S.A. 69, 2110–2114.

Davies, G., Henrissat, B., 1995. Structures and mechanisms of glycosyl hydrolases. Structure 3, 853–859.

Demchick, P., Koch, A.L., 1996. The permeability of the wall fabric of *Escherichia coli* and *Bacillus subtilis*. J. Bacteriol. 178, 768–773.

Dijkstra, A.J., Keck, W., 1996. Identification of new members of the lytic transglycosylase family in *Haemophilus influenzae* and *Escherichia coli*. Microb. Drug Resist. 2, 141–145.

Dmitriev, B.A., Ehlers, S., Rietschel, E.T., 1999. Layered murein revisited: a fundamentally new concept of bacterial cell wall structure, biogenesis and function. Med. Microbiol. Immunol. 187, 173–181.

Dramsi, S., Magnet, S., Davison, S., Arthur, M., 2008. Covalent attachment of proteins to peptidoglycan. FEMS Microbiol. Rev. 32, 307–320.

Dupont, C., Clarke, A.J., 1991. In vitro synthesis and O acetylation of peptidoglycan by permeabilized cells of *Proteus mirabilis*. J. Bacteriol. 173, 4618–4624.

Ehlert, K., Höltje, J.V., Templin, M.F., 1995. Cloning and expression of a murein hydrolase lipoprotein from *Escherichia coli*. Mol. Microbiol. 16, 761–768.

Engel, H., Smink, A.J., van Wijngaarden, L., Keck, W., 1992. Murein-metabolizing enzymes from *Escherichia coli*: existence of a second lytic transglycosylase. J. Bacteriol. 174, 6394–6403.

Evrard, C., Fastrez, J., Soumillion, P., 1999. Histidine modification and mutagenesis point to the involvement of a large conformational change in the mechanism of action of phage lambda lysozyme. FEBS Lett. 460, 442–446.

Ghuysen, J.M., 1968. Use of bacteriolytic enzymes in determination of wall structure and their role in cell metabolism. Bacteriol. Rev. 32, 425–464.

Ghuysen, J.M., Tipper, D.J., Strominger, J.L., 1966. Enzymes that degrade bacterial cell walls. Meth. Enzymol. 8, 685–699.

Glauner, B., 1988. Separation and quantification of muropeptides with high-performance liquid chromatography. Anal. Biochem. 172, 451–464.

Glauner, B., Höltje, J.V., 1990. Growth pattern of the murein sacculus of *Escherichia coli*. J. Biol. Chem. 265, 18988–18996.

Glauner, B., Höltje, J.V., Schwarz, U., 1988. The composition of the murein of *Escherichia coli*. J. Biol. Chem. 263, 10088–10095.

Gmeiner, J., Essig, P., Martin, H.H., 1982. Characterization of minor fragments after digestion of *Escherichia coli* murein with endo-N,O-diacetylmuramidase from *Chalaropsis*, and determination of glycan chain length. FEBS Lett. 138, 109–112.

Goffin, C., Ghuysen, J.M., 1998. Multimodular penicillin-binding proteins: an enigmatic family of orthologs and paralogs. Microbiol. Mol. Biol. Rev. 62, 1079–1093.

Goodell, E.W., 1985. Recycling of murein by *Escherichia coli*. J. Bacteriol. 163, 305–310.

Ha, S., Gross, B., Walker, S., 2001. *E. coli* MurG: a paradigm for a superfamily of glycosyltransferases. Curr. Drug Targets Infect. Disord. 1, 201–213.

Hancock, R.E., Carey, A.M., 1979. Outer membrane of *Pseudomonas aeruginosa*: heat- and 2-mercaptoethanol-modifiable proteins. J. Bacteriol. 140, 902–910.

Harz, H., Burgdorf, K., Höltje, J.V., 1990. Isolation and separation of the glycan strands from murein of *Escherichia coli* by reversed-phase high-performance liquid chromatography. Anal. Biochem. 190, 120–128.

Hash, J.H., 1967. Measurement of bacteriolytic enzymes. J. Bacteriol. 93, 1201–1202.

Heidrich, C., Ursinus, A., Berger, J., Schwarz, H., Höltje, J.V., 2002. Effects of multiple deletions of murein hydrolases on viability, septum cleavage, and sensitivity to large toxic molecules in *Escherichia coli*. J. Bacteriol. 184, 6093–6099.

van Heijenoort, J., 2001. Formation of the glycan chains in the synthesis of bacterial peptidoglycan. Glycobiology 11, 25R–36R.

Höltje, J.V., 1995. From growth to autolysis: the murein hydrolases in *Escherichia coli*. Arch. Microbiol. 164, 243–254.

Höltje, J.V., 1996. A hypothetical holoenzyme involved in the replication of the murein sacculus of *Escherichia coli*. Microbiology 142, 1911–1918.

Höltje, J.V., 1998. Growth of the stress-bearing and shape-maintaining murein sacculus of *Escherichia coli*. Microbiol. Mol. Biol. Rev. 62, 181–203.

Höltje, J.V., Kopp, U., Ursinus, A., Wiedemann, B., 1994. The negative regulator of β-lactamase induction AmpD is a *N*-acetyl-anhydromuramyl-L-alanine amidase. FEMS Microbiol. Lett. 122, 159–164.

Höltje, J.V., Mirelman, D., Sharon, N., Schwarz, U., 1975. Novel type of murein transglycosylase in *Escherichia coli*. J. Bacteriol. 124, 1067–1076.

Hoyle, B.D., Beveridge, T.J., 1984. Metal binding by the peptidoglycan sacculus of *Escherichia coli* K-12. Can. J. Microbiol. 30, 204–211.

Ikeda, M., Wachi, M., Jung, H.K., Ishino, F., Matsuhashi, M., 1991. The *Escherichia coli mraY* gene encoding UDP-*N*-acetylmuramoyl-pentapeptide: undecaprenyl-phosphate phospho-*N*-acetylmuramoyl-pentapeptide transferase. J. Bacteriol. 173, 1021–1026.

Jacobs, C., Joris, B., Jamin, M., Klarsov, K., Van Beeumen, J., Mengin-Lecreulx, D., van Heijenoort, J., Park, J.T., Normark, S., Frère, J.M., 1995. AmpD, essential for both β-lactamase regulation and cell wall recycling, is a novel cytosolic *N*-acetylmuramyl-L-alanine amidase. Mol. Microbiol. 15, 553–559.

Joris, B., Englebert, S., Chu, C.P., Kariyama, R., Daneo-Moore, L., Shockman, G.D., Ghuysen, J.M., 1992. Modular design of the *Enterococcus hirae* muramidase-2 and *Streptococcus faecalis* autolysin. FEMS Microbiol. Lett. 70, 257–264.

Kahne, D., Leimkuhler, C., Lu, W., Walsh, C., 2005. Glycopeptide and lipoglycopeptide antibiotics. Chem. Rev. 105, 425–448.

Kajie, S., Ideta, R., Yamato, I., Anraku, Y., 1991. Molecular cloning and DNA sequence of *dniR*, a gene affecting anaerobic expression of the *Escherichia coli* hexaheme nitrite reductase. FEMS Microbiol. Lett. 67, 205–211.

Karamanos, Y., 1997. Endo-*N*-acetyl-β-D-glucosaminidases and their potential substrates: structure/function relationships. Res. Microbiol. 148, 661–671.

Keck, W., van Leeuwen, A.M., Huber, M., Goodell, E.W., 1990. Cloning and characterization of *mepA*, the structural gene of the penicillin-insensitive murein endopeptidase from *Escherichia coli*. Mol. Microbiol. 4, 209–219.

Koch, A.L., 1990. Additional arguments for the key role of "smart" autolysins in the enlargement of the wall of Gram-negative bacteria. Res. Microbiol. 141, 529–541.

Koch, A.L., Doyle, R.J., 1985. Inside-to-outside growth and turnover of the wall of Gram-positive rods. J. Theor. Biol. 117, 137–157.

Koraimann, G., 2003. Lytic transglycosylases in macromolecular transport systems of Gram-negative bacteria. Cell. Mol. Life Sci. 60, 2371–2388.

Korndörfer, I.P., Danzer, J., Schmelcher, M., Zimmer, M., Skerra, A., Loessner, M.J., 2006. The crystal structure of the bacteriophage PSA endolysin reveals a unique fold responsible for specific recognition of *Listeria* cell walls. J. Mol. Biol. 364, 678–689.

Kraft, A.R., Templin, M.F., Höltje, J.V., 1998. Membrane-bound lytic endotransglycosylase in *Escherichia coli*. J. Bacteriol. 180, 3441–3447.

Kuroda, A., Sugimoto, Y., Funahashi, T., Sekiguchi, J., 1992. Genetic structure, isolation and characterization of a *Bacillus licheniformis* cell wall hydrolase. Mol. Gen. Genet. 234, 129–137.

Labischinski, H., Goodell, E.W., Goodell, A., Hochberg, M.L., 1991. Direct proof of a "more-than-single-layered" peptidoglycan architecture of *Escherichia coli* W7: a neutron small-angle scattering study. J. Bacteriol. 173, 751–756.

Laemmli, U.K., 1970. Cleavage of structural proteins during the assembly of the head of bacteriophage T4. Nature 227, 680–685.

Legaree, B.A., Clarke, A.J., 2008. Interaction of penicillin-binding protein 2 with soluble lytic transglycosylase B1 in *Pseudomonas aeruginosa*. J. Bacteriol. 190, 6922–6926.

Leung, A.K., Duewel, H.S., Honek, J.F., Berghuis, A.M., 2001. Crystal structure of the lytic transglycosylase from bacteriophage lambda in complex with hexa-*N*-acetylchitohexaose. Biochemistry 40, 5665–5673.

Leutgeb, W., Weidel, W., 1963. On a glycogen trapped in *E. coli* cell wall preparations. Z. Naturforsch. B 18, 1060–1062.

Lommatzsch, J., Templin, M.F., Kraft, A.R., Vollmer, W., Höltje, J.V., 1997. Outer membrane localization of murein hydrolases: MltA, a third lipoprotein lytic transglycosylase in *Escherichia coli*. J. Bacteriol. 179, 5465–5470.

Luker, K.E., Collier, J.L., Kolodziej, E.W., Marshall, G.R., Goldman, W.E., 1993. *Bordetella pertussis* tracheal cytotoxin and other muramyl peptides: distinct structure-activity relationships for respiratory epithelial cytopathology. Proc. Natl. Acad. Sci. U.S.A. 90, 2365–2369.

Mainardi, J.L., Villet, R., Bugg, T.D., Mayer, C., Arthur, M., 2008. Evolution of peptidoglycan biosynthesis under the selective pressure of antibiotics in Gram-positive bacteria. FEMS Microbiol. Rev. 32, 386–408.

Mengin-Lecreulx, D., Texier, L., Rousseau, M., van Heijenoort, J., 1991. The *murG* gene of *Escherichia coli* codes for the UDP-*N*-acetylglucosamine: *N*-acetylmuramyl-(pentapeptide) pyrophosphoryl-undecaprenol *N*-acetylglucosamine transferase involved in the membrane steps of peptidoglycan synthesis. J. Bacteriol. 173, 4625–4636.

Meroueh, S.O., Bencze, K.Z., Hesek, D., Lee, M., Fisher, J.F., Stemmler, T.L., Mobashery, S., 2006. Three-dimensional structure of the bacterial cell wall peptidoglycan. Proc. Natl. Acad. Sci. U.S.A. 103, 4404–4409.

Mohammadi, T., van Dam, V., Sijbrandi, R., Vernet, T., Zapun, A., Bouhss, A., Diepeveen-de Bruin, M., Nguyen-Disteche, M., de Kruijff, B., Breukink, E., 2011. Identification of FtsW as a transporter of lipid-linked cell wall precursors across the membrane. EMBO J. Advance online publication, 1–8.

Murray, R.G., Steed, P., Elson, H.E., 1965. The location of the mucopeptide in sections of the cell wall of *Escherichia coli* and other Gram-negative bacteria. Can. J. Microbiol. 11, 547–560.

Nanninga, N., 1998. Morphogenesis of *Escherichia coli*. Microbiol. Mol. Biol. Rev. 62, 110–129.

Nelson, D.E., Young, K.D., 2000. Penicillin binding protein 5 affects cell diameter, contour, and morphology of *Escherichia coli*. J. Bacteriol. 182, 1714–1721.

Neuhaus, F.C., Baddiley, J., 2003. A continuum of anionic charge: structures and functions of D-alanyl-teichoic acids in Gram-positive bacteria. Microbiol. Mol. Biol. Rev. 67, 686–723.

Nielsen, H., Engelbrecht, J., Brunak, S., von Heijne, G., 1997. Identification of prokaryotic and eukaryotic signal peptides and prediction of their cleavage sites. Protein Eng. 10, 1–6.

Packer, N.H., Lawson, M.A., Jardine, D.R., Redmond, J.W., 1998. A general approach to desalting oligosaccharides released from glycoproteins. Glycoconj. J. 15, 737–747.

Park, J.T., 1993. Turnover and recycling of the murein sacculus in oligopeptide permease-negative strains of *Escherichia coli*: indirect evidence for an alternative permease system and for a monolayered sacculus. J. Bacteriol. 175, 7–11.

Parquet, C., Flouret, B., Leduc, M., Hirota, Y., van Heijenoort, J., 1983. *N*-acetylmuramoyl-L-alanine amidase of *Escherichia coli* K12. Possible physiological functions. Eur. J. Biochem. 133, 371–377.

Pei, J., Grishin, N.V., 2005. COG3926 and COG5526: a tale of two new lysozyme-like protein families. Protein Sci. 14, 2574–2581.

Powell, A.J., Liu, Z.J., Nicholas, R.A., Davies, C., 2006. Crystal structures of the lytic transglycosylase MltA from *N.gonorrhoeae* and *E.coli*: insights into interdomain movements and substrate binding. J. Mol. Biol. 359, 122–136.

Quintela, J.C., Caparrós, M., de Pedro, M.A., 1995. Variability of peptidoglycan structural parameters in Gram-negative bacteria. FEMS Microbiol. Lett. 125, 95–100.

Reid, C.W., Blackburn, N.T., Clarke, A.J., 2004a. The effect of NAG-thiazoline on morphology and surface hydrophobicity of *Escherichia coli*. FEMS Microbiol. Lett. 234, 343–348.

Reid, C.W., Blackburn, N.T., Clarke, A.J., 2006. Role of arginine residues in the active site of the membrane-bound lytic transglycosylase B from *Pseudomonas aeruginosa*. Biochemistry 45, 2129–2138.

Reid, C.W., Blackburn, N.T., Legaree, B.A., Auzanneau, F.I., Clarke, A.J., 2004b. Inhibition of membrane-bound lytic transglycosylase B by NAG-thiazoline. FEBS Lett. 574, 73–79.

Reid, C.W., Brewer, D., Clarke, A.J., 2004c. Substrate binding affinity of *Pseudomonas aeruginosa* membrane-bound lytic transglycosylase B by hydrogen-deuterium exchange MALDI MS. Biochemistry 43, 11275–11282.

Romeis, T., Höltje, J.V., 1994. Specific interaction of penicillin-binding proteins 3 and 7/8 with soluble lytic transglycosylase in *Escherichia coli*. J. Biol. Chem. 269, 21603–21607.

Romeis, T., Vollmer, W., Höltje, J.V., 1993. Characterization of three different lytic transglycosylases in *Escherichia coli*. FEMS Microbiol. Lett. 111, 141–146.

Sanger, F., 1945. The free amino groups of insulin. Biochem. J. 39, 507–515.

Sauvage, E., Kerff, F., Terrak, M., Ayala, J.A., Charlier, P., 2008. The penicillin-binding proteins: structure and role in peptidoglycan biosynthesis. FEMS Microbiol. Rev. 32, 234–258.

Scheurwater, E., Reid, C.W., Clarke, A.J., 2008. Lytic transglycosylases: bacterial space-making autolysins. Int. J. Biochem. Cell Biol. 40, 586–591.

Scheurwater, E.M., 2008. Identification of YfhD from *Escherichia coli* as membrane-bound lytic transglycosylase F, the archetype for family 1B lytic transglycosylases. Ph.D. thesis. University of Guelph.

Scheurwater, E.M., Clarke, A.J., 2008. The C-terminal domain of *Escherichia coli* YfhD functions as a lytic transglycosylase. J. Biol. Chem. 283, 8363–8373.

Scheurwater, E.M., Pfeffer, J.M., Clarke, A.J., 2007. Production and purification of the bacterial autolysin *N*-acetylmuramoyl-L-alanine amidase B from *Pseudomonas aeruginosa*. Protein Expr. Purif. 56, 128–137.

Schiffer, G., Höltje, J.V., 1999. Cloning and characterization of PBP 1C, a third member of the multimodular class A penicillin-binding proteins of *Escherichia coli*. J. Biol. Chem. 274, 32031–32039.

Schleifer, K.H., Kandler, O., 1972. Peptidoglycan types of bacterial cell walls and their taxonomic implications. Bacteriol. Rev. 36, 407–477.

Smith, T.J., Blackman, S.A., Foster, S.J., 2000. Autolysins of *Bacillus subtilis*: multiple enzymes with multiple functions. Microbiology 146, 249–262.

Stoker, N.G., Pratt, J.M., Spratt, B.G., 1983. Identification of the *rodA* gene product of *Escherichia coli*. J. Bacteriol. 155, 854–859.

van Straaten, K.E., Dijkstra, B.W., Vollmer, W., Thunnissen, A.M., 2005. Crystal structure of MltA from *Escherichia coli* reveals a unique lytic transglycosylase fold. J. Mol. Biol. 352, 1068–1080.

Strohalm, M., Hassman, M., Kosata, B., Kodicek, M., 2008. mMass data miner: an open source alternative for mass spectrometric data analysis. Rapid Commun. Mass Spectrom. 22, 905–908.

Strohalm, M., Kavan, D., Novak, P., Volny, M., Havlicek, V., 2010. mMass 3: a cross-platform software environment for precise analysis of mass spectrometric data. Anal. Chem. 82, 4648–4651.

Thunnissen, A.M., Dijkstra, A.J., Kalk, K.H., Rozeboom, H.J., Engel, H., Keck, W., Dijkstra, B.W., 1994. Doughnut-shaped structure of a bacterial muramidase revealed by X-ray crystallography. Nature 367, 750–753.

Thunnissen, A.M., Rozeboom, H.J., Kalk, K.H., Dijkstra, B.W., 1995. Structure of the 70-kDa soluble lytic transglycosylase complexed with bulgecin A. Implications for the enzymatic mechanism. Biochemistry 34, 12729–12737.

Touhami, A., Jericho, M.H., Beveridge, T.J., 2004. Atomic force microscopy of cell growth and division in *Staphylococcus aureus*. J. Bacteriol. 186, 3286–3295.

Ursinus, A., Höltje, J.V., 1994. Purification and properties of a membrane-bound lytic transglycosylase from *Escherichia coli*. J. Bacteriol. 176, 338–343.

Vollmer, W., 2008. Structural variation in the glycan strands of bacterial peptidoglycan. FEMS Microbiol. Rev. 32, 287–306.

Vollmer, W., Joris, B., Charlier, P., Foster, S., 2008. Bacterial peptidoglycan (murein) hydrolases. FEMS Microbiol. Rev. 32, 259–286.

Vollmer, W., Pilsl, H., Hantke, K., Höltje, J.V., Braun, V., 1997. Pesticin displays muramidase activity. J. Bacteriol. 179, 1580–1583.

Vollmer, W., von Rechenberg, M., Höltje, J.V., 1999. Demonstration of molecular interactions between the murein polymerase PBP1B, the lytic transglycosylase MltA, and the scaffolding protein MipA of *Escherichia coli*. J. Biol. Chem. 274, 6726–6734.

Vollmer, W., Seligman, S.J., 2010. Architecture of peptidoglycan: more data and more models. Trends Microbiol. 18, 59–66.

Vollmer, W., Tomasz, A., 2000. The *pgdA* gene encodes for a peptidoglycan *N*-acetylglucosamine deacetylase in *Streptococcus pneumoniae*. J. Biol. Chem. 275, 20496–20501.

Vollmer, W., Tomasz, A., 2002. Peptidoglycan *N*-acetylglucosamine deacetylase, a putative virulence factor in *Streptococcus pneumoniae*. Infect. Immun. 70, 7176–7178.

Vötsch, W., Templin, M.F., 2000. Characterization of a β-*N*-acetylglucosaminidase of *Escherichia coli* and elucidation of its role in muropeptide recycling and β-lactamase induction. J. Biol. Chem. 275, 39032–39038.

Ward, J.B., 1973. The chain length of the glycans in bacterial cell walls. Biochem. J. 133, 395–398.

Watt, S.R., Clarke, A.J., 1994. Initial characterization of two extracellular autolysins from Pseudomonas aeruginosa PAO1. J. Bacteriol. 176, 4784–4789.

Wiedemann, B., Dietz, H., Pfeifle, D., 1998. Induction of β-lactamase in *Enterobacter cloacae*. Clin. Infect. Dis. 27 Suppl 1, S42–47.

Wientjes, F.B., Woldringh, C.L., Nanninga, N., 1991. Amount of peptidoglycan in cell walls of Gram-negative bacteria. J. Bacteriol. 173, 7684–7691.

Wilkins, M.R., Gasteiger, E., Bairoch, A., Sanchez, J.C., Williams, K.L., Appel, R.D., Hochstrasser, D.F., 1999. Protein identification and analysis tools in the ExPASy server. Methods Mol. Biol. 112, 531–552.

Wolf-Watz, H., Normark, S., 1976. Evidence for a role of *N*-acetylmuramyl-L-alanine amidase in septum separation in *Escherichia coli*. J. Bacteriol. 128, 580–586.

Xu, N., Huang, Z.H., Watson, J.T., Gage, D.A., 1997. Mercaptobenzothiazoles: A new class of matrices for laser desorption ionization mass spectrometry. J. Am. Soc. Mass Spectrom. 8, 116–124.

Yao, X., Jericho, M., Pink, D., Beveridge, T., 1999. Thickness and elasticity of Gram-negative murein sacculi measured by atomic force microscopy. J. Bacteriol. 181, 6865–6875.